OpenAIR@RGU

The Open Access Institutional Repository
at Robert Gordon University

http://openair.rgu.ac.uk

Citation Details

Citation for the version of the work held in 'OpenAIR@RGU':

GAZEY, R. N., 2014. Sizing hybrid green hydrogen energy generation and storage systems (HGHES) to enable an increase in renewable penetration for stabilising the grid. Available from *OpenAIR@RGU*. [online]. Available from: http://openair.rgu.ac.uk

Sizing Hybrid Green Hydrogen Energy generation and Storage systems (HGHES) to enable an increase in renewable penetration for stabilising the grid

Ross Neville Gazey

A thesis submitted in partial fulfilment of the requirements of the Robert Gordon University for the degree of the Doctor of Philosophy

January 2014

Acknowledgments

I would like to express my sincere gratitude to my project supervisors **Dr. Dallia Ali, Dr. Daniel Aklil-D'Halluin** and **Dr Stephen Finney** for their continual valuable advice, help, understanding and enthusiasm during this project. I have genuinely enjoyed working with everyone during this time and trust that future research students will also have the pleasure of working with you.

I would also like to thank all my family and friends, and in particular **Frances Browne**, who have supported and encouraged me through the course of my research. Without that support I would not have been able to achieve the outcomes reached.

Special dedication to all of those involved in the **Energy Technology Partnership (ETP)** and **Robert Gordon University IDEAS Research Institute** teams that this research was conducted under. Their continued support ensured that I had the opportunity to complete this work, Thank you for your friendship support and help.

I would particularly like to take this opportunity to thank all those I have had the pleasure of working with during this research project. In particular **all those at the Pure Energy Centre**, without their continued belief and commitment to the successful outcome of this research I would not have managed to reach the full potential of this research.

Dedication

In memory of the late **Alexander Andrew Macaulay (Sandy)**, a true inspiration

Abstract

A problem that has become apparently growing in the deployment of renewable energy systems is the power grids inability to accept the forecasted growth in renewable energy generation integration. To support forecasted growth in renewable generation integration, it is now recognised that Energy Storage Technologies (EST) must be utilised. Recent advances in Hydrogen Energy Storage Technologies (HEST) have unlocked their potential for use with constrained renewable generation. HEST combines Hydrogen production, storage and end use technologies with renewable generation in either a directly connected configuration, or indirectly via existing power networks.

A levelised cost (LC) model has been developed within this thesis to identify the financial competitiveness of the different HEST application scenarios when used with grid constrained renewable energy. Five HEST scenarios have been investigated to demonstrate the most financially competitive configuration and the benefit that the by-product oxygen from renewable electrolysis can have on financial competitiveness. Furthermore, to address the lack in commercial software tools available to size an energy system incorporating HEST with limited data, a deterministic modelling approach has been developed to enable the initial automatic sizing of a hybrid renewable hydrogen energy system (HRHES) for a specified consumer demand. Within this approach, a worst-case scenario from the financial competitiveness analysis has been used to demonstrate that initial sizing of a HRHES can be achieved with only two input data, namely – the available renewable resource and the load profile.

The effect of the electrolyser thermal transients at start-up on the overall quantity of hydrogen produced (and accordingly the energy stored), when operated in conjunction with an intermittent renewable generation source, has also been modelled. Finally, a mass-transfer simulation model has been developed to investigate the suitability of constrained renewable generation in creating hydrogen for a hydrogen refuelling station.

Key Words: Hybrid, Renewable, Hydrogen, Energy, Electrolyser, Refuelling, Cascade

Glossary of Abbreviations

EST	Energy Storage Technology
HEST	Hydrogen Energy Storage Technology
ESS	Energy Storage System
PHS	Pumped Hydro Storage
CAES	Compressed Air Energy Storage
NaS	Sodium Sulphur
NiCd	Nickel Cadmium
LiOn	Lithium Ion
RES	Renewable Energy Source
RFB	Redox Flow Battery
DSM	Demand Side Management
VPP	Virtual Power Plant
LCM	Levelised Cost Model
RPM	Revolutions Per Minute
HHES	Hybrid Hydrogen Energy System
PV	Photovoltaic
GA	Genetic Algorithm
PSO	Particle Swarm Optimisation
SA	Simulated Annealing
AI	Artificial Intelligence
PEM	Proton Exchange Membrane
FC	Fuel Cell
H_2	Hydrogen
O_2	Oxygen
HRHES	Hybrid Renewable Hydrogen Energy System
DNO	Distribution Network Operator
LSHPST	Large Stationary High Pressure Storage Tank
LP	Low Pressure
HP	High Pressure
ROC	Renewable Obligation Certificate
LHV	Lower Heating Value Higher
HHV	Heating Value
IEA	International Energy Association

List of notations

Wind Turbine Model

Notation	Description
Cp	Coefficient of performance
λ	Tip speed ratio
β	Blade pitch angle
n	Turbine RPM
D	Turbine rotor diameter
v	Wind speed.
P_{wind}	Wind turbine output
ρ	Air density
A	Swept rotor area

Photovoltaic Model

Notation	Description
I_{SC}	Short circuit current
V_{OC}	Open circuit voltage
MPP	Maximum Power Point
V_{MP}	Maximum power point Voltage
I_{MP}	Maximum power point Current
C_1	Constant
C_2	Constant
Φ	Solar Irradiance
T	Cell Temperature
T_{ref}	Reference Temperature
α	Coefficient of I_{sc}
β	Coefficient of V_{oc}
R_s	Series Resistance

Electrolyser Model

Notation	Description
U	*Cell Voltage*
U_{rev}	Reversible voltage
$r_{1,2}$	Empirical ohmic resistance parameter of electrolyte

T	Temperature
$t_{1,2,3}$	Empirical over voltage parameter of electrode
s	Over voltage parameter of electrode
A	Electrode area
I	Current
η_F	Faraday Efficiency
f_1	Faraday efficiency parameter
f_2	Faraday efficiency parameter
$\dot{n}_{H_2}$	Molar flow rate
z	number of electrons transferred per reaction
F	Faraday constant
n_c	Number of cells in electrolyser cell stack
η_e	Energy Efficiency
U_{tn}	Thermo Neutral Voltage
$\dot{Q}_{gen}$	Thermal Energy Created by electrolysis process
$\dot{Q}_{loss}$	Thermal Energy lost to the environment
$\dot{Q}_{cool}$	Thermal energy dissipated by cooling system
C_t	Thermal capacity (or inertia) of electrolyser
R_t	Thermal resistance of electrolyser
T_a	Ambient temperature
t	Time
T_{ini}	Initial temperature
Δ_t	Change in time

Pressurised Hydrogen Storage Model

Notation	Description
P	Absolute pressure
ρ	Molar density
T	Absolute temperature
R	Universal gas constant
a_i	Constants associated with the density equation for normal hydrogen
b_i	Constants associated with the density equation for normal hydrogen
c_i	Constants associated with the density equation for normal hydrogen
M	Molar Mass

Z	Pressure correction factor

PEM Fuel Cell Model

Notation	Description
U_{rev}	Reversible cell voltage
U	Overall cell voltage
U_a	Activation losses
U_o	Ohmic losses
U_c	Concentration losses
P_{h2}	Partial pressure of hydrogen
P_{O2}	Partial pressure of oxygen
T	Cell temperature
i_{fc}	Cell operating current
C_{O2}	Concentration of oxygen at the catalytic interface of the cathode
ξ	Parametric coefficients of each FC Cell
R_C	Resistive constant
L	Membrane Thickness
A	Membrane Active Area
Ψ	Humidification level of the membrane
j	Current density (I_{FC}/A)
j_{max}	maximum current density
B	parametric coefficient

List of figures

List of Tables

Table Of Contents

1

1 Introduction

Since the turn of the 21st Century great progress has been made in understanding the impact of human activities on the global climate. Since the publication of the Stern review, the Political, Environmental and Economical pressures together with the recent significant increase in the fossil fuel costs have led to the rapid expansion of electricity generation from Renewable Energy Sources (RES). In reviewing the Political, Environmental and Economical issues, the Stern review has found out that almost quarter of the global green-house emissions were produced from the power generation (24%) sector [1].

Additionally, a recent report from the International Panel on Climate Change (IPCC), stated that one of the greatest challenges facing humanity in the 21st century is climate change [2]. In the IPCC Special Report on Renewable Energy Sources and Climate Change Mitigation (SRREN), it was concluded that, if implemented properly, renewable energy can play a vital role in addressing many of the political, economical, and environmental pressures that climate change is bringing.

Furthermore, the International Energy Agency (IEA) indicated that as much as 46% of global electricity could be delivered from RES by 2050 [3]. In addition British Petroleum (BP) 2011 "energy

outlook2030" [4] energy forecast predicted Fossil fuel energy source growth to fall from 83% to 64% of market share in favour of renewable energy sources. This trend is continued in their revised 2013 "Energy outlook 2030" with over half the increase in energy for the power market sector projected to be derived from non-fossil fuels. BP estimates that renewable sources will contribute to at least 27% of the growth in the power sector. This is in combination with a total projected growth in overall energy demand of 40% between 2010 and 2013 [5].

Due to these factors, power networks used around the world must become much more robust.   This is to allow the integration of increasing quantities of intermittent RES and the growing number of small decentralised power producers [6].

Nowadays, electrical networks are required to develop the means to absorb and potentially store the excess power fed into the grid from fluctuating sources (such as RES) in order to remain stable. Integrating more capacity into power transmission, and distribution systems in the form of energy storage and deferrable loads can facilitate the projected increase in the variable generation from RES.   Unfortunately, lack of demonstration sites to develop understanding, technical limitations, and high capital costs of energy storage technologies have constrained large scale deployment of such technologies to be used for balancing power networks.

The recent advances in hydrogen technologies are of significant interest. These advances are slowly but surely unlocking the potential for their use in Hybrid Hydrogen Energy Systems (HHES). HHES combines hydrogen production, storage and end use technologies with RES in either a directly connected off grid configuration, or indirectly via existing power networks.

HHES has the potential to be integrated into power networks to allow both the absorption of the excess energy from fluctuating RES, and the supply of supplementary energy when RES production is insufficient to meet demand. This enables balancing of supply and demand over a power network, while integrating increasing quantities of variable RES output.

However, a major drawback has been found to the wide deployment of HRHES in the final report of the International Energy Agencies - Hydrogen Implementing Agreement (IEA-HIA) Task 18, Subtask B for Integrated Systems Evaluation. This drawback is due to the current existing modelling techniques, where a two year period is typically required to develop a detailed HHES evaluation as per the statement below [7]:

> *"Proper validation of data, detailed modelling and system analysis is a tedious process; a minimum of two person-years should be allowed in each detailed evaluation"*

This major drawback means that substantial amounts of human resources will be required to develop the application of HRHES projects, while other technologies benefit from simple modelling and analysis tools. The IEA-HIA task 18 has also concluded in their final report, that simulation models are needed to enable the operation and design of hydrogen energy storage systems. In addition, the IEA-HIA defined that generic hydrogen energy models are needed in the commonly available simulation environments including Matlab/Simulink.

In essence, the existing limitation in modelling software and tools identified by the International Energy Association is a key barrier to realising the potential of hydrogen energy storage technology. Therefore, the research presented in this thesis aims to address the aforementioned opportunities and /or barriers by:

1) Identifying the most appropriate application for hydrogen energy storage technology when used in conjunction with constrained power networks.
2) Develop a financial model to define the financial competitiveness of hydrogen energy storage technology.
3) Develop a rapid system sizing model for the initial sizing of HRHES.
4) Investigate the effect of thermally compensated electrolyser (hydrogen generator) modelling on the simulation of HRHES.
5) Develop an analysis model to identify HRHES suitability for transport applications when applied in a constrained RES situation.

1.1   Thesis Overview

Chapter 1, this chapter, introduces the global energy situation and identifies the need for more flexible energy networks to accommodate increasing renewable energy generation. From the IEA hydrogen implementing agreement task 18 work, it has been identified that there is a requirement for quicker modelling techniques to reduce the time needed in initially assessing and sizing hydrogen energy storage projects. Furthermore, it has been identified that there is a need to develop more hydrogen energy models to overcome the barriers to adoption of the technology.

Chapter 2 explores the improvements that have been made in balancing supply and demand on electrical grids. It provides the rationale behind the need for Energy Storage Technologies (EST) in general. It then illustrates the limitations of the existing ESTs and discusses the opportunity that hydrogen energy technology presents. The existing barriers towards the adoption of hydrogen technology are also described alongside the limitations of existing modelling techniques to simulate hydrogen technology within the context of a grid constrained renewable energy.

Chapter 3 investigates the financial competitiveness of a hydrogen energy storage technology in order to define when, and under which conditions, a hydrogen energy storage system will attain financial competitiveness. The existing extent of constrained renewable energy in the UK is examined along with the balancing mechanism payments that are in place to manage these constraints. A financial model, that can be applied to capture the full economic potential of a hydrogen energy storage system, is then proposed. Five scenarios are developed for the deployment of hydrogen energy storage, and a comparison versus other EST's is made.

Chapter 4 examines the limitation of the existing software available for the initial sizing (define the size of an electrolyser, storage tank, fuel cell, etc) of a renewable energy system that uses hydrogen energy storage technology. A deterministic modelling method is then developed for sizing a HRHES. The proposed modelling method allows the initial sizing of a hybrid renewable hydrogen energy system with a minimal amount of input data and computer resources. Moreover, through the use of the proposed modelling method in a case study, the benefits that hydrogen energy storage technology can bring to constrained renewable generation, is identified.

Chapter 5 investigates the adverse effects of thermal transient characteristics on hydrogen production efficiency, when constrained renewable generation is used as a source of energy for electrolysis. The limitations that existing software have in assessing the impact of thermal transients in electrolysers in a renewable hydrogen production setup, is illustrated. In this chapter, a thermally compensated electrolyser model is developed with a proposed algorithm to examine the overall effect on hydrogen production when using an electrolyser operated either directly in response to a renewable resource, or as part of a power grid network balancing mechanism.

Chapter 6 inspects the dynamic mismatch that can occur between renewable resource availability and the use of hydrogen in refuelling stations. The limitation of existing models is identified and a hydrogen mass transfer model is proposed. The proposed mass transfer model is then applied to a case study to analyse the replenishment dynamics of a hydrogen refuelling station between refuelling operations, when supplied from a grid constrained renewable source.

Chapter 7 then concludes the work done in this thesis, together with recommendations of further work that can contribute to the development of hydrogen energy storage technologies as a an enabling technology for constrained renewable generation.

2

2   Context for Hydrogen as an Energy Vector

The consumption of electrical energy across the world grows continually every year. The increasing demand for electrical energy is also having a detrimental impact on the environment. It is approaching an unsustainable level within the limitations of existing centralised electrical infrastructure and design concepts.

The United States Energy Information Administration (EIA) predicts global renewable energy output to increase by over 50% (excluding bio-fuels) between 2010 and 2035 [8]. On the other hand, modelling of power networks suggests that the grid will become unstable if more than 20% of the energy mix comes from renewable sources [9]. Hence, to accommodate the projected increase in renewable energy output, electrical power networks not only need to become more flexible, but must also develop the capacity to store excess power fed into the grid from fluctuating and intermittent power sources [10].

This chapter provides the background to this research. It illustrates the improvements that have been implemented in balancing supply and demand in electrical grids and the rationale behind the need for energy storage technologies. The limitations of the existing improvements are also discussed with the opportunity that hydrogen energy technology can present. The barriers towards the adoption of hydrogen technology are then described. Finally, the limitations of existing modelling techniques that simulate hydrogen technology within the context of a grid connected energy system are described.

2.1 Balancing Demand and Supply

There are a number of methods available to Distribution Network Operators (DNOs) to help guarantee the stability of electrical networks. However, with the integration of increasing quantities of renewable and distributed generation over the last few decades, it has become necessary to develop new methods to ensure the power grid remains balanced.

To continually achieve equilibrium under increasingly demanding conditions, it has now become crucial that electrical grids increase their capacity through the implementation of energy storage technologies [11]. Without increased capacity, power grids are at risk of ending up in a total black out similar to that which happened in the North American power grid in August 2003 [12].

In the following sections, the fundamental challenge of maintaining the supply and demand balance will be introduced together with how this challenge has led to the development of new control and management techniques, which have then led to the need to energy storage integration and in particular the novel application of hydrogen technologies.

2.1.1 Why Traditional Generation, Transmission And Distribution Are Out Of Date?

Traditional developed electrical infrastructure has a relatively simple topology compared to that of a decentralised smart grid. The traditional infrastructure design has been developed to bring electricity from a relatively small number of large scale centralised fossil fuelled electrical power stations to a large number of domestic and industrial/commercial consumers. Conventionally fuelled hydrocarbon and nuclear power stations are load following in nature and can at least partially adjust

their electrical generation output to follow demand as required. As the turbine output follows demand, the electrical grid is maintained in equilibrium at all times as all the energy generated is consumed.

As time has progressed, the transmission of power from power stations to the 'periphery' of the network has developed. This has created a transmission network topology that is suited for power flow in one direction from generation to load as shown in Figure 2-1 [13].
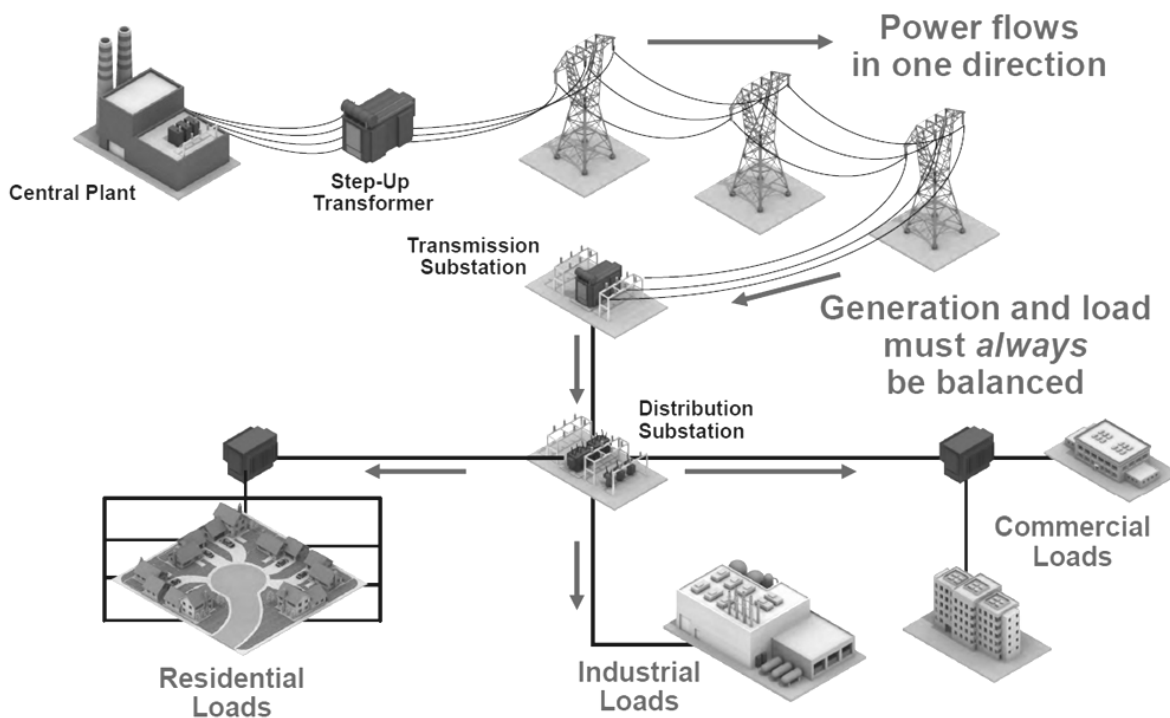
Figure 2-1: Traditional Power network topology delivering power from generation to load [13]

As can be seen in Figure 2-1, should any interconnection between the generation and consumption points become disconnected, the power from the generation station cannot be transmitted to the consumer.

In order to improve the robustness of the network shown in Figure 2-1, more interconnections have been introduced to allow alternative paths for power flow between generation stations and the consumers. The additional interconnections, known as network nodes (and sometimes referred to as substations), improves the robustness of the network and enables power to flow from more than

one source to the points of consumption. Such interconnection also allows greater flexibility in the event of a sudden demand shift (for example if an interconnection fails, or a large load is switched on). However if demand exceeds supply the network will be unable to meet these demands, and some of the network will automatically disconnect itself which is known as a black out.

In situations where power networks move towards an imbalanced condition, network operators are obliged to implement their control mechanisms to return the electrical network to its balanced state. One common example of this is having electrical generation equipment in a ready to generate state. This is an electrical generation that is running, but under a no-load condition. When the electrical network requires additional generation to meet demand, this generator is connected onto the electrical network and loaded up according to demand. This is known in the power industry as spinning reserve [14]. Spinning reserve is a highly costly and inefficient method of maintaining network stability as it requires a large number of generating stations running and consuming fuel in order that they can be brought online very quickly to maintain the supply and demand balance.

It can be said that electrical generators operating in the mode of spinning reserve can be considered to have a 0% or negative efficiency as they are consuming fuel resources. In this mode of operation they produce no output onto the electrical network until brought on-line by network operators. Research has shown that the costs of maintaining spinning reserve increase as the requirement for reserve capacity continues to rise in line with the expansion of RES onto the existing electrical infrastructure [15].

The increase (and the future forecasted further increase) in RES integration is forcing the change in the traditional operation of the electrical infrastructure. In fact, power network operators have to manage much larger numbers of RES power generators distributed over an increasingly wide geographic area [16]. Unfortunately renewable sources cannot adjust their electrical power output in the same way traditional power stations can. For example a photovoltaic array or wind turbine will continue to produce electrical energy for as long as the sun is shining or the wind is blowing. Due to this fundamental difference in operational profile, a traditional power network will develop a significant deviation from the supply and demand balance required for a stable electrical network.

In extreme cases, the operators of RES connected to an increasingly congested electrical transmission and distribution networks have to incur financial penalties. This is the result of producing electrical energy at times when demand is low. Conversely network operators will have to pay compensation to RES operators when constraints have to be introduced to maintain network supply and demand balance [17].

New strategies have therefore been developed to reduce the effect that RES can have on the grid stability, while reducing the need for expensive and inefficient spinning reserve resources. The development of intelligent load and generation management (Smart grid) and operational concepts of Virtual Power Plants (VPP) coupled with energy storage are amongst these strategies. They have been investigated and implemented to provide a valuable mechanism to unlock the full potential of RES and increase valuable electrical network flexibility [18].

In the UK context, Grid operators have invested greatly to reduce grid stability issues that can be seen when substantial amount of RES are introduced onto the grid [19]. This has been achieved through greater interconnections. There has also been a push towards more telemetry and smarter management systems that allows a more intelligent way of operating the grid. Such systems are seen by many as the precursor to the wider application of energy storage technologies [20]. The enhanced management systems are known as Smart Grids, Virtual Power Plants (VPP) and Demand Side Management (DSM) [21]. Each of these systems is further described in the coming sub-sections. It is important to note that combining these concepts serve to rationalise the load demands in a power network and can act as a facilitator for the introduction of large scale EST.

2.1.2 Why Smart Grids?

A Smart Grid can be thought of as an electrical power network that is enhanced to accommodate the introduction of many variable and intermittent sources such as RES. In contrast to traditional power networks, a smart grid is not necessarily dominated by a small number of very large scale generation stations. Decentralised energy production is a major defining element of a Smart Grid that maintains a continual supply and demand balance [22]. The supply and demand balance is managed by a number of modern advanced control techniques within which EST can make a significant contribution [23]. A smart Grid is actively managed by reading strategically placed network status sensors and operating load management controls on both transmission and distribution levels in a

power network [24]. Whilst there is no globally recognised definition for Smart Grids the most commonly understood description of a Smart Grid is an electrical power network combined with a data network [25] that enables the gathering of information about supply and demand data in order to adjust load and generation to maintain equilibrium. Figure 2-2 illustrates a smart grid, with the dashes used to define the data flow for decision making.

In essence, smart grids have been incorporated within the power grid to help maintain the demand and supply balance whilst enabling further integration of distributed energy sources such as RES. Though the concept of smart grids can make substantial improvements to the power grid, they are not capable of fully stabilising it if larger numbers of RES become connected [26]. To counteract this problem a new concept, Virtual Power Plants (VPP) has been introduced.
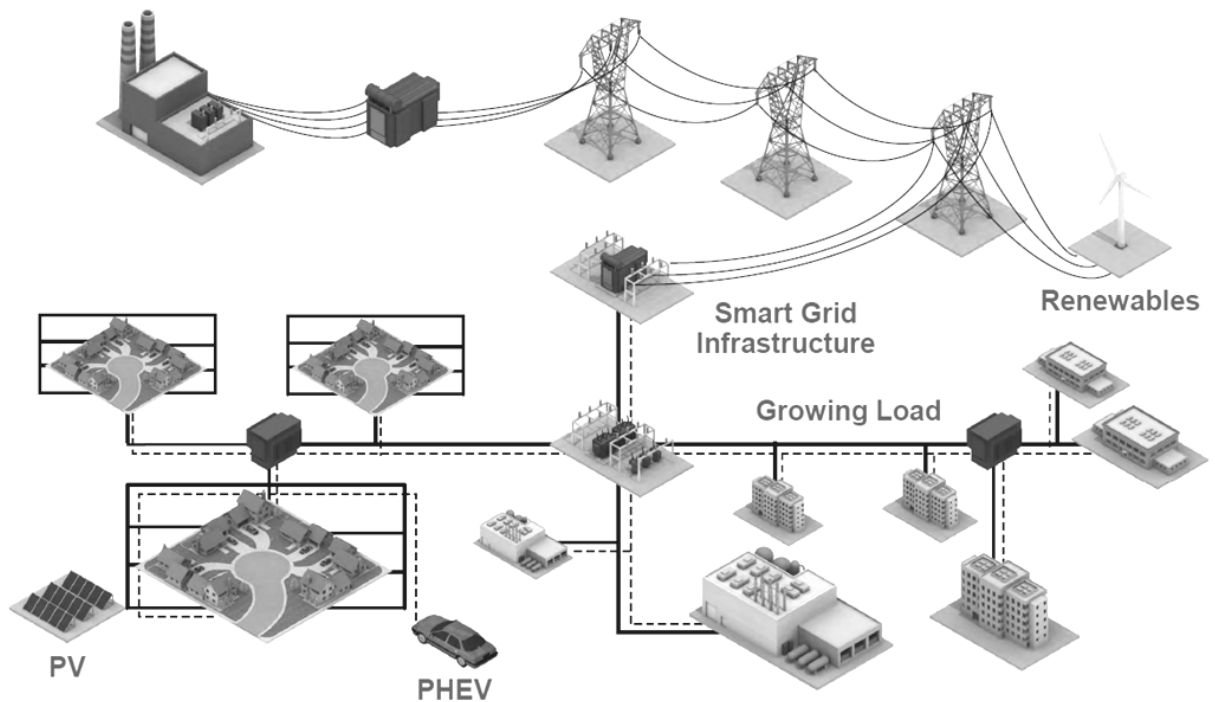
Figure 2-2: Addition of 'Smart Grid' to electrical grids [13]
Dashed line represents the flow of information between embedded and renewable generators

2.1.3 Virtual Power Plants (VPP)

In geographic areas where there are a number of distributed generators and controllable consumers (loads), there is the concept to combine them into what is known as a Virtual Power Plant (VPP). The fundamental concept behind a VPP is that small scale producers of electrical energy can be operated as if they are formed from one single large generation source [27].

Individually distributed generation sources cannot guarantee network stability on a continual basis. However, the idea behind VPP is the combination of generation sources together to form one bulk virtual generation node which provides improvements by evening out the peaks and troughs in energy production.

In conjunction with the clustering of distributed generation sources, it is also possible to integrate the VPP concept together with the control of consumer loads within a smart grid using Demand Side management (DSM). The effect of disconnecting a large proportion of load over a geographic area has the same impact on capacity in electrical networks as turning on an additional generation source to meet peek demands. However, the control of consumer loads cannot be achieved by VPP and smart grids alone. Smart grids facilitate the gathering of consumer demands information, whilst VPP facilitates the control of grouped distributed generation into one virtual node. Hence there is a need for an additional layer of intelligent control. This additional layer (which has been used for decades, but not utilised for the purpose of controlling and managing large numbers of distributed RES), is known within the power industry as Demand Side Management, or DSM [28, 29]. DSM is further described in the next section.

2.1.4 Demand Side Management (DSM)

The central element to a VPP and a smart grid is a management mechanism to facilitate the control of consumer loads. This management mechanism is in most cases referred to as DSM. Within the concept of DSM a management mechanism takes logical decisions to keep the grid stable. Using the data gathered from smart grid telemetry, a DSM mechanism monitors the available number of distributed generation stations and their status through a VPP (production level, availability etc). It also monitors the level of end users electrical demands.

A DSM manages end user demands (load) placed upon the grid network in accordance with the available generation sources available to meet that demand. This is achieved by disconnecting deferrable loads such as heating and cooling systems where some time delay is acceptable to the end user. The DSM therefore manages the peaks of demand by reducing or removing them to deliver a predictable and stable electrical grid network.

Combining consumer loads DSM with the clustering of distributed generation sources (VPP) can provide a large increase in network flexibility. Therefore the combination of Smart grid, VPP and DSM improves stability without the need to operate large spinning generation reserves. However the use of DSM in the context of VPP and smart grids has some significant recognised limitation.

The majority of electrical network loads can only be deferred for a short time period without causing noticeable disturbance in consumer activities (keeping fridges and freezers cold, or maintaining an industrial process temperature for example). In addition, the exchange of high quantities user consumption data has been found to raise many issues over the security of end users privacy [30]. Also, for DSM to work most effectively there is a need for a significant flexibility in pricing to actively change consumer habits [31]. Finally, the available number of energy storage systems currently connected to electrical grids for control is still very low [32]. The present lack of grid connected energy storage is a limiting factor in the full application of smart grids, VPP and DSM. To reduce these limitations, and increase the level capacity to connect RES onto the grid, there is a need for a larger deployment of energy storage technologies (EST) [33]. Therefore, without the introduction of ESTs used in conjunction with smart grids, VPP and DSM, it is documented that the grid will not have the capacity to cope with any significant increase in RES above 30% of the generation mix [34]. As such this provides a global opportunity for energy storage technologies if combined correctly with RES. Hence, there is a need to investigate the different energy storage technologies for grid connected energy management.

Consequently, the next sections will describe the most suited energy storage technologies, their strength, weaknesses and why hydrogen can play a major role in stabilising the grid. This will accordingly form the background for the further research developed in this thesis, namely, Sizing Hybrid Green Hydrogen Energy generation and Storage systems (HGHES) to enable an increase in renewable penetration of stabilising the grid.

2.2 Energy Storage

It is now becoming clear that energy storage technologies will play a crucial role in supporting the wider integration of distributed RES into electrical networks. The rationale for Energy storage becoming so crucial is that it will act as a stabiliser by increasing the power grid capacity to

accommodate increasing fluctuations in supply and demand [35]. Indeed, the integration of EST into electrical networks allows more flexibility in accommodating the demands of increased amounts of RES [36].

An example of how energy storage may be introduced into the electricity grid infrastructure within a 'Smart grid' configuration is shown in Figure 2-3. This illustrates how enhancing the flexibility of an electrical network increases its capacity to accommodate more decentralised RES within the generation mix. As illustrated, distributed energy storage nearer to consumers can assist in reducing power quality issues (such as brown-outs). Larger energy storage further up at the supply chain can assist in bulk energy management of the network. The consumer obtains a better quality of power supplied and the Distribution Network Operator (DNO) attains a more flexible grid management system. In addition, the grid acquires the capacity to accept more renewable energy.
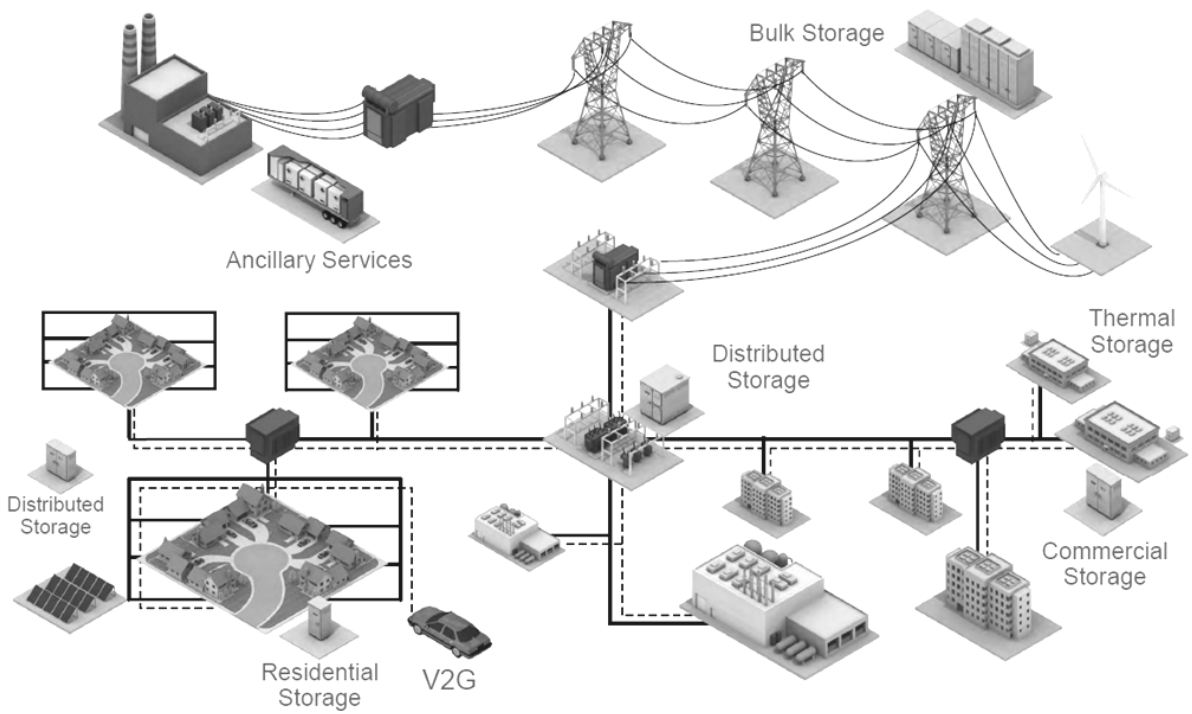
Figure 2-3: Introduction of energy storage within a smart grid infrastructure [13]

As aforementioned, the increased flexibility that storage brings to the grid reduces the risks that additional RES integration may destabilise the electrical supply and demand balance. However, the inclusion of an energy storage system brings additional costs over and above the initial costs of energy generation. It also incurs additional capital and operational costs associate with the energy

conversion loss efficiencies [37]. There is also limited large scale operational and testing experience of energy storage technologies available (with the exception of pumped hydro). However, despite these potential limitations, EST is considered to provide a vital role in enabling the projected increase in RES onto power network [38].

2.2.1 Why Energy Storage Technologies?

Research conducted by the Boston Consulting Group (BCG) [39] identified that DSM on its own will have a limited contribution to the smoothing of large quantities of grid connected RES. In a high RES penetration scenario, BCG has highlighted the limited impact that DSM can contribute to maintaining the supply and demand balance. Due to this limitation it has now become necessary to utilise Energy Storage Technology (EST).

It is becoming clear that EST can fit well within existing power grid systems that operate as smart grids with VPP and DSM. The purpose of EST integration within smart grids utilising VPP and DSM concepts is to stabilise the electrical network and balance supply and demand. Within a coordinated VPP mechanism, EST can be considered as a DSM controllable consumer load during charging and as a VPP controllable generation source during discharging. The central element to a VPP consists of a management mechanism that will take logical decisions regarding the number of distributed generation stations available and the consumers of the electrical energy. This will result in a more predictable and stable electrical network.

Therefore, applying the principles of DSM to EST within a VPP and smart grid infrastructure can greatly reduce the data requirements as described previously. The rationalised approach to energy management means that RES connected to the power network will have their energy utilised in the most effective manner possible. For instance, the RES generation can be delivered to the load when load demands require it and diverted to storage when generation is in excess of consumption. This would remove a considerable quantity of the constraint issues that are becoming an increasing problem on traditional centralised power networks.

In addition to the above EST has the potential to reduce spinning reserve requirements. Hence, allowing operational costs for spinning reserve to be diverted to the operational costs for EST [40].

The DNO will also be able to reduce the need for grid interconnection upgrades, as energy storage will be able to absorb excess renewable energy generation between weakly connected network segments.

As energy storage technologies have such high potential for reducing grid energy management issues and facilitating high levels of RES connection, it is important then to understand the different energy storage technologies, their weaknesses, strengths and why hydrogen has the potential to provide significant additional benefits compared to other ESTs.

EST energy storage duration ranges between a few seconds of operation to several hours [41]. Shown in Figure 2-4 is a summary of the different storage technologies conducted by AEA technologies for the Scottish government [42] and how they are best suited for use. It can be seen that hydrogen has a role to play in durations between several minutes to hours. It is also potentially best suited for applications larger than 100 kW.

*SMES = Superconducting Magnetic Energy Storage
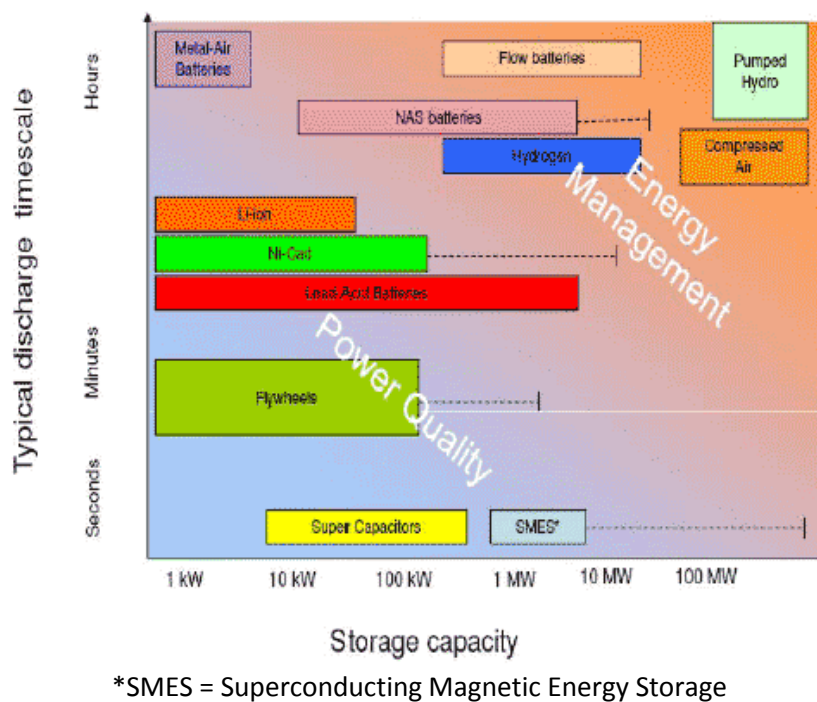
Figure 2-4: Energy storage technology overview from Scottish Government report [42]

One of the challenges in selecting the most appropriate EST when interconnected to the electricity network is related to how much storage should be installed and in what form. As can be seen in Figure 2-4, there are a variety of storage technologies that have been researched for either improving power quality or improving energy management.

The energy storage technologies best suited to short duration and low to medium power outputs are typically seen as performing better in improving power quality. Energy storage technologies that provide medium to high power outputs with long durations are seen as better suited to energy management of electrical networks. The technologies that have been suggested by the AEA research as the most appropriate for Energy management of electricity networks are:

- Large Lead Acid Batteries
- Sodium Sulphur (NAS)
- Flow Batteries (RFB)
- Pumped Hydro
- Compressed Air Energy Storage (CAES)
- Hydrogen (H_2).

The above ESTs are briefly described in the following sections.

2.2.2 Large Scale Lead Acid Batteries

Lead acid battery technology has been in use for more than 140 years in a wide variety of applications and is still among the most commonly used battery based energy storage technologies today. Continuous improvements in this technology have resulted in modern lead acid batteries having a relatively low cost with a very high reliability. Their energy densities have also been improved by as much as 50% since the 1950's. However, the overall energy density remains low at around 35 to 50 Wh.Kg^{-1} of material [71].

Lead acid technology performs poorly in low temperatures. Therefore they require advanced thermal management systems when used in large volumes. Nevertheless, a good management system and optimised charging regime will enable modern lead acid battery systems to withstand up to 10 years of continued use. In contrast to the other storage technologies, it should be noted that Lead Acid

battery technology at large scales will require a significant quantity of lead. It is known that lead is a poisonous and toxic substance if allowed to enter the environment [43].

When compared to previously listed ESTs and at a large scale, other technologies will not have significant quantities of lead to deal with after the system has reached the end of its working life. Thus lead acid batteries, though a widely accepted technology, have not been as successful in entering the energy storage market as other technologies. This can be seen in Figure 2-5.
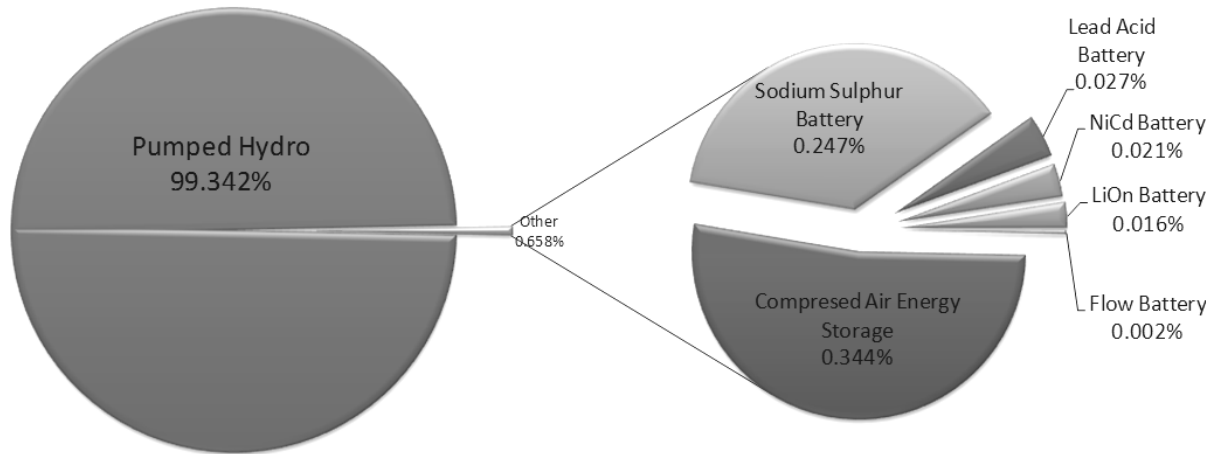
Figure 2-5: Pumped Hydro dominance of existing grid connected energy storage [49]

2.2.3 Sodium Sulphur (NaS)

Sodium-sulphur battery technology operates at an internal temperature of between 300 to $350^{\circ}C$. Batteries that operate at elevated temperatures demonstrate improved performance compared with ambient temperature batteries. However, they do require insulating to prevent rapid heat loss.

Due to the high temperatures of operation a heat source is required which adds an operational overhead to the battery's own stored energy. This partially reduces the battery performance. However, no self-discharge occurs within the battery. This results in an overall efficiency as high as 85% including heat losses [71].

One of the largest NaS battery systems is to be installed within the Shetland Islands power grid as part of a collaborative project led by Scottish and Southern Energy (SSE). The project is known as the 'Northern Isles New Energy Solutions' or NINES project. The NaS battery that is proposed for installation in the Shetland Islands electrical transmission system is to have a 6MWh capacity with a 1MW charge and discharge power capability.

However, safety concerns have arisen in many large scale systems of NaS batteries and they have been taken out of service [44] due to unexplained outbreaks of fire. Additionally the production of these batteries from the world's largest manufacturer NGK has been halted until further notice [45].

When compared to other technologies discussed in this chapter the NaS battery has potential to offer the scale and density of energy storage needed for electrical network energy management. However, due to the ongoing safety concerns around the quantities of highly reactive sodium used within NaS batteries, many of the other technologies would seem to provide a safer alternative. Even if manufacturers of NaS battery technology declare a newer safer version of the NaS battery to be available, it is likely to take several years of work before the industry confidence rebuilds.

2.2.4 Flow Batteries (RFB)

Flow Batteries, or Redox Flow Batteries (RFB) as they are also commonly known, store energy in the form of two electrochemical electrolytes. Energy is realised by flowing the electrolytes through a cell stack. The cell stack converts the stored energy in the electrolytes into electrical power using the redox reduction principle [46].

Recent research has identified that RFB technology has been deployed much faster than the fundamental understanding of the science behind the technology has developed [47]. It was found that the membranes used in the Redox reduction reaction to release stored energy were prone to failure. This represented a significant limiting factor to the large scale uptake and deployment of the technology. In contrast, many of the chemical reaction phenomena in hydrogen EST have been widely applied and understood for many decades [48].

2.2.5   Pumped Hydro Storage (PHS)

Many technologies for the large scale storage of electrical energy are still relatively undeveloped, with pumped hydroelectric energy storage as the one notable exception to this.   As shown in Figure 2-5, presently pumped hydro systems account for over 99% of all grid-connected energy storage systems [49].

Pumped hydroelectric requires two water reservoirs. These are separated vertically to enable high flow rates between upper and lower reservoirs to generate significant power levels. During off-peak hours, water is pumped from the lower reservoir to the upper reservoir. To release energy, the flow is reversed to generate electricity as water flows from the upper reservoir to the lower reservoir through hydro turbines.

However, increasing storage capacity significantly using pumped hydro-electric is unlikely to be feasible. It requires specific geographic circumstances in order to create the large water reservoirs necessary to store renewable energy over longer time periods [50]. To reduce the need for two water storage reservoirs, ideas have been developed to use sea water as the main reservoir. However, to date only one such system has ever been built [51]. For this system the elevated reservoir is built on land, where sea water is pumped up to it during low demand periods. This is then released back to the sea during high demand periods through hydro turbines generating electrical power.

2.2.6   Compressed Air Energy Storage (CAES)

Compressed Air Energy Storage (CAES) is another potential option, and the only other mainstream mechanically based energy storage. However, in common with hydropower, it requires suitable and stable geographical conditions for large-scale energy storage. Low energy density associated with CAES also restricts the extent to which it can be exploited [71].

Small-scale CAES systems can use high-pressure cylinders to store compressed air. However heat generated during compression must also be stored for use in expanding the air. If waste heat is not recovered during compression, the additional heat required for warming expanding air during energy

release negates its stored energy. In addition, industry analysis's predicts that CAES will ultimately be partially or completely replaced by hydrogen [52] technology in the medium to long term. Furthermore, CAES does not have the flexibility of end use that hydrogen energy storage has the potential to deliver. For instance hydrogen energy storage technology has been demonstrated for use in many applications [53], while CAES is restricted to grid connected application with gas turbines.

The numerous applications of hydrogen as an energy vector (transport, stationary generation etc.) provides a unique opportunity for the wide spread use of hydrogen as an energy storage technology. The opportunity that this versatility can bring is described in the following section.

2.3 Hydrogen Storage

Storing energy over long periods of time requires a stable storage medium, which can be scaled up and which is not subject to restrictions on its location. Additionally the storage mechanism should not have a high rate of self-discharge or degradation in performance. Chemical storage in the form of hydrogen (either as gas or liquid) has the potential to meet all of these requirements.

2.3.1 The Global Opportunity Hydrogen Presents

Hydrogen can be stored for long periods of time without degradation. Hydrogen can also be stored in a gaseous or liquid form, or in some instances adsorbed onto a solid form in the case of metal hydride storage technology. Hydrogen is also mixable with other gases making it suitable for mixing into the existing natural gas grid in a process known as sector shifting [54]. Furthermore, hydrogen can be used as a reactive agent in the chemical transformations of synthetic natural gas and fuels. Finally, hydrogen can be used to generate electricity, or to power fuel cell or combustion engine powered vehicles.

As aforementioned hydrogen production systems can be operated as a deferrable and controllable load within a smart grid infrastructure. It can also be used in other energy intensive sectors such as the gas grid, transport as a fuel, and industrial processes. In fact, larger industrial and commercial users can play a vital role in balancing the electrical network through the intelligent use of their

electrical loads for different processes. One significant example of this has been demonstrated in the Tessenderlo Groups chemical processing activities [55]. A vital component in their chemical production is both oxygen and hydrogen gases.

Tessenderlo, utilises one of the world's largest scale electrolysis hydrogen production systems [56, 57] in the order of multiple Mega Watt (MW) scale. To assist their local DNO to maintain the electrical network in a balanced state, Tessenderlo are charged at a lower cost per kWh of electrical energy to allow the DNO to adjust their electrolytic hydrogen and oxygen production. The DNO make these adjustments in accordance with the demands on the electrical network using DSM techniques.

In a concept that is not new [58], Tessenderlo will reduce their hydrogen production when the electrical network is experiencing a period of high demand and low energy production. Conversely they will increase their hydrogen production when generation on the electrical network is in excess of consumption. This trading arrangement with a preferential tariff minimises the need for the local network operators to waste money on highly inefficient and wasteful rolling reserves. In this example both hydrogen and oxygen gases are used in chemical processes.

The above Tessenderlo hydrogen production example demonstrates that hydrogen technologies can be used for balancing the grid. As this is not new, hydrogen is in a strong position to be applied widely as an energy storage vector for balancing the grid.

Hydrogen is seen by many energy industry experts as a means to store surplus renewable energy from sources such as wind, solar, wave and tide [59, 60]. It has also been shown to have market potential for vehicle fuelling stations in both urban and remote rural areas [61, 62].

It is important to note that over the last decade, several renewable hydrogen concepts have been investigated [63, 64], and a number of installations have been implemented. Many have been based around small-scale wind turbines of only a few tens of kilowatts. Exceptions to this in recent years are the Hydrogen Mini Grid System (HMGS) in Rotherham, Yorkshire [65, 66], the Utsira (Norway)

energy system [67] and the Hydrogen Office [68] where large scale RES have been utilised. All these systems use commercially available alkaline electrolysers with rated hydrogen production capacities in the range of 0.2 to 10Nm^3/h and operating pressures in the range of 7 to 20 bar. An important exception to this was the PURE Project (3.5Nm^3/h, 55bar prototype). These systems have been specifically designed to demonstrate energy storage in the form of hydrogen to balance supply and demand on constrained grids.

Research recently published by LUX Research [69] indicates that grid connected energy storage market will have a value of 117bn US dollars by 2017. They also indicate that constraints will develop on the supply and availability of storage technologies by this time, limiting market opportunity. As can be seen, hydrogen has a degree of flexibility not available in other energy storage technologies. It is not geographically restricted and offers the potential to shift constrained renewable generation into other energy intensive sectors. It is clear that as governments around the world are strategically moving towards a low carbon economy, hydrogen storage will undoubtedly play an important role as a solution to make use of grid constrained 'green' energy [70] within a rapidly growing market.

2.3.2   Hydrogen Limitations

Regardless of the apparent benefits and potential that hydrogen energy storage technology presents, there are two significant limitations that exist. These are related to high capital cost and low turn around efficiency [11, 71] (electricity to hydrogen stored then back to electricity).

Furthermore, the storage of bulk quantities of hydrogen is still limited by the extremes of pressures and temperatures required to store significant quantities in a low volume. The storage technology is still also heavy in weight and limits the range of hydrogen as transportable fuel in Fuel Cell Electric Vehicles. None the less these issues are being addressed with the introduction of lightweight and high pressure composite material vessels. However, there is currently a lack of legislative framework in many countries to allow these new composite tanks to be used in transport applications [72]. In addition to this there is requirement to develop appropriate financial mechanisms to encourage the use of the technology. These financial mechanisms should interleave with present mechanisms that currently only exist for a short time period (as limited grant funding). In fact, it is said that the best method could be to develop a mechanism similar to the Feed in Tariff for renewable energy [73].

Nevertheless, significant efforts are being made by industry to lobby for financial mechanisms and address cost and efficiency concerns. In addition, many countries have started the process of publishing draft guidelines for the use of hydrogen energy storage technologies [72]. Despite the lack of a financial mechanism, the existing technology can already be used effectively in niche areas today if implemented in the appropriate manner.

However, in order to achieve an effective implementation of HEST, there is a need for effective HEST Modelling techniques. This is especially important where hydrogen energy storage systems are operated in combination with variable RES. In fact, the International Energy Agencies task 18 hydrogen working group (as discussed in chapter 1 section 1) has identified that such tools and models are not readily available, and this is restricting the wider implementation and deployment of hydrogen technologies.

Therefore this research develops a new application of modelling techniques that will support the deployment of hydrogen ESS. This will in turn support the wider deployment of RES, and help stabilise the grid. This research work proposes the following;

1. Levelised cost modelling to identify the most financially competitive application of HEST for grid balancing
2. Deterministic model for initially sizing a hybrid renewable hydrogen energy system (HRHES)
3. Analysis of the impact that thermal transients have on overall hydrogen production in a HRHES
4. Cascade refuelling station replenishment dynamics when used with constrained renewable generation

2.4 Summary

This chapter has shown that despite improvements that have been implemented into the electrical networks through the application of Smart Grids, VPP and DSM, there is still a need to increase electrical grid capacity. This can be achieved through the application of energy storage, with a market estimated to be worth $117 billion USD by 2017 [69].

It has been illustrated that energy storage methods such as batteries have been used at large scale. They offered the benefit of being much less geographically restrictive than PHS and CAES. However, this type of EST is only realistic for short duration energy storage (as depicted in Figure 2-4). Unfortunately, battery energy storage tends to require very large sized facilities containing many tens of thousands of battery cells. They also need substantial associated control and safety equipment. It has also been seen that the high number of electrochemical battery cells requires significant safety management of the incorporated toxic chemicals and heavy metals, to protect the environment.

More advanced high capacity Battery technology, such as NAS, have some significant safety concerns to overcome before they are to become usable. In addition mature technology such as pumped hydro is highly dependent on local geography. Whilst it currently accounts for over 99% of existing grid connected storage capacity, future development opportunities are likely to be restricted due to their being a limited quantity of suitable sites. The same is also true for compressed air energy storage. As CAES is relatively new in comparison to pumped hydro, its application is significantly restricted by geographic constraints.

It has been concluded that energy storage employing hydrogen technologies is best suited for use with renewable energy. This is achieved through the absorption of surplus energy (for example when renewable energy production is greater than consumption) via electrolysis. Hydrogen created by electrolysis can then be stored in the form of compressed gas to be later re-used in many different applications such as:

- Controllable generation reserve via Fuel cells and/or gas turbines and/or Internal combustion engines (ICE)
- Fuel for transport applications
- Means to transfer renewable energy into the gas grid
- A chemical process gas for food, fertilisers, etc

Furthermore, it has been shown that when taken within the context of Smart Grid, electrolysis can offer the additional benefit of becoming a deferrable controllable load using DSM and VPP techniques. This can further boost the potential benefit that a Hydrogen Energy Storage System (HESS) can bring to a constrained electrical network.

Evidence has been provided to illustrate that the adoption of HEST has been significantly restricted due to high costs and limited modelling tools.

In conclusion this thesis supports the deployment of hydrogen energy storage technologies through new hydrogen energy storage modelling techniques that allows;

a) Identification of the niche applications of hydrogen energy storage technology that are nearing financial competitiveness
b) the initial sizing of a hydrogen system
c) the utilisation of stored hydrogen as transport fuel to facilitate the use of grid constrained renewable energy

3

3   Financial Competitiveness of HEST

Chapter two has shown that there is a need for modelling tools to support the uptake of hydrogen energy technologies. The first step identified to support this uptake, is to investigate the financial competitiveness of a hydrogen energy storage system. As such, there is a need to define when, and under what conditions, a hydrogen energy storage system will attain financial competitiveness.

This chapter is therefore aimed at investigating the different techniques currently available to analyse the financial competitiveness of an energy storage system. It then proposes a new financial model that can be applied to capture the full economic potential of a hydrogen energy storage system. Finally, a comparison versus other EST's is made.

3.1   Financial Competitiveness Background

In general, EST is only compared in terms of lifetime, efficiency, energy density, power density, and technological-maturity [74].   Often these technologies are compared on the basis of application-specific benefits and specific characteristics of interest [75-76]. However these do not take into consideration their financial competitiveness.

Different methods can be employed for analysing the financial competitiveness of energy storage technologies. The idea behind these methods is to define the price per kWh of stored energy over the lifetime of the energy storage system. This price per kWh determines how much each kWh will cost to store using a specific technology. By understanding and knowing the cost per kWh, it is possible to define how an energy storage system compares financially to other technologies. Therefore, analysing the cost competitiveness of an energy storage technology must be performed prior to any capital investment [77].

Financial models found in literature often focus on the sensitivity to life-cycle cost parameters such as capital expenditure, operating lifetime, storage capacity, etc [78]. This is known as a sensitivity analysis and is relatively simple to implement. It gives useful information on parameter changes that have the greatest impact on an EST financial competitiveness. It does not take into consideration the probability that changes may take place. Nevertheless, recent research has shown that probability can be included in defining the competitiveness of an EST through the application of Genetic Algorithms (GA) [79]. Thus, GA techniques have been used to perform probabilistic analysis to identify the likelihood that cost sensitive changes may take place. In addition, probabilistic models have also been applied to identify the optimal (a) size; (b) capacity; and (c) network connection locations for EST [80] in power grid networks.

Incorporating ESTs into the aforementioned modelling techniques is challenging and require the use of temporal models. This is because it requires a high level of detailed time series data. Such data are required in order to reflect the full effects of intermittent sources combined with EST on system balancing. Therefore, temporal type models can be found to simulate the effects of ESTs application onto the power grid network with respect to time [81]. Unfortunately, temporal models require a significant quantity of detailed time series information in order to perform well. Often, this level of detailed time series data is unavailable for immature ESTs. This leads to a higher level of uncertainty in results obtained making comparison of ESTs financial competitiveness difficult.

As an alternative, however, the Electric Power Research Institute (EPRI) [82] have developed and documented a method that analyses costs associated with grid connected energy storage applications. The EPRI utilises a Levelised Cost Model (LCM) approach to perform a cost benefit analysis for a number of energy storage technologies.

LCM is a method for comparing the annualised cost of power generation. In other words, the Levelised Cost (LC) represents the present value of the 'total cost' of building and operating a power plant. The LC is modelled over the power plants economic life represented as equal annual payments. Costs are levelised in order to remove the effect of inflation. In its most basic form the LC is calculated by dividing the annual expenditures by the annual income, corrected for inflationary effects. The LC therefore reflects a number of capital and operational expenditures. This includes upfront capital costs, fuel expenses, Operating and Maintenance (O&M) charges, financing costs etc.

Levelised Cost analysis is often used in regulatory review and longer term resource planning [83]. This is to compare the costs of different investment strategies and resources against future possible scenarios. In contrast to temporal modelling techniques the calculation of levelised costs can be done using a limited number of input data. This makes them very useful for evaluating the real costs of technologies which have limited operating experience or available data.

The main benefit of LCM is their ability to use a limited amount of input data to determine the cost effectiveness and competitiveness of ESTs. LCM is therefore an essential financial comparison technique when there is a lack of available financial and/or operational data. Therefore if an EST LCM is conducted, it will not perform hourly analysis against market prices or system loads, but instead provide an important indicator of the competitiveness of EST.

To date, HEST have not been included within the annual EPRI analysis [84]. They have also not been included in the other cost analysis modelling as found in literature. HEST appears to be commonly excluded from cost comparative studies largely due to the high capital cost of hydrogen energy storage technology. They have also been excluded due to the comparatively low turn-around efficiency that HEST has in comparison to other bulk ESTs. Conversely, studies that examined HEST have not included the additional revenue streams that HEST can derive. Recent work completed by the National Renewable Energy Laboratories (NREL) has introduced the value of grid connected stored hydrogen for transport applications [85]. Whilst this builds upon the work of EPRI, it unfortunately has not investigated the potential value of by-product Oxygen gas from electrolysis. If the by-product oxygen gas is included it should have either a positive or negative effect on the cost competitiveness of HEST.

Therefore, this chapter proposes a new LCM to explore the additional financial benefits that can be derived from HEST and are not available from other ESTs. This includes the potential to sell hydrogen as a gas (for example to be used in transport, chemical processing or power to gas applications) as well as the by-product oxygen gas. As such, in contrast to existing methods, the additional value of the by-product oxygen is also investigated.   The additional hydrogen and oxygen gas revenue streams are compared to the typical energy-in -> energy-out approach for energy storage cost modelling.

3.2   Competitive Opportunity

As afore mentioned, the financial competitiveness of HESTs often only considers the value of the stored energy at the time it is released onto the electrical grid. HEST is often excluded from cost comparative studies due to its high capital cost. In addition the comparatively low turn around efficiency that HEST has in comparison to other bulk energy storage technologies places it at a disadvantage to more mature grid connected energy storage.

However, hydrogen as an energy storage mechanism has the ability to store surplus RES electrical energy for re-use as electricity. It also offers the potential to sell both hydrogen and oxygen gases as commodities.

As discussed previously hydrogen gas has the potential to be used either directly as a chemical process gas, or to shift grid constrained RES into other sectors such as the gas grid, or as transport fuel. Figure 3-1 illustrates the differences between traditional energy storage systems and hydrogen energy storage.
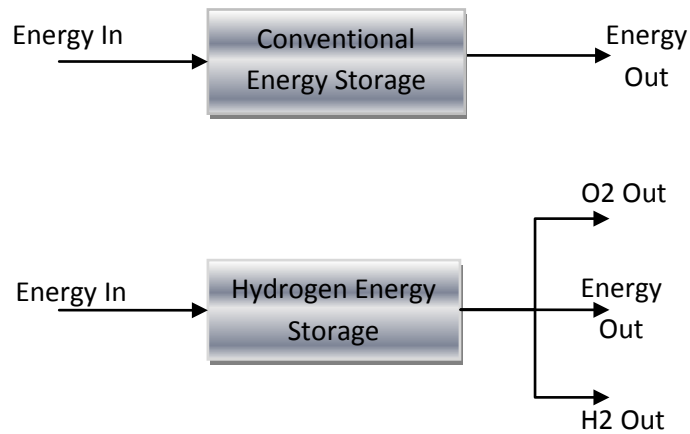
Figure 3-1: Comparison of conventional EST and HEST

As shown in Figure 3-1, hydrogen energy storage systems can realise three possible revenue streams. This is in contrast to conventional energy storage systems where there is only one possible revenue stream. Conventional network-connected energy storage systems allow for energy to be stored and released in the form of electrical energy only. On the contrary, hydrogen energy storage provides a unique opportunity for extra income from two further outputs. It is these additional income streams that have the potential for hydrogen energy storage systems to offer greater financial competitiveness. By applying the two new income streams, it is reasonable to envisage that the low energy efficiency and high capital costs associated with an HEST system could be offset. This highlights the need for a new HEST financial competitiveness model. The developed model is presented and investigated in the following sections.

3.2.1 Context for a new HEST model

The UK power grid system is selected as a case study in order to investigate the new HEST financial competitiveness model.

3.2.1.1 The UK power grid situation

In the UK, wind farms over 5MW in size receive Renewable Obligation Certificate (ROC) income valued at around £55 per MWh [86]. However, the recent increase in renewable energy generation onto electrical infrastructure has resulted in a loss of traded energy. This is because generation is constrained off-grid to maintain electrical network stability [87]. The implication for renewable

energy generators is that if no mitigating measures are taken, then the value of their energy will fall. This is due to the insufficient demand to absorb the excess in their energy production.

However, it is important to note that the value of energy constrained off grid is not lost to the generator. In the context of the UK energy market, compensation payments are made to the generator whose energy is constrained. However, the value of these constraint payments is considered to be very high for renewable generation. This is widely publicised and summarised in the Renewable Energy Foundation (REF), "Scottish wind power constraint payments update". For instance, the average constraint payments that have been recorded between the 30th May 2010 and 16 June 2011 were £215 per MWh. During the same time period 23,747 MWh of renewable energy were constrained off-grid. Therefore, in this single example, the total cost for constraining RES generation off-grid was £5.1m.

Further to this, since the REF started collating publically available data on constraint payments, their records indicate that a total of 383 GWh of RES have been constrained off-grid between the 30th May 2010 and the 11 of October 2013. This adds up to a total cost over £43m in reimbursement payments to RES generators for lost revenue through the sale of their electricity and their subsidies. A summary of these data is presented in Figure 3-2. It should be noted that the REF data published do not include private contracts signed with RES generators outside of the balancing mechanism (BM) system operated on the UK national grid.

UK Grid constrained RES and associated Cost
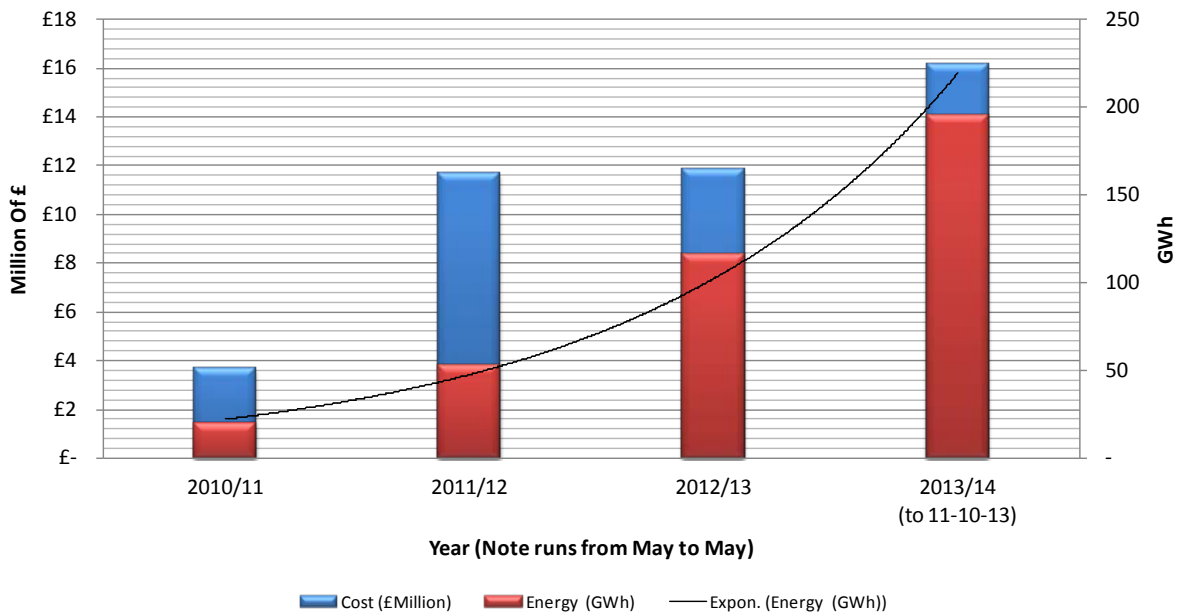
Figure 3-2: UK Grid annually constrained RES data and associated cost [88]

It can be seen in Figure 3-2 that since RES constraint payments has begun in 2010, the annual constrained RES is increasing at an exponential rate. Worryingly, the constrained RES energy has increased by almost 10 times since constraint payment were introduced in 2010 until 11th October 2013 (from approximately 19GWh to 190GWh). Similarly the cost of constraint payments has also increased in the same period by almost 4 times. Industry experts widely agree that the level of constrained RES will continue to rise as the UK power grid network moves towards its 2020 targets for renewable generation. [89]

The planned increase in annual RES generation of 11TWh by 2016 will further stretch the existing electrical power grid [90]. Therefore, there will be a significant requirement to increase the capacity of the electrical power grid through the integration of EST. Conventional EST will initially resolve the balancing issues, so that integration of new RES will run smoothly. However, it is foreseeable that there will be a time where the conventional ESTs will run out of capacity to store surplus RES. As such, it is understood that conventional energy storage technologies will become difficult to integrate onto the grid, hence restricting the uptake of RES. Thus, there will be a need for a flexible storage technology for absorbing large scale energy in a form that can be used in other applications. Due to the increasingly constrained RES, it can be seen that there is a need to investigate the

competitiveness of EST in general and HEST in particular. Therefore, in common with global RES constraints, the UK context leads to the need for a new financial competitiveness model for HEST.

In the following section the detailed application of the proposed LCM, that allows comparing the competitiveness of different HEST configurations, is given.

3.3 Proposed Levelised Cost Model (LCM) for HEST

The costs of energy storage are considered using a levelised cost of ownership approach. The capital costs of an energy storage facility are typically expressed as £/kW installed. This cost includes all expenses involved in the purchase and installation of a facility. The £/kW capital expenditure (CapEx) multiplied by the size of the facility produces the total cost of the project. In the proposed model, all costs relating to an energy storage facility are expressed as (a) total £/kW of usable discharge capacity (in kW) and (b) total £/kWh of usable energy storage capacity. Typically EST with a deeper Depth of Discharge (DoD) and higher turn-around efficiency will have a lower unit cost of usable power (kW) and energy (kWh) [91].

In order to investigate the potential for the existing financial balancing mechanism in the UK grid to facilitate the opportunity to utilise HEST there is a need to examine an arbitrage style scenario. This scenario assumes that the energy stored in the EST is purchased at the Renewable Obligation Certificate (ROC) rate. Energy sold from the storage is done at the difference between the ROC and the constraint payment value.

Taken from the example given in the previous section, the RES generators are rewarded £55/MWh of generated energy. Instead of constraining the RES off-grid as is presently done, the energy that otherwise would be lost is diverted to energy storage. Therefore the cost of the electrical energy for filling the energy storage system (EC) can be considered as £55/MWh for this case study.

Conversely, the price for selling electrical energy is considered as the difference between the costs of RES generation (i.e. the ROC payment) and the cost of the constraint payments (£215/MWh – see

previous section). Therefore, the difference, or potential selling price, for electrical energy output (EO) from the storage system can be considered as £160/MWh (where; EO = constraint payment – ROC payment = £215/MWh-£55/MWh = £160/MWh).

A Levelised Storage Cost (LSC) for a conventional grid connected energy storage systems can then be expressed using equation 5-1 [92].

$$LSC = \frac{\sum_{t=1}^{n} \dfrac{ISC_t + SOM_t + EC_t}{(1+r)^t}}{\sum_{t=1}^{n} \dfrac{EO_t}{(1+r)^t}}$$

(5-1)

Where: ISC_t = Invested Storage Capital in year (t)

SOM_t = Storage Operation and Maintenance costs in year (t)

EC_t = input energy cost (t)

r   = Annual discount rate (typically 10%) [93]

EO_t = Value of released energy in year (t)

However, Energy storage developed around hydrogen technology will have additional revenue potential. This can be realised in the sale of both hydrogen and oxygen gases as a commodity. A new equation can therefore be developed to include H_{2t} and O_{2t}. The H_{2t} and O_{2t} in this case are the realisable value of both hydrogen and oxygen gas in year (t). The new levelised cost of HEST can then be expressed as shown in equation 5-2.

$$LSC = \frac{\sum_{t=1}^{n} \dfrac{ISC_t + SOM_t + EC_t}{(1+r)^t}}{\sum_{t=1}^{n} \dfrac{EO_t + H_{2t} + O_{2t}}{(1+r)^t}}$$

(5-2)

Where: ISC_t = Invested Storage Capital in year (t)

SOM_t = Storage Operation and Maintenance costs in year (t)

EC_t = Input energy cost (t)

r   = Annual discount rate (typically 10%)

EO_t = Value of sold energy in year (t)

H_{2t} =Value of sold hydrogen gas year (t)

O_{2t} =Value of sold Oxygen gas in year (t)

3.4 HEST Scenario Analysis

To investigate the HEST financial competitiveness, five possible scenarios for hydrogen energy storage systems have been developed and compared. Levelised costs have been calculated for each scenario using equation 5-2. In each scenario, the energy storage system is operated within the context of grid constrained RES. As such, in simulating these 5 scenarios for the case study under consideration, the energy cost (EC) has been taken as £55/MWh, and the energy output cost has been taken as £160/MWh. The quantity of constrained RES available for storage was taken from section 3.2.1, and is quantified as 23,747MWh. Outlined below a further description of the proposed five scenarios,

Scenario A. No Fuel Cell (FC) - (no energy sale), 100% O_2 & H_2 gas sold

Scenario B. 100% energy sale using 3MW FC, 100% O_2 sold, no H_2 sale

Scenario C. 50% H_2 sold as Energy through a 3MW FC, 50% O_2 & H_2 gas sold

Scenario D. No FC - (no energy sale), No O_2 Sold, 100% H_2 sold

Scenario E. 100% Energy sold (3MW FC), no O_2 nor H_2 sold

The proposed levelised cost model does not consider detailed timing of surplus power and energy availability. It proposes a 3MW electrolyser to absorb the constrained RES in all scenarios listed above. On the other hand, a 3MW fuel cell is proposed in scenarios B, C, and E to release the stored energy back to the power grid network. Furthermore, pressurised bulk storage tanks capable of storing 36MWh of energy (this equates to 12hrs of fuel cell operation at full power, and it will take 12 hrs of electrolyser operation to fill the tank from empty) is proposed for storing the hydrogen produced.

In scenario A, the electrolyser produces hydrogen and oxygen gas which are sold directly as gases.

In scenario B, the energy stored in the form of hydrogen gas is injected back to the power grid network via the fuel cell. At the same time the by-product oxygen gas is sold.

In scenario C, 50% of the hydrogen produced is sold as gas, while the other 50% is sold as energy via the fuel cell. In addition, 50% of the oxygen is sold as gas and the remaining 50% vented to the atmosphere.

In scenario D, 100% of hydrogen gas is sold (no sale of Oxygen and no sale of electrical energy). Finally, in Scenario E all the stored hydrogen is sold as electricity back to the power grid with no oxygen being sold. For the avoidance of doubt, both scenarios D & E do not utilise any by-product oxygen gas.

For each scenario, the Capital expenditure (CapEx) and Operational Expenditure (Opex) data used is shown in Table 3-1

CapEx & OpEx Data	
Hydrogen CapEx	
Electrolyser (£/kW)	£ 2,500.00
Storage (£/kWh)	£ 27.00
Fuel Cell (£/kWh)	£ 4,000.00
Hydrogen OpEX	
Electrolyser (£/kW)	£ 50.00
Storage (£/kWh)	£ 2.00
Fuel Cell (£/kW)	£ 100.00

Table 3-1: Hydrogen technology capital and operational data [94]

Table 3-2 summarises the market value for hydrogen and by-product oxygen gases.

Market Data	
O_2 Sale (£/Tonne)	£ 3,000.00
H_2 Sale (£/Tonne)	£ 5,000.00

Table 3-2: Market value for Oxygen and Hydrogen gas [94]

The LCM simulation results for the 5 scenarios, calculated using equation 5-2, are given in Figure 3-3. Results show that the most financially competitive configuration for the hydrogen energy storage system can be realised in scenario A. Additionally a favourable result is also seen in Scenarios B and

C. The least competitive configuration is seen in scenario E. Though hydrogen has a high financial value when sold as a gas, scenario D demonstrates that it is not competitive on its own.
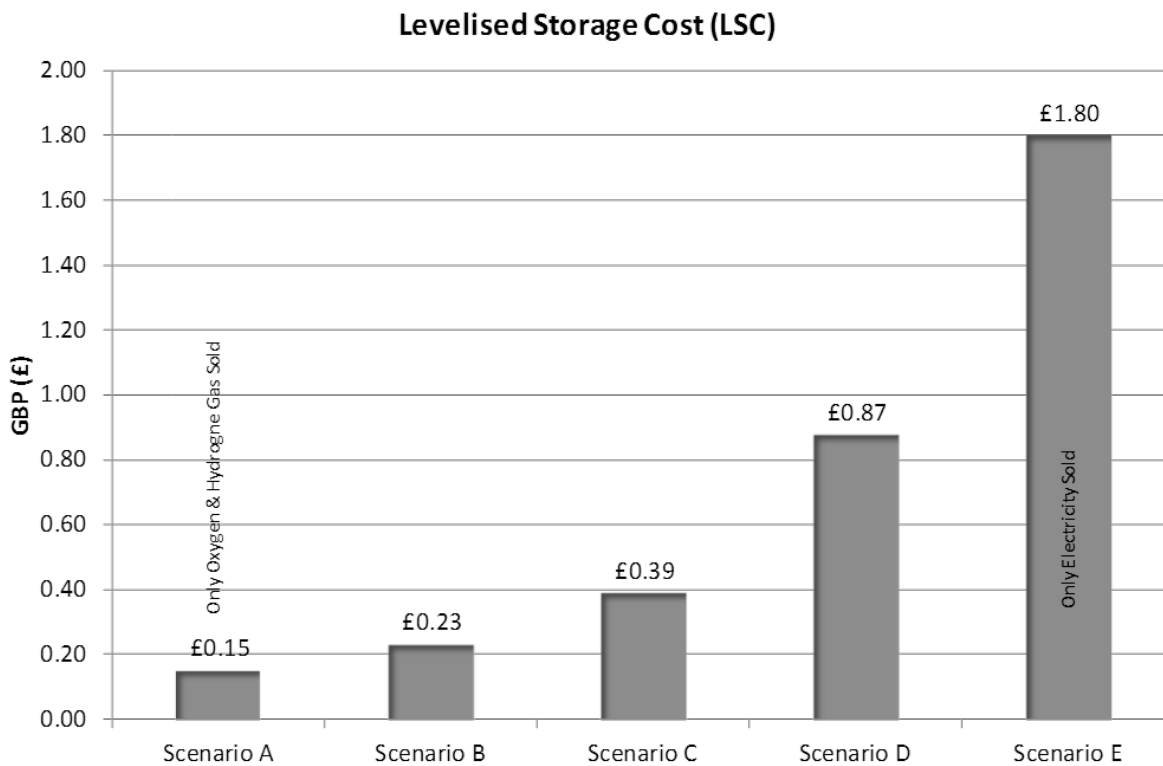
Figure 3-3: LCM simulated output costs for HEST scenarios

Research conducted by NREL [95] has shown that conventional energy storage systems exhibit levelised costs as summarised in Table 3-3. For comparison purposes, these levelised energy storage costs are illustrated in Figure 3-4 alongside the hydrogen energy storage scenario results.

Technology	Levelised storage cost
NiCd Battery	£ 0.52
NaS Battery	£ 0.16
Redox Flow Battery	£ 0.17
Pumped hydro	£ 0.08
CAES	£ 0.06

Table 3-3: Levelised costs of other energy storage technology [95]
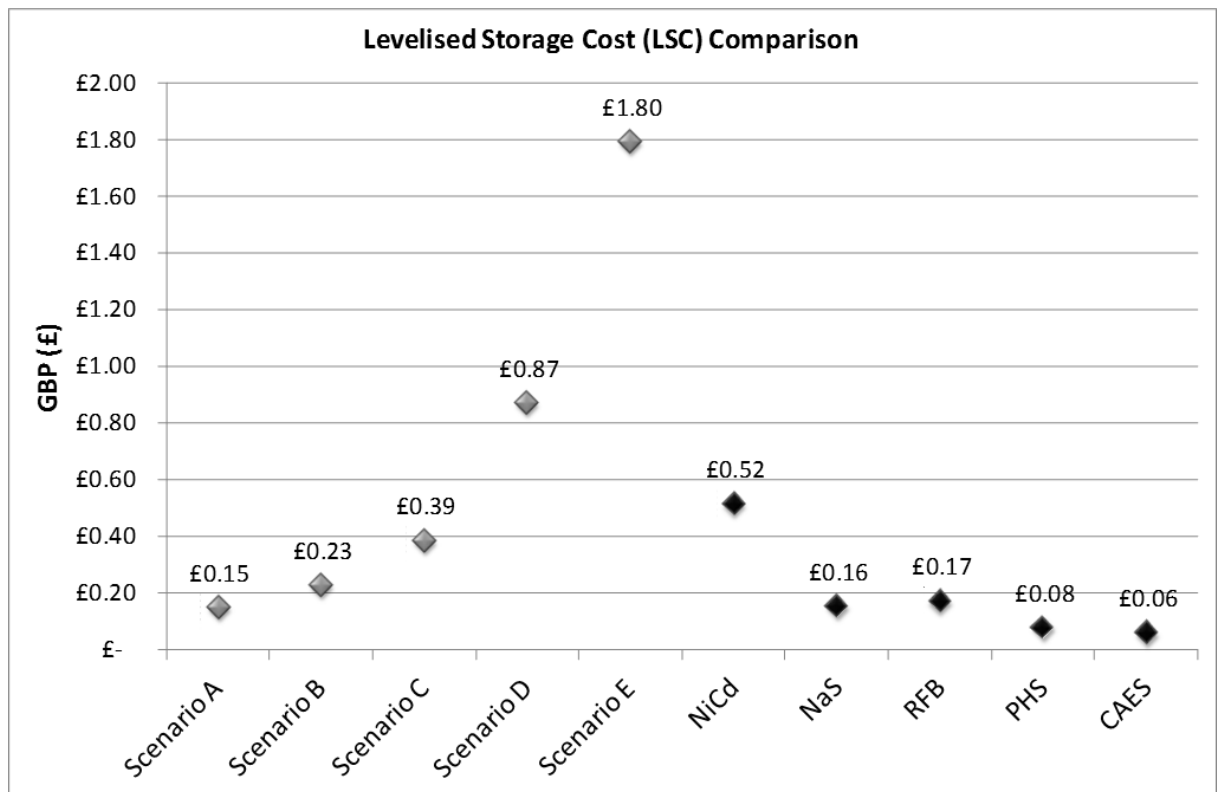
Figure 3-4: Levelised cost comparisons

The non-HESTs are represented in Figure 3-4 by the black diamonds. The values displayed are the values for the technologies when used in a grid connected energy arbitrage scenario. It can be concluded from Figure 3-4 that CAES and PHS are more cost competitive than the proposed five hydrogen scenarios. However, HEST when used in conjunction with by-product oxygen sale can compete with NaS and RFB technologies. Additionally, HEST also competes with NiCd battery technology when only 50% of the oxygen is sold, and the hydrogen is equally divided between hydrogen gas sale and electrical energy sale. Therefore this shows that HEST can be competitive in three different scenarios when compared to other EST. However, it can also be seen that when HEST is used for the storage and sale of electrical energy only (scenario E), it becomes un-competitive against the existing EST. Furthermore, it can be concluded that the sale of H_2 on its own (scenario D) without the sale of by-product O2 is currently not competitive. Finally, the LCM model has shown that there is still a need for either the reduction in CapEx or the increase in turn around efficiency of HEST to become more financially competitive. If these can be achieved then hydrogen could become a mainstream energy storage mechanism.

3.5   Conclusion

A financial competitive assessment of HEST has been conducted within the example of constrained RES from a power grid network. It has been found that whilst there are many examples of financial modelling techniques available, it is difficult to obtain the appropriate level of detailed input data required to compare HEST against other EST options. Furthermore, it has also been found that whilst detailed cost analysis has been conducted for HEST in traditional cost arbitrage markets, many do not consider the energy stored in the form of hydrogen as an output product. Moreover, no model in literature has included oxygen as a potentially valuable by-product from the electrolytic hydrogen production process, to support the uptake of HEST.

Using the proposed LCM in five scenarios, it has been shown that hydrogen used as an energy storage mechanism has the most potential where the oxygen by-product is sold. The oxygen by-product value has been introduced into the LCM through the proposed equation 5-2. The best scenario is achieved when by-product oxygen is sold and hydrogen gas is also sold as a high value commodity for other applications such as sector shifting to transportation fuel, gas grid or other chemical processes.

It has been further shown that within the existing balancing mechanism of constraint payments in the UK power network that HEST does not perform competitively in an energy arbitrage model. This is largely due to the comparatively low turn-around efficiency for electrolysis of constrained RES, storage as hydrogen gas, and conversion back to electrical energy via a fuel cell. Typical turn around efficiency for this process is in the region of 35 % to 40% for HEST, whilst other bulk energy storage technologies such as PHS, CAES, NAS and NiCd have much higher turn around efficiencies that range from 65% to 85%. HEST financial competitiveness is also adversely affected in an energy arbitrage scenario due to its high capital costs.

4

4   Sizing a Hybrid Hydrogen Energy System

This chapter proposes a model for sizing a hybrid hydrogen energy system. In the previous chapter, the financial competitiveness of five scenarios has been discussed. Each scenario took into consideration one application of the hydrogen production and use. The most complex scenario to model is scenario E (from chapter 3) and therefore this scenario will be modelled in this chapter. Scenario E has been considered for developing the sizing model, as it includes a fuel cell for the conversion of stored hydrogen back into electrical energy.

There are numerous examples of analytical models that have been developed for simulating hybrid energy systems. These are generally used with wind/diesel and hybrid energy systems employing battery technology as a renewable energy store. In addition, most of these modelling platforms and tools are for simulating off-grid/stand alone energy systems without any grid connection or network 'backup' or support. Most of the available software and associated models suffer from two main drawbacks; the requirement for a large number of input data (several system size options for wind, solar, diesel, etc.) and the substantial amount of computing resources to dimension a system size.

In this chapter, a novel modelling tool that allows the sizing of a hybrid renewable hydrogen energy system (HRHES), with the minimal amount of input data and computer resources, is proposed. This tool has been developed by utilising the individually developed Matlab/Simulink models of the proposed HRHES components (i.e. the RES (wind and PV), electrolyser, H_2 Storage and the fuel cell). Each component developed model is detailed in Appendix A.

4.1 Sizing Methods

There are many sizing methods available for sizing a HRHES, each with their associated benefits and drawbacks [96, 124]. These can be categorised into two main categories:

- Commercial software
- Standalone modelling techniques

Each of the above two categories is discussed in the following sections.

4.1.1 Commercially Available Software Tools

Commercially existing simulation tools are commonly used for evaluating the performance of hybrid renewable energy systems, typically before anything is built. Using such tools enable the comparison of different systems by manually entering alternative configurations to identify the best one. Whilst looking into the potential software tools, it has been found that many are not capable of simulating HRHES. These tools included, EMCAS, EnergyPLAN, energyPRO, GTMax, IKARUS, Invert, MiniCAM, NEMS, ORCED, PERSEUS, ORCED, PERSEUS, PRIMES, ProdRisk, RAMSES, RETScreen, SIVAEL , STREAM, WASP and WILMAR [96, 124].

However, a small number of software tools have been found able to simulate hybrid renewable energy systems incorporating HEST. Among these, the most commonly used software in modern literature is HOMER (from National Renewable Energy Laboratories (NREL)).

HOMER offers several HRHES component models including PV, Wind, Hydro, Batteries, Fuel Cells, Electrolysers, Grid connections etc.   To work effectively the software requires a number of initial input data including energy resources, technical and economic constraints, energy storage

requirements and control system strategies. Also required are details of the component types, Capex, Opex, operational life, efficiency etc.

The advantage of Homer is that it can take all of the financial and economic constraints of a project, and produce an energy system that that can fit within those constraints. However, this advantage can also be a drawback. Unfortunately, in the majority of early HEST system development, most of the required HOMER input data is not available. Also in the very early stages of a project, there is a need for a rapid initial system sizing that meets the technical requirements. Unfortunately, this cannot be performed easily using HOMER unless major assumptions are made, leading to the potential for inaccurate results.

In common to HOMER, a few other available commercial software packages have been found that are able to simulate HRHES. These included BALMORAL, H_2RES, ENPEP-BALANCE , HYDROGEMS (Now incorporated into Transys16), SimREN and UniSyD3.0 [96,124].

UniSyD3.0 has been found able to simulate hydrogen production but unable to simulate hydrogen storage. Additionally SimREN is not available for use outside the Institute of Sustainable Solutions & Innovations, however literature detailing the model use identifies the requirement for a significant amount of input data (for example, weather data from 153 weather stations) covering large geographic areas [97].

On the other hand, although Hydrogems (now incorporated into Transys16) does detailed simulation of HRHES, it is not capable of sizing an energy system. The user is required to manually enter the details of each component in the HRHES once the system component sizes are known. In common with Hydrogems, H_2RES also requires the user to manually enter known system sizes before the performance of a system can be simulated. The same is also true for ENPEP-BALANCE and BALMORAL. In addition, BALMORAL and ENPEP-BALANCE also require detailed information about the existing electrical infrastructure that is already in operation.

4.1.2 Stand-Alone Modelling Techniques

In addition to the commercially available software, there are a number of intelligent techniques that have been investigated in literature for automatically sizing a HRHES. The most commonly used modelling techniques are:

- Genetic Algorithms (GA)
- Particle Swarm Optimisation (PSO)
- Simulated Annealing (SA)

Each of the above techniques is described in the following sections while illustrating their strength and weaknesses.

4.1.2.1 Genetic Algorithms (GA)

Genetic algorithm is a process of optimisation based upon the observed genetic process of biological organisms. GA mimics this process to offer potential solutions to a complex problem. The concept was first proposed in 1975 and has been widely utilised in many applications.

A GA sizing process provides an iterative method aimed at finding the best solution of a given problem. A GA utilises user defined operators until a predefined termination criteria or maximum iteration number is reached. Input data to a GA based algorithm for sizing a HRHES could be for example weather (resource) conditions and load demand.

Constraints are also added to a GA in order to define the boundaries of analysis. An example of a constraint in HRHES might be limiting the number of wind turbines installed on a specific land area constrained by geographic boundaries. Constraints can be defined based on the type of application in order to retain the returned solutions within real-world limitations.

A fitness function (for example, ability to provide power and energy within a pre-defined set of parameters) must also be entered as a defined input to a GA optimisation algorithm. The fitness function acts as a measure of possible solutions suitability to meet the required output constraints. Both the fitness and constraint definitions are known as "operators". In addition, operator values must also be entered for the rate of mutation of the genetic algorithm.

Parameters for GA operators, such as the rate of mutation and percentage of selection, require to be provided by the user before a GA-based sizing algorithm is started. A GA typically consists of five basic components. These include an initial random population generator to start the process, an evaluation of "fitness" and genetic operators for "selection", "crossover" and "mutation" operations. With a random population generation at the start, GA algorithm offers random sizes for the hybrid energy system components that satisfy the load demand/power generation balance at each step.

The GA begins with a random population created before the algorithm starts. It then provides random sizes for the components of a hybrid energy system that satisfy the fitness requirements that have been defined. This could be for example the ability to satisfy the requirements for a load demand and maintain a power/generation balance. The selection parameters (or operator as it is commonly known) select the pre-defined percentage of the initial population based on their fitness value.

Advantages of the GA include the ability to exit from a local minimum situation through the use of the mutation operator and the ability to find global system optimum if the criteria given is of a good enough quality. Another significant advantage of a GA is its ability to code an infinite number of system parameters. This makes it particularly suited to a sizing algorithm for a hybrid renewable energy system. In particular systems that are comprised of more than 3 components, such as a PV, Wind, Hydro, Battery, Diesel system as those used in many island and off grid communities. This ability to optimise many parameters is a capability that is not easily found in other techniques. Nonetheless, one of the most significant drawbacks to a GA is that it is much harder to code in software compared to other techniques due to its highly complex structure. In addition as the number of parameters to optimise becomes larger, the complexity increases and the computational time and resource requirement of the GA increase significantly. [96]

Due to the previously discussed advantages that a GA inherently presents, GA's has been used widely in several energy system optimisation projects. There are a number of published articles [98-101] that utilised the GA in order to identify the optimum size of a hybrid energy system. Additionally, investigations have been completed using GA as the mechanism to find optimal component sizing for hybrid renewable energy systems [102-106]. However, it should be noted that none of the references found in recent literature has appeared to utilise GA for the sizing of HRHES components in

conjunction with a renewable energy source. Instead many studies examine the optimal sizing of a fuel cell backup generator supplied by fuel from an external source (e.g. bottled gas supplied to a site derived from a hydrocarbon resource).

4.1.2.2   Particle Swarm Optimisation (PSO)

Particle swarm optimisation is a technique that is based on the intelligent movement of swarms. It belongs to a group of optimisation techniques known as Evolutionary Computational Techniques (ECT). It has been originally developed in 1995 for the analysis of social structures, and since then it has found increased use in engineering related problem solving. PSO's are population based stochastic optimisation algorithms where each potential solution within a PSO population is known as a particle. In a PSO based algorithm, each particle co-ordinates (in an X, Y or X, Y, Z plot) represent a possible solution associated with a position and a velocity vector. Each particle is initialised with a random velocity and is 'flown' thought the search space. During iterations, the PSO particles (potential solutions) move towards an optimum solution through its present velocity, personal best, and global best solution for all particles [96].

Whilst PSO (in common with GA algorithms) is very effective at utilising similar iterative search techniques, the PSO does have some advantages over the GA approach. A PSO involves a concept of using as few equations as possible that are easily implemented in software. This makes the execution time shorter and the memory and processing resource requirement less in comparison to GA. However, a PSO does have a lower reliability of finding the best solution than its GA equivalent. In addition, the PSO is limited to a maximum of three parameters (coordinates) that are defined on a three dimensional X, Y, Z plot. Therefore if a complex energy system comprising of more than 3 components is to be considered for optimisation, it would not be possible to achieve this using a PSO approach and the GA would be more suitable in this case.

Despite this limitation, PSO algorithms have found common use in optimising low component count hybrid renewable energy systems [107-111]. This has included hydrogen production storage and re-use through fuel cells (HEST). However, if PSO were to be considered within the context of a hybrid energy system comprising multiple renewable sources, together with HEST (hydrogen production storage and re-use), alongside with power grid network and load constraints; there would be too many parameters to consider a PSO approach. Therefore, the use of a PSO modelling technique

would not be suited for the initial sizing of a hybrid energy system comprising of more than three elements, such as that in scenario E in the previous chapter.

4.1.2.3 Simulated Annealing (SA)

First introduced in 1983, Simulated Annealing (SA) was a general optimisation technique for solving optimisation problems. SA considers how a cold solid immersed in a hot environment is warmed by increasing the temperature of the environment and then cooled by slowly lowering the temperature of the environment as is done in the annealing of materials. In an SA algorithm, a candidate (a solution possibility) is moved through a random selection of solution possibilities. The move is accepted if it leads to a better solution with improved objective function (similar to fitness in GA and PSO) over the present candidate [96].

The use of SA in hybrid energy system sizing is not as common as PSO or GA algorithms. However, there is an increasing interest in how it may be applied, particularly in the integration of hydrogen technologies [112]. In common with GA's, SA requires a significant amount of processing resource in order to compute the high number of variables that are found in a HRHES. Additional system uncertainty models are also required to be completed before an SA input parameters can be defined, thus making their use HRHES very time consuming and complex.

Therefore, with the previously mentioned limitations of the above tools, it is necessary to explore an alternative method for sizing a HRHES. In the following sections, a description of the proposed model for the initial sizing of a hybrid renewable hydrogen energy system is given.

4.2 Why Use a Deterministic Sizing Algorithm

It has been shown in the previous sections that there are numerous available modelling techniques that can be used to define the size of a hybrid renewable energy system. The literature review conducted suggests that the use of a GA based model would tend to provide the best optimisation approach for defining the size of a HRHES. The rationale behind this is that a GA is capable of handling many variables at once, while PSO techniques cannot handle more than 3 variables. The down side of GA based models is their associated high computational resources requirements,

particularly where many variables and possible solutions are available. Alongside this main limiting factor, very complex coding is required to implement an optimisation routine for a HRHES with more than 3 components.

Although GA, PSO and SA methods would be considered to deliver the best result when sizing a hybrid renewable hydrogen energy system, recent research has found that they do not provide the best results for this type of system simulation [113]. In fact, it has recently been documented that the best method for sizing a hybrid renewable energy system with hydrogen energy storage is the application of a simple technical sizing technique [113]. Such a technique can be referred to as being deterministic [114].

The advantage of a deterministic approach is that it can provide very rapid and reasonably accurate [115] system size options. This can be achieved with relatively simple input data that can easily be obtained. The proposed model is therefore based on the development of a deterministic method for the sizing of a HRHES. The proposed deterministic method is described in the following sections.

4.3   Proposed Deterministic Sizing Algorithm

The aim of the deterministic sizing algorithm is to properly size the system components to ensure a reliable electricity supply. Hence, the financial aspects involved with a hybrid renewable hydrogen energy system will not be considered in this algorithm. HRHES components sizing included in this section are based on the integration of solar and wind renewable resources, combined with HEST to meet the demands of an electrical load. An outline of the proposed deterministic algorithm is shown in Figure 4-1:

```
┌─────────────────────────┐
│   Select Wind Turbine   │
│        (Step-1)         │
└─────────────────────────┘
             │
             ▼
┌─────────────────────────┐
│   Size supporting PV    │
│        (Step-2)         │
└─────────────────────────┘
             │
             ▼
┌─────────────────────────┐
│    Size Electrolyser    │
│        (Step-3)         │
└─────────────────────────┘
             │
             ▼
┌─────────────────────────┐
│      Size Fuel Cell     │
│        (Step-4)         │
└─────────────────────────┘
             │
             ▼
┌──────────────────────────────────┐
│    Run simulation with no storage │
│              (Step-5a)            │
└──────────────────────────────────┘
             │
             ▼
┌──────────────────────────────────┐
│ Size storage vessel by summing all energy │
│   values not met by renewable source       │
│              (Step-5b)            │
└──────────────────────────────────┘
```
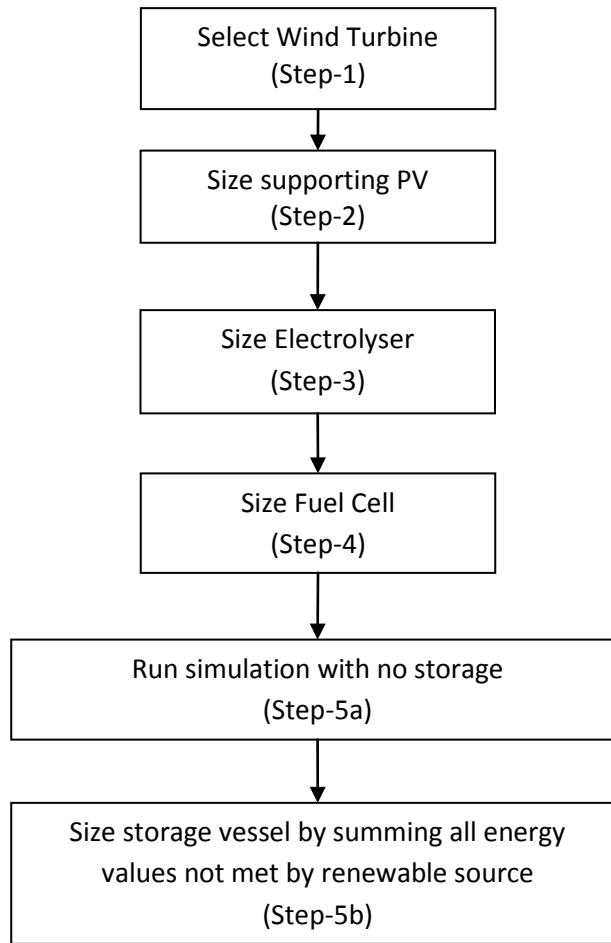
Figure 4-1: Proposed Deterministic Sizing Algorithm

Detailed description of each of the algorithm steps is given in the following sections

4.3.1   Sizing a Wind Turbine and Solar Photovoltaic

The first criterion to investigate in sizing a HRHES is the primary renewable source. The wind turbine here constitutes the primary RES, followed by a photovoltaic (PV) system as the second renewable generation source. Hence, the capacity factor for each technology must first be found.

A wind turbine or PV Capacity Factor (CF) is defined as the average power ($\bar{P}$) output from a renewable device as a percentage of the maximum power output (P).   For a wind turbine the capacity factor (CF_{wind}) is given by equation 4-1. For a PV installation the capacity factor (CF_{PV}) is given by equation 4-2. In these two equations, $\bar{P}_{Wind}$ and $\bar{P}_{PV}$ are the average power output from

the wind turbine and PV respectively, while P_{wind} and P_{PV} are the rated power output from the wind turbine and PV respectively.

$$CF_{wind} = \frac{\bar{P}_{wind}}{P_{wind}} \qquad (4\text{-}1)$$

$$CF_{PV} = \frac{\bar{P}_{PV}}{P_{PV}} \qquad (4\text{-}2)$$

The objective of including the RES generator component (wind turbine or solar) in the sizing routine is to minimize the average difference between load demand ($\bar{P}_{dem}$) and generated renewable energy ($\bar{P}_{gen}$). Typically the duration of the analysis is considered to be 1 year in order to incorporate the seasonal peaks and troughs of demand and renewable generation.

Wind turbine sizes and availability are usually restricted to the unit sizes commonly available in the market. The size steps available are in general 3, 5, 6, 10, 15, 20, 50, 250, 330, 500, 850, 900, 1200, 2200, 3200kW. Therefore it has been concluded that the average power of the turbine ($\bar{P}_{wind}$) should be first selected, such that it is close to the average demand for a defined load ($\bar{P}_{dem}$) as shown in equation 4-3.

$$\bar{P}_{dem} \cong \bar{P}_{wind} \qquad (4\text{-}3)$$

The average power output for the wind turbine is then found by using the annual average site wind speed together with the proposed wind turbine model described in appendix A, (section 9.1).

The second step is then to define the rated power (P_{PV}) of a supporting PV array. The PV array rated power is calculated as shown in equation 4-4. In equation 4-4, P_{PV} is calculated by using the values obtained from equations 4-1 to 4-3.

$$P_{PV} = \frac{\bar{P}_{dem} - (CF_{wt}P_{wt})}{CF_{PV}} \qquad (4\text{-}4)$$

4.3.2 Sizing the Electrolyser

After determining the RES system size, the size of the electrolyser is then identified. The size of the electrolyser (P_{EL}) is calculated by subtracting the minimum load demand (P_{dem_min}) from the total rated power that can be delivered by the renewable sources as shown in equation 4-5. It has been found out that the size of electrolyser using this method can be very large and underutilised [116]. As electrolysers can be very expensive to purchase (as discussed in chapter 3), it is desirable to operate them with a high level of utilisation. Therefore the calculated value, as suggested in literature, is to be reduced by around 50%. This has the effect of increasing the electrolyser level of utilisation (i.e. it will run at higher production rates more often). The potential disadvantage is that there are times when the total renewable generation exceeds the total power absorbable by the combined load and storage.

$$P_{EL} = (P_{PV} + P_{wind} - P_{dem\_min})/2 \qquad (4\text{-}5)$$

4.3.3 Sizing the Fuel Cell

When the load demand exceeds the renewable generation, the deficit is met by the fuel cell. The fuel cell converts the chemical energy stored within the stored hydrogen into electrical energy to supply the demand. The fuel cell size is selected to meet or exceed the maximum power demanded ($P_{dem_{MAX}}$) by the load. Typically a margin of 20% [117] is added to the size of the fuel cell to accommodate any modest increase in peak demands. Fuel cell power output (P_{FC}) is, therefore, calculated as shown in equation 4-6.

$$P_{FC} \cong 1.2(P_{dem_{MAX}}) \qquad (4\text{-}6)$$

4.3.4 Sizing the Hydrogen Storage

The renewable energy devices have been sized to provide enough energy to supply a specified load on an annual average basis. This has been described within equations 4-1 to 4-4. The size of an

appropriate electrolyser and fuel cell has then been identified using equations 4-5 and 4-6. However, demand may occur when there is no (or insufficient) renewable generation available to supply the load. Therefore, there is a need to assess the correlation of the load demand and the renewable energy production. Thus, the energy system is first modelled with no energy storage, as illustrated in Figure 4-2.
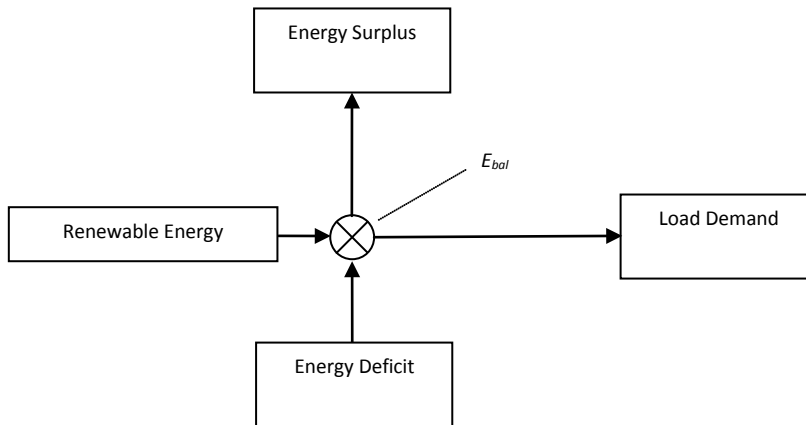
Figure 4-2: Simulating the energy system without energy storage

On simulating the energy system with the calculated PV and wind turbine sizes with the recorded renewable resource, it is possible to identify the correlation between load demand and generation.

However, the difference between the load demand and the renewable generation at different timings can be found by subtracting the load demand from the renewable energy available for each sample interval of recorded load and renewable resource. It can then be concluded that summing the difference for all the sample intervals is what yields a negative value (indicating a supply deficit) which defines the energy storage size. This is shown by equation 4-7 where E_S is the value for the size of energy storage, and E_{bal} is the negative value of the energy balance between renewable generation and power demand.

$$E_S = \sum E_{bal} < 0 \qquad (4\text{-}7)$$

On calculating the size of the hydrogen tank to supply the fuel cell, the average fuel cell conversion efficiency has been considered. The hydrogen storage tank must hold enough hydrogen so that the

fuel cell can deliver the energy requirements ($\bar{E}_S$). Therefore the energy that is required to be stored within the hydrogen storage tank ($\bar{E}_{tank}$) can be defined as shown in equation 4-8. In equation 4-8, $\bar{\eta}_{FC}$ represents the fuel cell conversion efficiency considering the Lower Heating Value (LHV) of hydrogen gas.

$$\bar{E}_{tank} = \bar{E}_s . \frac{1}{\bar{\eta}_{FC}}$$

$$(4\text{-}8)$$

The average volume of hydrogen that needs to be stored in the hydrogen tank is then calculated based on the absolute energy content of the hydrogen gas. This is known as the Higher Heating Value (HHV) of the hydrogen gas which is known to be 3.55kWh/Nm^3 [63]. Therefore the volume of hydrogen to be stored ($\overline{VL}_{tank}$) is found as shown in equation 4-9

$$\overline{VL}_{tank} = \frac{\bar{E}_{tank}}{3.55}$$

$$(4\text{-}9)$$

4.4   Applying the Proposed Deterministic Sizing Algorithm – A Case Study

The hypothetical case study considered here is based upon Scenario E (Chapter 3). Surplus renewable energy is stored as hydrogen and used via a fuel cell to generate electrical energy during times of renewable deficit. The case study system to be sized is outlined in Figure 4-3. In this case study an industrial load is to be supplied by a HRHES. The deterministic sizing method described in the previous section is applied to size a HRHES to supply the load. The wind turbine, PV, electrolyser, hydrogen storage, and fuel cell sizes that are found, are then simulated with the renewable resource (weather) and load demand data using the component models described in appendix A.
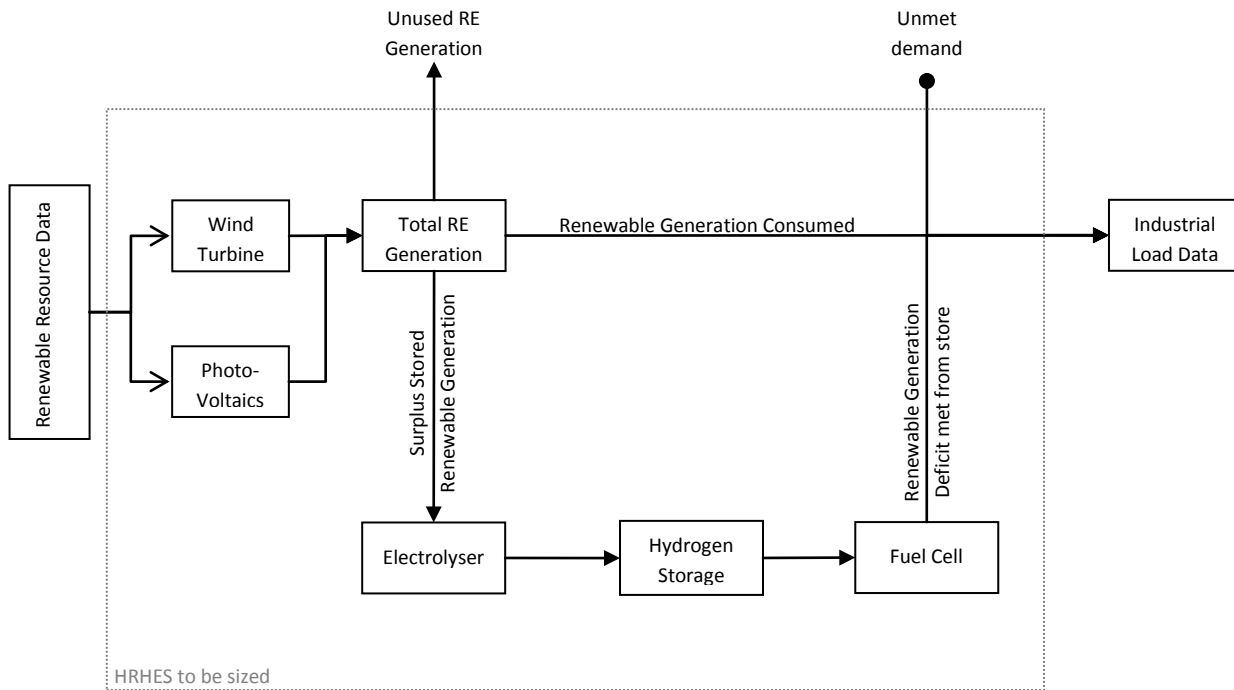
Figure 4-3: HRHES Case Study

The input data to the deterministic method are the recorded values of wind speed and solar irradiance for a period of a year. This data has been acquired at an industrial processing plant and is shown in Figure 4-4. The renewable wind and solar resources have been recorded using a weather station mounted onto the roof of the building in which the load demands were recorded. The height of the instrumentation was approximately 10m Above Ground Level (AGL). The average recorded annual wind speed (v) and insolation data (Ø) are shown in Table 4-1.

Average overall insolation (Ø) (W/m^2)	79.46
Average Mean Wind speed ($\bar{v}$) (m/s)	7.91

Table 4-1: Average recorded solar and wind resource

During the same period, the industrial processing plant electrical demands have also been recorded and are shown in Figure 4-5. These are also used as input data to the deterministic algorithm.
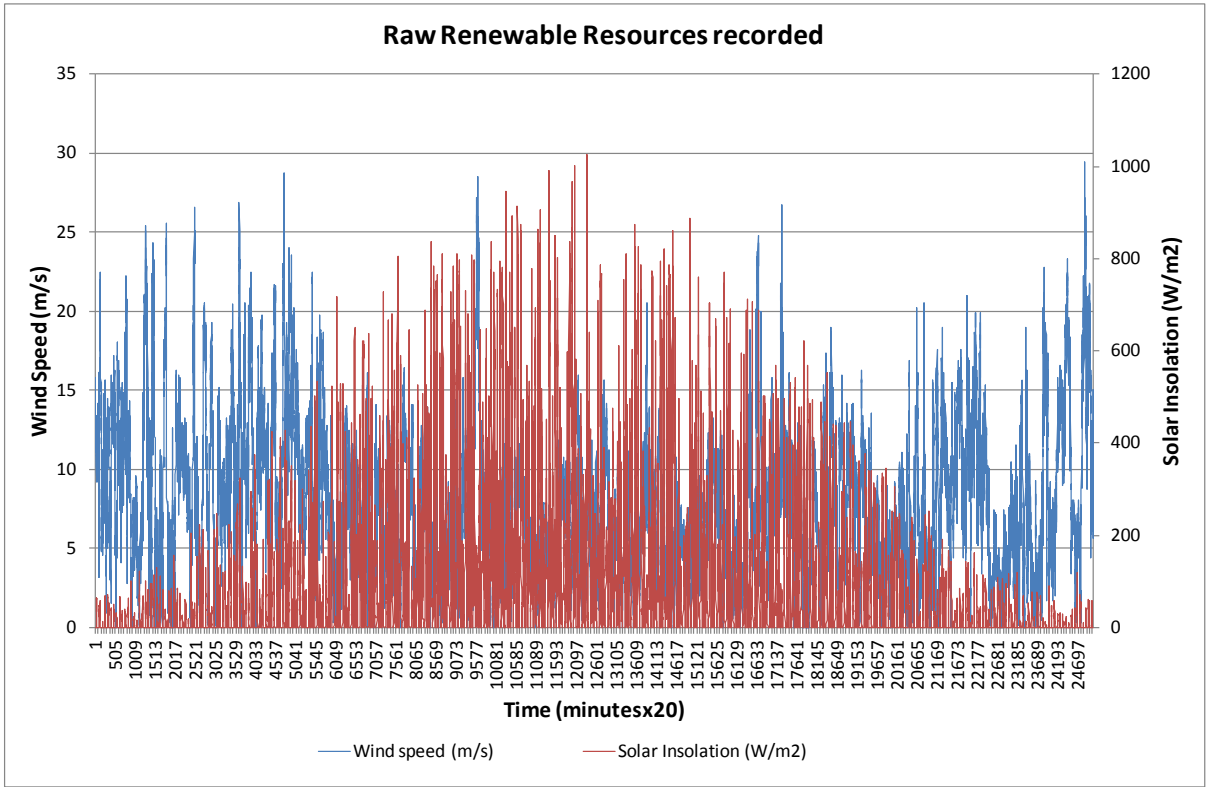
Figure 4-4: Renewable resource data recorded every 20 min
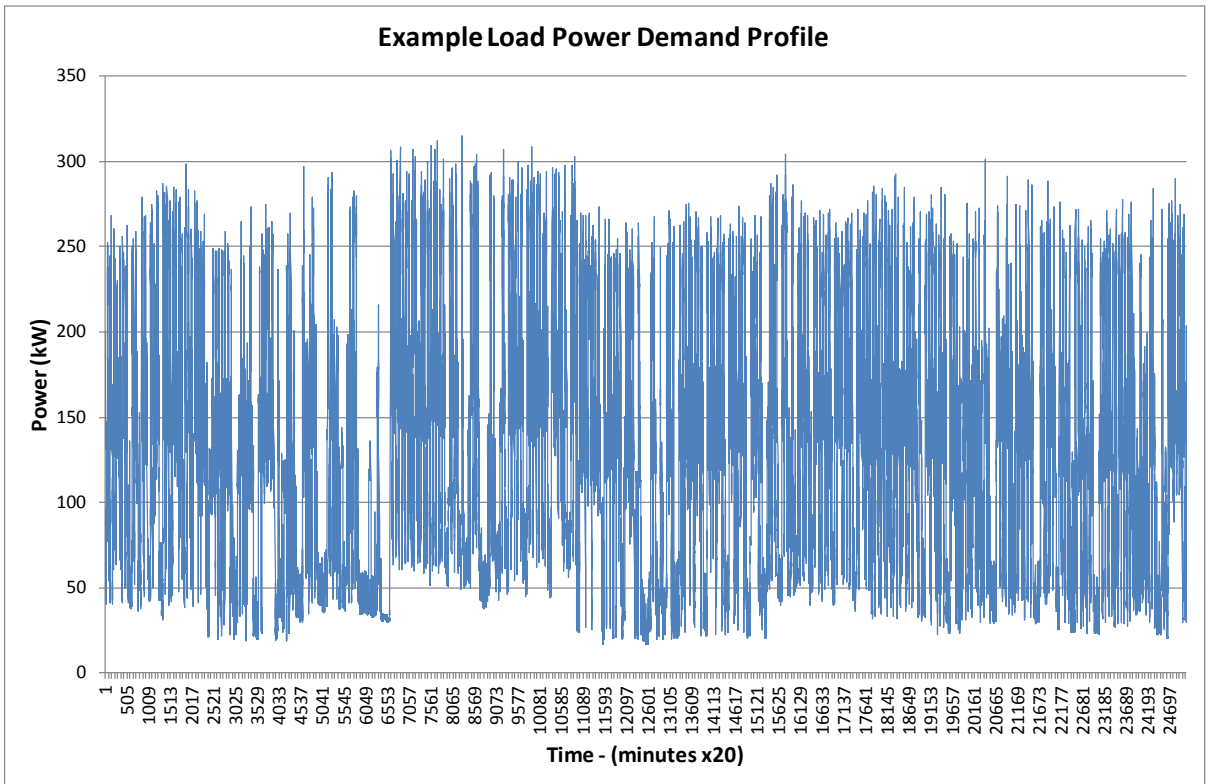
Figure 4-5: Industrial load demand profile for 1 year

From the aforementioned input data it is required to define the size of an appropriate wind turbine, PV array, electrolyser, hydrogen storage tank and fuel cell. The inputs and outputs of the proposed deterministic modelling approach are all illustrated in Figure 4-6.
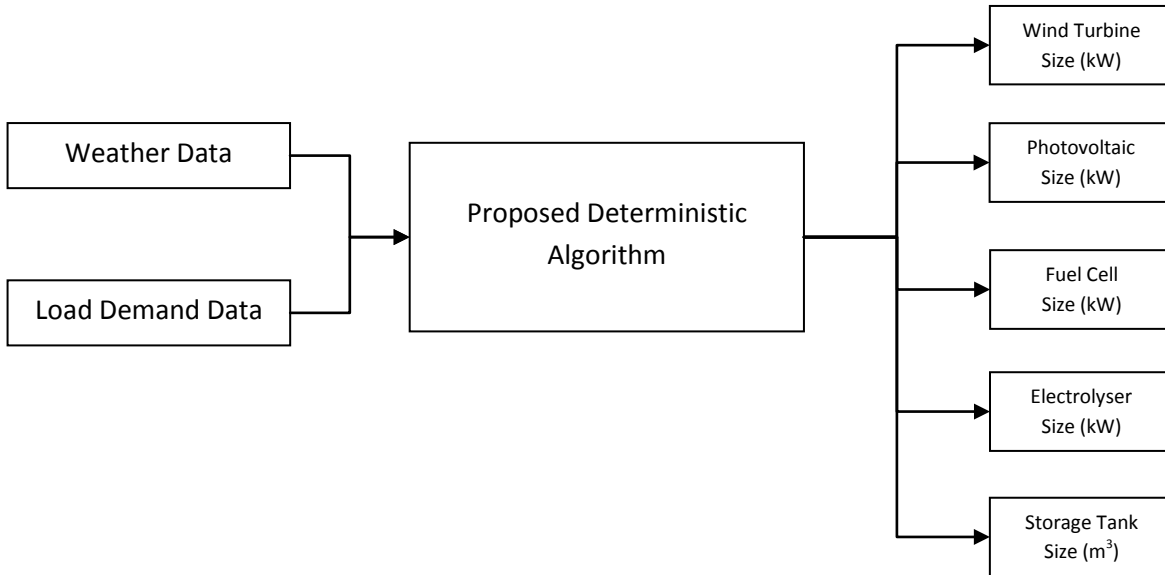
4.4.1   Step-1: Sizing the Wind Generator

To calculate the size of the wind generation, there is a need to first find the average power demands required by the load. The average demand of the load ($\bar{P}_{dem}$), as shown in table 4-2, is found by taking the mean average of the recorded demand data shown in Figure 4-4.

Total Load Consumption	1049507	kWh
Average power demand ($\bar{P}_{dem}$)	125	kW
peak power ($P_{dem_{MAX}}$)	315	kW
minimum power demand (P_{dem_min})	17	kW

Table 4-2: Required load demand data

As can be seen in Table 4-2 the average load demand is 125kW. Thus the selected wind turbine must be able to provide an average output ($\bar{P}_{wind}$) approximately equal to this demand. To find the average output of the wind turbine, the average wind-speed ($\bar{v}$) is used from Table 4-1. The wind

speed (v) in the wind turbine model (described and referenced in appendix A), is then replaced with $\bar{v}$ as shown in equation 4-10:

$$\bar{P}_{wind} = \frac{1}{2}\rho A \bar{v}^3 \left(0.5(\lambda - 0.02\beta^2 - 2.9)e^{(\lambda)} - 0.0303\lambda\right) \tag{4-10}$$

Where: $\bar{P}_{wind}$ = Average wind turbine output
ρ = Air density
A = Swept rotor area
$\bar{v}$ = Average wind speed
λ = Tip speed ratio
β = Blade pitch angle

It has been found that by choosing an Enercon E33 wind turbine (Appendix B), an average output approximately equal to the average demand of the load is obtained. In fact, an Enercon E33 wind turbine results in an average power output of 118kW. This is almost equivalent to the loads average demands, which is 125kW. The average power output from the wind turbine corresponds to a capacity factor (CF_{wind}) of 35.8%. The developed model' resulting power curve, using equation 4-10, is then compared with the manufacturer recorded data in Figure 4-5. The figure illustrates that the model outputs correlates with recorded manufacturer data. This accordingly confirms the viability of the proposed model.
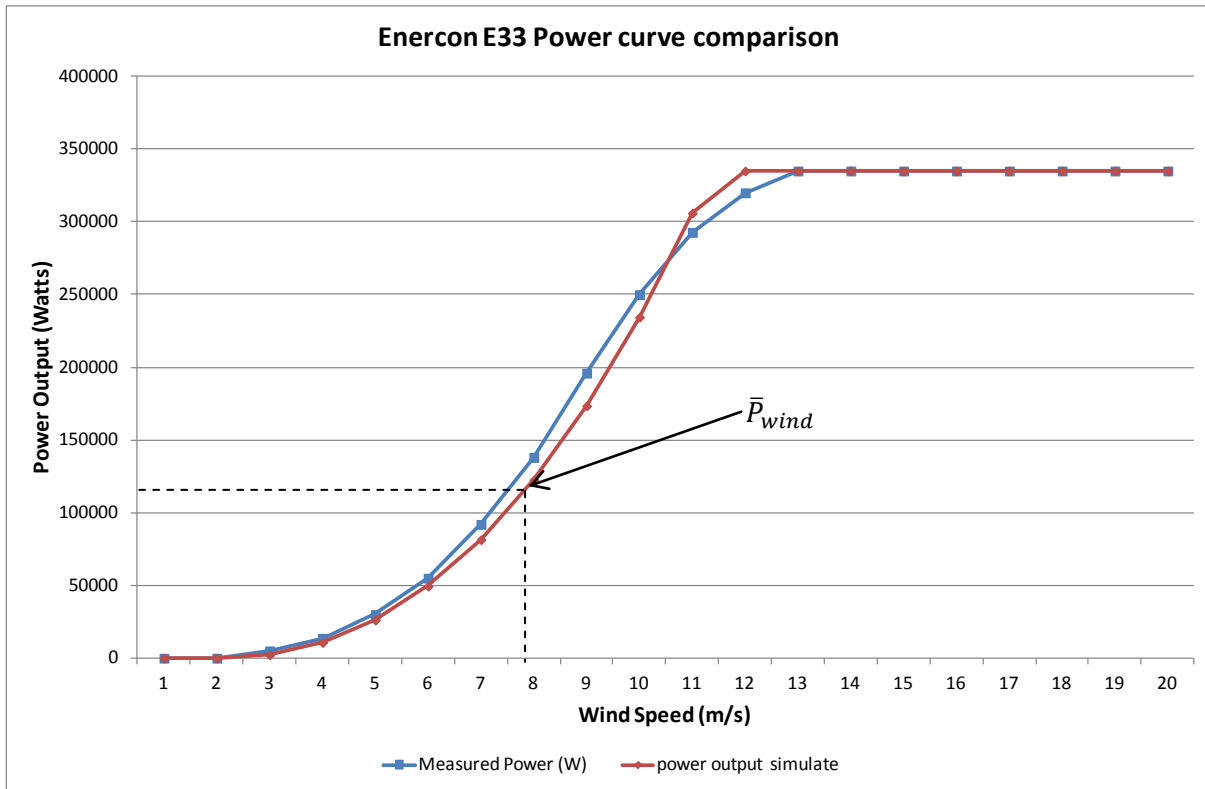
Figure 4-7: E33 modelled power curve comparison

4.4.2 Step-2: Sizing the PV array

PV panels are rated by manufacturers in standard conditions with a reference illumination of $1000W/m^2$. Dividing the measured average solar insulation with the reference $1000W/m^2$ yields a capacity factor of 7.75%. In other words, the expected capacity factor for a PV array used with the solar resource depicted in Figure 4-3 and Table 4-1 is 7.75%.

Therefore, using equation 4-4 it is possible to define the size of the photovoltaic array. This is found to be a size of 92kW.

4.4.3 Step-3: Sizing the Electrolyser

The electrolyser size is identified by employing equation 4-5. This is calculated using the size of the wind turbine found in step 1 (330kW) and the size of the PV array found in step 2 (92kW). The minimum demand P_{dem_min} (required in equation 4-5) is taken from the load analysis table, Table 4-2, to be 17kW. This gives the size of the electrolyser as 202.5kW. However, the precise size of 202.5kW is not a commonly market available electrolyser size, therefore an electrolyser size of 200kW is to be used in the model simulations described later in this chapter.

$$P_{EL} = \frac{P_{PV} + P_{wind} - P_{dem\_min}}{2} = \frac{(92 + 330 - 17)}{2} = 202.5 \cong 200kW$$

4.4.4 Step-4: Sizing the Fuel Cell

Using the value for maximum load power demand in Table 4-2 in equation 4-6, the fuel cell size has been found to be 378kW. . Similar to the electrolyser, the precise size of 378kW for a fuel cell is not possible to obtain. Due to this, a 300kW PEM fuel, that has been successfully used in Guangdong, China [118], is considered in the simulation here.

4.4.5 Step-5: Sizing the storage tank

To identify the storage tank size, it is first necessary to simulate the energy system without any hydrogen energy storage connected. Simulating the renewable energy generators (wind and PV) sized in steps 1 and 2, and comparing their output with the measured load depicted in Figure 4-5,

identifies the correlation between load demand and generation. The summary of findings of a 'no-storage' simulation scenario is given in Table 4-3:

Item	Value	
Total Load Demand	1,049,507	kWh
Total Wind generation	1,176,707	kWh
Total PV generation	57,668	kWh
Total Renewable Generation	1,234,375	kWh
Renewable generation not utilised	619,071	kWh
Load demands not supplied	434,164	kWh
Load demand supplied from renewable generation	615,304	kWh
% RES not used	50%	
% load demand supplied from renewable generation	59%	
% Load demand not satisfied	41%	

Table 4-3: Simulation with no storage

It can be seen from Table 4-3 that when there is no storage attached, approximately 50% of the renewable generation is not used by the load demand due to the generation occurring at times of low demand. Therefore the unused renewable generation will not be used and must be constrained or dumped. Conversely, 41% of the loads demand requirements are not met by the renewable generation due to insufficient renewable energy generation at the time of demand. In this case, the amount of additional energy required to supply the load is 434MWh. This is found by subtracting load demands from the renewable generation during a 'no-storage' simulation of the energy system as described by equation 4-7. Therefore, the energy that needs to be available for release from an energy store can be said to be 434MWh. Applying equations 4-8 and 4-9 gives a hydrogen tank storage volume of 305,749m^3 of hydrogen. The fuel cell efficiency based on the Low Heating Value (LHV) of the hydrogen gas is assumed to be 38.3%

Table 4-4 summarises the computed system component sizes for the given case study using the 5 step deterministic algorithm:

System Component Size	Value
Wind turbine rated power (step-1)	330kW
Solar PV rated power (step-2)	92kW
Electrolyser rated power (step-3)	200kW
Fuel Cell rated power (step-4)	378kW
Hydrogen Storage Tank cubic meter H_2 capacity (step-5)	305,749m^3

Table 4-4: Summary of case study energy system components sizes using the proposed sizing algorithm

4.5 Verification of the Proposed Deterministic Algorithm

In the previous section, the renewable energy generation resources together with the electrolyser, hydrogen storage and fuel cell have all been sized using the proposed deterministic algorithm for the case study under consideration. To assess the suitability of the system sizes that has been calculated using the proposed deterministic method, an overall system simulation is conducted. The simulation of the sized system, for scenario E, is conducted using the component models described in appendix A. In scenario E (chapter 3), the surplus renewable energy that is not consumed by the load is absorbed by the electrolyser and converted into hydrogen gas for storage. Conversely, any energy that cannot be met by the renewable resources is supplied from the storage through the fuel cell. The results of the overall system simulation, sized by the proposed deterministic method, are shown in Table 4-5.

Item	Value	
Total Load Demand	1,049,507	kWh
Total Wind generation	1,176,707	kWh
Total PV generation	57,668	kWh
Total Renewable Generation	1,234,375	kWh
Renewable generation not utilised	136,749	kWh
Renewable energy electrolysed	482,322	kWh
Load demand supplied from fuel cell (store)	269,779	kWh
Load demands not supplied	164,384	kWh
Load demand supplied from renewable generation	885,083	kWh
% RES not used	11%	
% load demand supplied from renewable generation	84%	
% Load demand not satisfied	16%	
Average electrolyser efficiency simulated	59%	
Average fuel cell efficiency simulated	50%	
Overall storage efficiency simulated	29%	
Storage capacity at start	100%	
Storage capacity at end	8%	
Storage capacity minimum	0%	

Table 4-5: Performance of HRHES sized using the proposed deterministic method

The simulation results indicate that the integration of hydrogen energy storage significantly improves the utilisation of renewable energy generation by 39%. This is found from the difference between the percentage of unused renewable energy generation (i.e. constrained) when HEST has not been utilised and the unused renewable energy generation when HEST is utilised (50%-11% = 39% as taken from Table 4-3 and Table 4-5 respectively).

Additionally 84% of the load demands are met by the renewable energy sources when HEST is applied. This represents an increase of 34% from when HEST has not been applied to the energy system. Unfortunately, it is not possible to absorb all the renewable generation by the energy storage system in any of the following three circumstances:

1. When the storage tank is full and no additional hydrogen can be stored
2. When the total renewable energy production is greater than the maximum power of the electrolyser

3. When the surplus renewable energy is less than the minimum starting power of the electrolyser (20% of the name plate rating for an industrial alkaline electrolyser)

The average overall storage 'turn-around' efficiency, for the given system case study is found to be 29.5%. This is found by multiplying the electrolyser and fuel cell efficiencies to find the overall turn-around efficiency (59% x 50%=29.5%). The 'turn-around' efficiency is a measure of the losses from the energy input to the electrolyser to the energy output through the fuel cell. The value of 29.5% calculated is very low; however, a typical Proton Exchange Membrane (PEM) fuel cell can only recover the Lower Heating Value (LHV) of hydrogen gas and not the Higher Heating Value (HHV). This represents an additional efficiency penalty of approximately 16% in turn around efficiency when using HEST as described by scenario E. To mitigate the case where the demand of the load is not met by the Hybrid renewable hydrogen energy system, the demand could be either imported from the power grid, or a stand-by generator can be installed.

4.5.1 Effect of Storage Capacity at Start of Simulation

The impact of the storage state (empty and full) before starting the simulation has also been examined. Comparison results are shown in Figure 4-6. The utilisation of the renewable generation is found to be slightly improved if starting with a partially filled storage tank. However, a greater portion of the load demand remains unmet due to the storage system becoming empty at times. Therefore, it can be concluded that the best scenario for supplying the load is when the storage is full from the beginning.
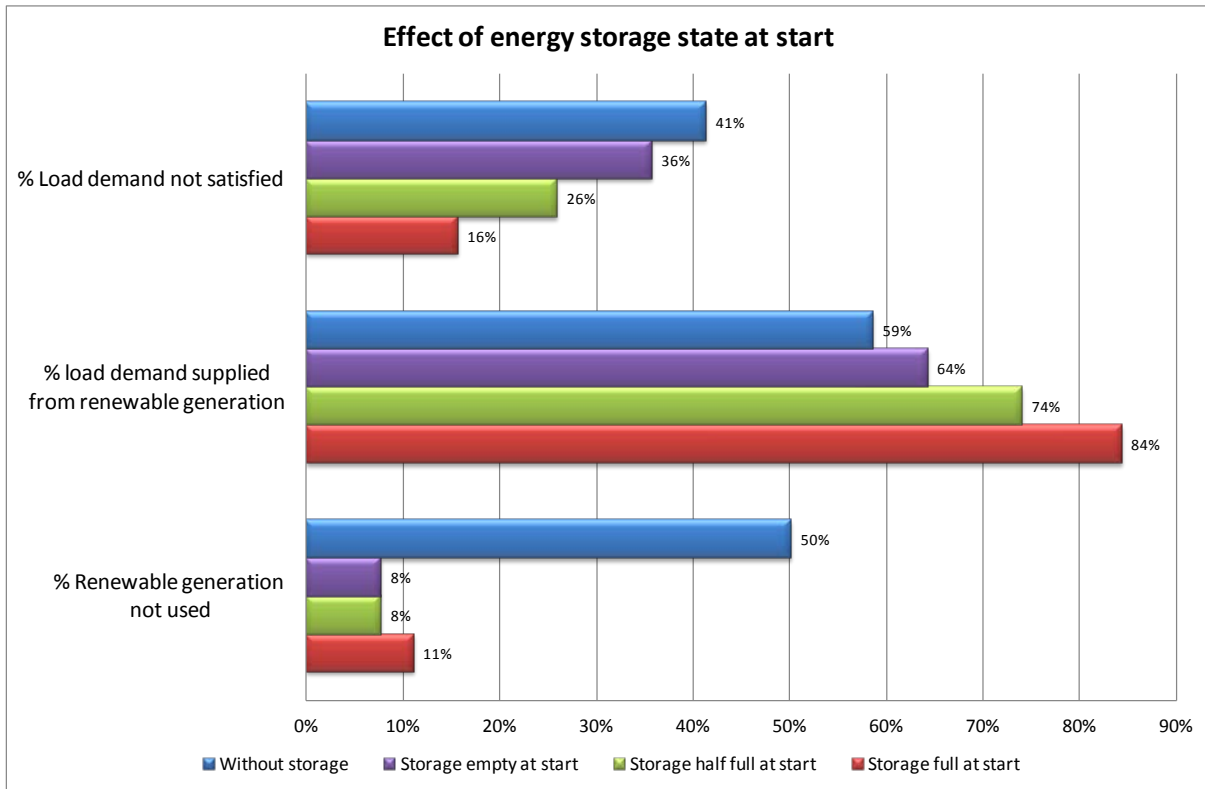
Figure 4-8: Effect of energy storage state at simulation start

4.5.2 Effect of Using a Smaller Storage Tank

The simulation has also been conducted to investigate the impact of reducing the storage tank size. The results are shown in Figure 4-9. By reducing the storage system size to become 1% of the originally defined size, a renewable energy utilisation factor similar to that of having a large storage system is observed. On using a much smaller storage tank, surplus renewable energy can still be absorbed, however, and as expected, the load demands that are achievable by the overall energy system are reduced considerably from 84% to 66%. Nonetheless this is still a 7% improvement from having no storage present at all. This is found by repeating the HRHES simulation as described previously in section 4.4; however the size of hydrogen storage tank is reduced to 3,057m^3 (1% of the size of storage tank given in Table 4-4).
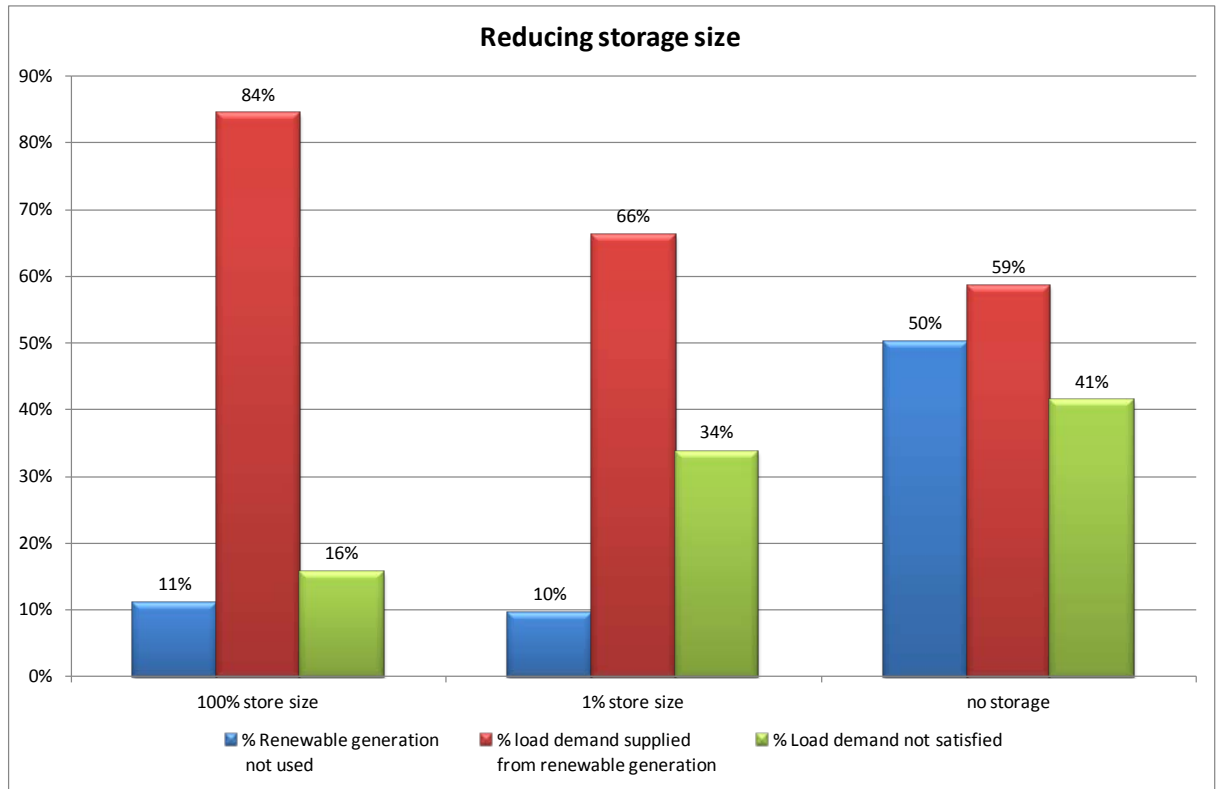
Figure 4-9: Effect of reducing storage size

In addition the storage system is utilised much more when the hydrogen storage tank is reduced in size. The impact of the storage systems size on its utilisation can be seen in Figure 4-9.
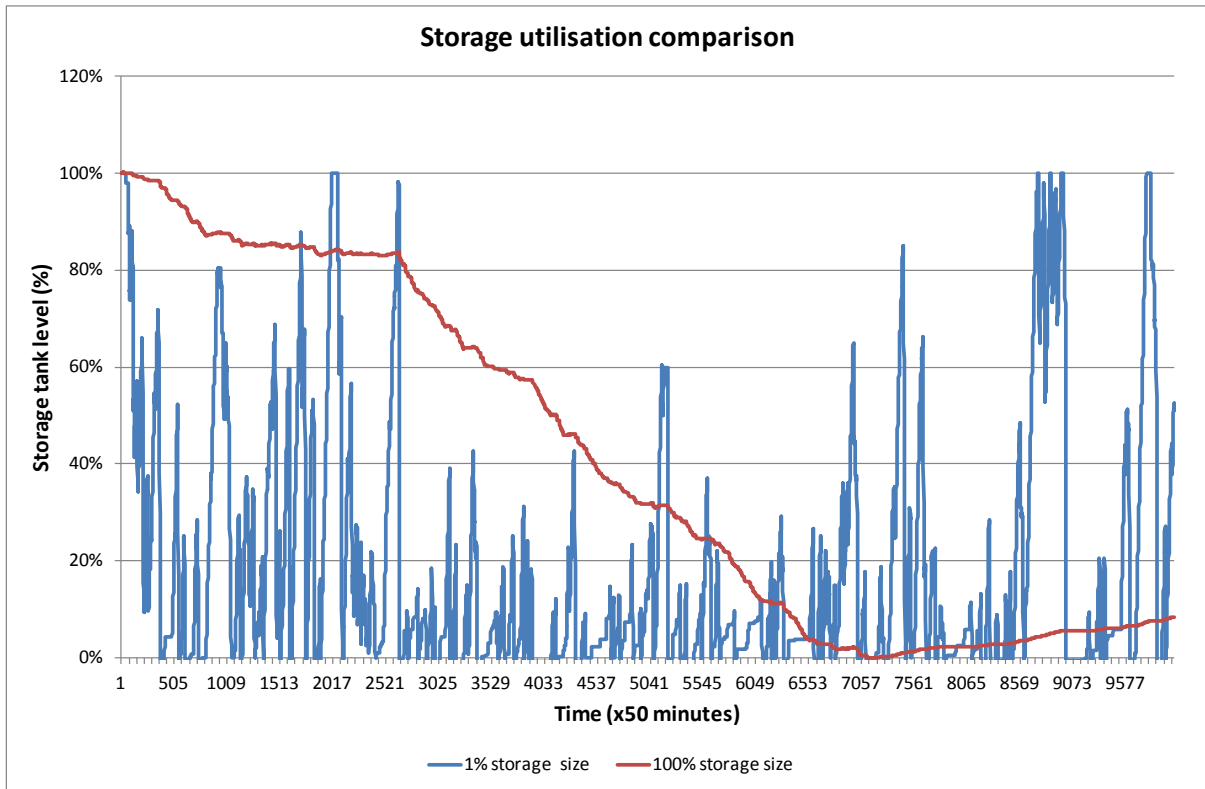
Figure 4-10: Impact of the storage systems size on its utilisation - storage level comparison

4.6 Deterministic Sizing Method Summary

This chapter has shown that many of the commercially available software do not offer the capability to simulate HEST as part of a hybrid renewable energy system. It has been found that software which can simulate HEST require a significant quantity of input data as well substantial computing resource, in order to perform well.

Essentially, and in common with commercially available software, the use of techniques such as GA, PSO and SA also requires a large volume of input data to perform well. In addition GA, PSO and SA methods require a significant quantity of computing resources and highly complex code in order to size and simulate a HRHES. Furthermore, PSO techniques are limited to the number of system components that can be sized due to the vectored nature of the solving algorithm. The requirement for an X, Y or X, Y, Z plot, limits their application to very simple three-component energy systems.

Due to the large input data requirements of commercially existing software and the significant computing resources needed for more advanced GA, PSO and SA techniques, a new deterministic sizing methodology that offers a very rapid initial system sizing, has been proposed here. The proposed methodology requires a very limited number of input data and can offer an initial system size for a HRHES very quickly. This approach plays an important role in appropriately sizing a renewable hydrogen energy system in the initial design phase, thus assisting in the early decision making process for the implementation of such a system.

The proposed deterministic sizing approach has shown that the application of electrolytic hydrogen production, storage and re-use can significantly increase the utilisation of renewable generation that would otherwise not be used. However, it has also shown that the "turn-around" efficiency of a HEST system was only 29.5%, which confirms that scenario E (Chapter 3) is highly inefficient and would need substantial increases in efficiency before being considered a viable solution. One of the main reasons for the low turn-around efficiency is that typical commercially available fuel cells are not able to utilise the HHV of the hydrogen gas. Finally, it has been found that the application of hydrogen technologies for renewable energy storage to supply an electrical load results in potentially very large storage requirements.

Nevertheless, the application of HEST has been found to increase the utilisation of constrained renewable energy. Even with a very modest storage system it has been shown that the level of constrained renewable energy can be greatly reduced. Therefore, where grid constrained renewable energy exists the application of even a small HEST solution can enable a greater renewable penetration without causing additional constraints.

It can be concluded that whilst the production of hydrogen provides a positive benefit to the increased penetration of renewable energy, the utilisation of the produced hydrogen may be better in other applications. For example it could be utilised as a transport fuel where a much higher value can potentially be realised for the gas. In addition, the utilisation of hydrogen gas as a transport fuel will also facilitate the use of much smaller hydrogen storage tanks, while still enabling the increased penetration of renewable energy.

5

5   Effect of thermal transients on renewable hydrogen production

Throughout the years, different electrolyser modelling tools have been developed and used to examine many aspects of an electrolysis process when coupled with renewable energy [119, 96]. The most common purpose of the modelling tools that simulate electrolysis, when combined with renewable energy generators, is to predict their overall hydrogen output. However, the majority of the electrolyser models currently used, within the limited commercially available software tools that offer HRHES simulation, do not take into account the thermal characteristics of an electrolyser.

At present, electrolysers are typically switched on and off for producing hydrogen at scheduled times for industrial processes. When using an electrolyser operated either directly in response to a renewable resource, or as part of a power grid network balancing mechanism, it will be regularly switched on and off and operated at variable power levels. This is in contrast to the way large scale industrial electrolysers are typically being used today. In essence, an electrolyser operating in response to renewable generation will often operate in its transitory dynamic states. Thus, in this mode of operation, an electrolysers overall hydrogen output will be affected by its thermal transient characteristic.

In a real working electrolyser, the exothermic electrochemical reactions taking place inside the electrolyser will cause an electrolyser to warm up. The warmer the electrolyser becomes, the more efficient the hydrogen production becomes. This is true until the electrolyser reaches its full working temperature. Therefore the electrolysis of water to produce hydrogen occurs most efficiently when the electrolyser is working at its rated temperature.

During the period between electrolyser switch on and full working temperature, electrolysis of water occurs at a lower efficiency. In other words, before the electrolyser reaches its full working temperature, it requires more electrical input energy in order to produce hydrogen. Therefore, this will have an adverse effect on the quantity of hydrogen being produced.

A number of models capable of simulating an electrolyser's transient thermal behaviour has been documented [96, 120, 124]. These have shown that thermal transients will adversely impact hydrogen production of an electrolyser. However, none of these models explored the impact of the transient thermal behaviour of an electrolyser's overall hydrogen production when connected to renewable generation. In other words, none of the available models and software tools has been utilised to explore the effect of thermal transients on the overall hydrogen production of an electrolyser when applied in a grid balancing system or connected directly to renewable generation.

Consequently, this chapter explores the effect that thermal transients are likely to have on cumulative hydrogen production when an electrolyser is operated in conjunction with renewable generation. Determining the cumulative effect on overall hydrogen production, and therefore energy stored, will provide valuable insight into whether or not there is a need to incorporate electrolyser thermal transient effects on efficiency when examining the use of HEST with renewable generation. This is also applicable where the use of electrolysers is incorporated as a balancing mechanism to absorb constrained renewable generation in the power grid.

5.1 The Issue of Electrolyser's Thermal Transient Effect on Hydrogen Production

Commercially available simulation tools are commonly used for evaluating the performance of an electrolyser within renewable energy systems. Among these, HOMER, developed at the National Renewable Energy Laboratories (NREL), is the most widely used software in modern literature with over 92,000 users worldwide [121].

HOMER is probably the most widely recognised and used modelling tool across the academic and industrial community. Unfortunately, this tool has a significant drawback when simulating hydrogen production from electrolysis in response to renewable generation. In HOMER, the thermal transient effect on an electrolysers' hydrogen production efficiency is not taken into consideration. Instead, HOMER relies on a single assumed value of average production efficiency [122] . This single value assumption disregards an electrolysers operating temperature and represents an important deviation from the performance of a real operating electrolyser.

Whilst examples of a single assumed value for average production efficiency such as that used by HOMER can be found in other commercial software, the application of a thermally compensated model is limited to very few modelling tools. Indeed, the only example found in literature where a thermally compensated model has been applied in commercially available software for simulating a hybrid renewable hydrogen energy system is HydroGems [123].

HydroGems is now only available as part of the Transys16 simulation environment. The empirical parts of the HEST models within HydroGems are calibrated based on data found in literature and manufacturer data sheets. However, it is a significant challenge to calibrate the model parameters effectively within the HydroGems software environment platform. In addition to this, access to the electrolyser source code for calibration within the Transys16 platform is not available. This therefore restricts its use to the pre-programmed model.

Whilst it would appear that Hydrogems would provide the ideal software platform to perform hybrid renewable hydrogen energy system simulations, access to real data from the hydrogen

demonstration systems being modelled is essential to ensure correct model operation [124]. In addition to the above identified significant drawbacks, work undertaken by the International Energy Association (IEA) in evaluating renewable hydrogen projects around the world found that it took at least two years of analysis on an already operating system in order to calibrate the HydroGems/Transys16 models to work effectively.

Therefore to simulate the effects of thermal transients on overall hydrogen production efficiency, a thermally compensated electrolyser model from literature, similar to that used in HydroGems, is used. This model is then applied to the proposed algorithm developed in the following sections to define the overall impact on hydrogen production efficiency when using an electrolyser in conjunction with renewable energy.

The model used in the proposed algorithm is based on a combination of heat transfer theory, fundamental thermo-dynamics, and empirical electro-chemical relationships measured from operating systems. The thermally compensated model is detailed in appendix A, (section 9.3). The simulations conducted use the 26kW and 30kW electrolyser model parameters from appendix B, (tables 10-1, and table 10-2 respectively).

Figure 5-1 illustrates the effect of the temperature on production efficiency. The effect of temperature across the full range of production has been simulated using the 30kW electrolyser details from appendix B. It can be seen that at lower temperatures the production efficiency is lower than at full production temperature, the full operating temperature being 60°C in the illustrated example. Therefore disregarding the effects of temperature, similar to HOMER, to simulate HEST may lead to over optimistic, unrealistic simulation results.
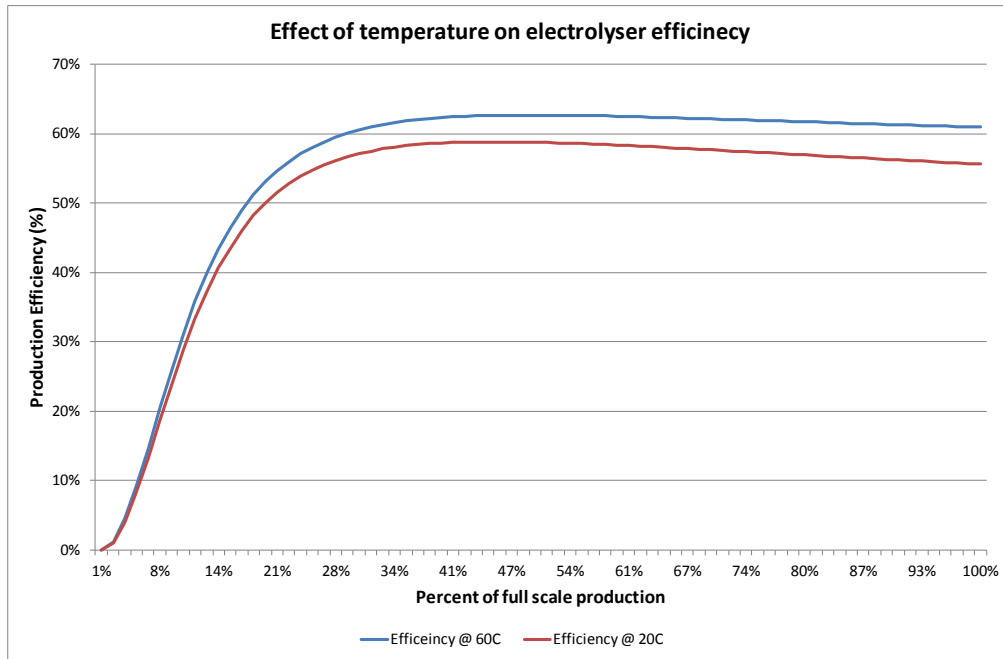
Figure 5-1: Impact of hydrogen production on the efficiency of a 30kW electrolyser

5.2 Algorithm Development

To identify the effects of thermal transients on the overall hydrogen production from an electrolyser operated in conjunction with a renewable source, a three step algorithm has been developed. In the developed algorithm, a simulation has been first run to determine hydrogen production from a renewably powered electrolyser using the configuration shown in Figure 5-2. In this initial simulation the electrolyser model is compensated for the effects of temperature on its hydrogen production and the results are saved.

The simulation is then repeated, however this time with the electrolyser temperate being fixed at its full working temperature. Therefore the effects of thermal transients are ignored this time, and the results are again saved.
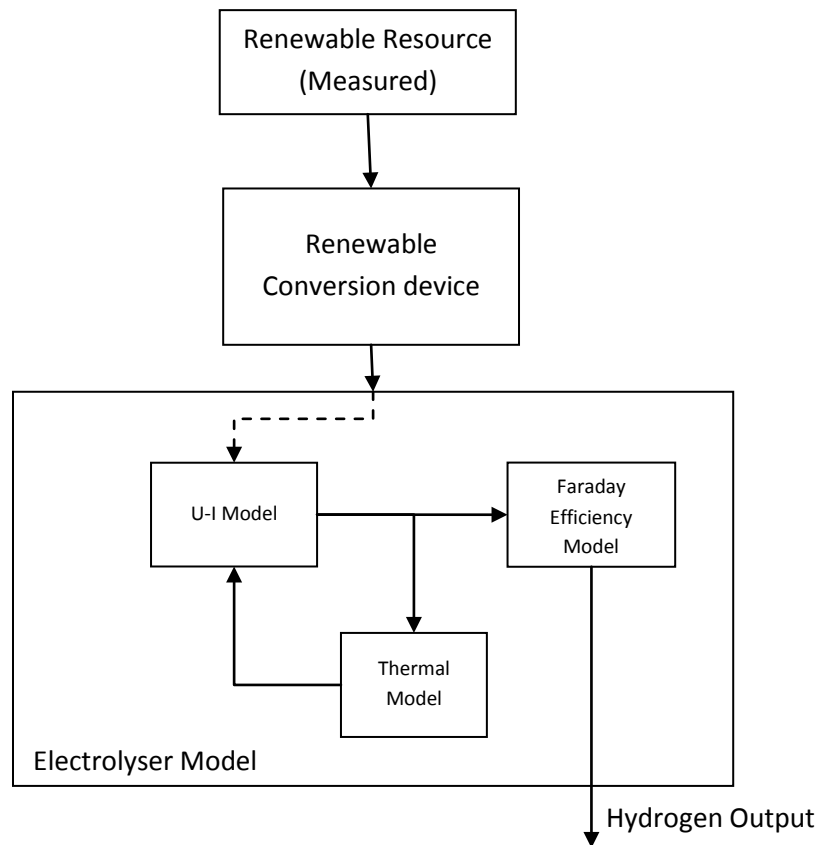
Figure 5-2: Electrolyser simulation incorporating thermal effect on efficiency

In the final step of the proposed algorithm, the overall effect of thermal transients on hydrogen production is calculated by subtracting the hydrogen output of the thermally compensated model in step 1 from the hydrogen output of the fixed temperature model in step 2. This yields the cumulative effect of the thermal transients on overall hydrogen production. The proposed algorithm is shown in Figure 5-3.
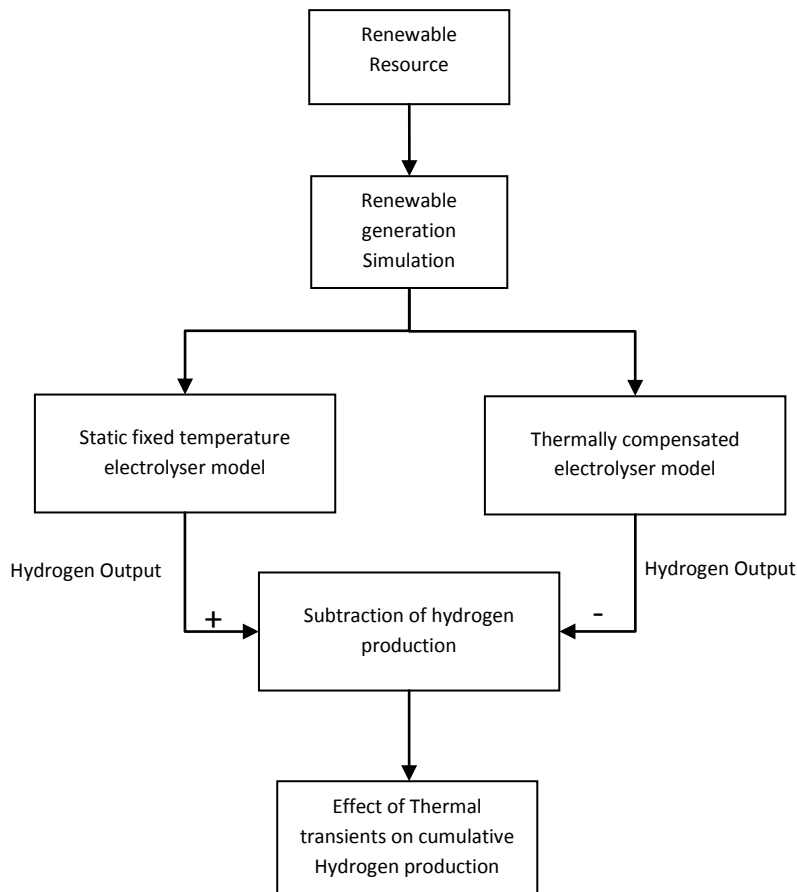
Figure 5-3: Proposed algorithm to find cumulative impact of thermal transients on hydrogen production

5.3 Thermal Transient Response

Using the simulation configuration depicted in Figure 5-2, the thermal response of a 30kW electrolyser has been simulated and compared against the measured thermal response. The comparison is shown in Figure 5-4. As can be seen, the simulated electrolyser output correlates positively with the data from the infield electrolyser data. The production rate of the electrolyser has been set to 50% of maximum production. For this case, the thermal transient between switch on and full working temperature is 3,210 seconds (about 53 minutes). At approximately 14,000 seconds the electrolysis is switched off, and then is switched back on again at around 17,500 seconds (approximately 8 minutes after the electrolyser was switched off). During the electrolyser down time, the working temperature of the electrolyser can be seen falling and then rising again when electrolysis is resumed. This profile is typical to what would be expected when operating an electrolyser in conjunction with grid constrained renewable generation.
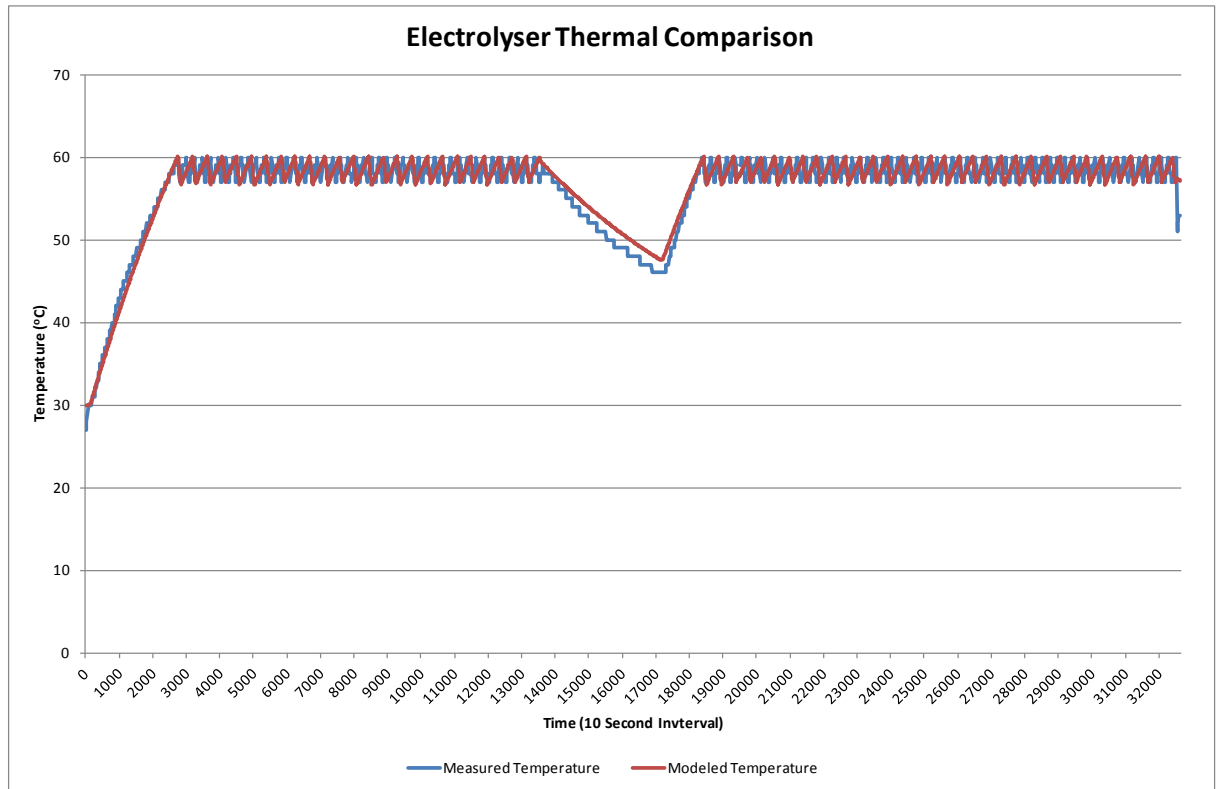
Figure 5-4: Comparison of modelled thermal response with actual response

The 53 minute time period taken by the electrolyser to get from an ambient of 30°C to full working temperature, illustrates the long duration of thermal transients. This is further demonstrated when the electrolyser is switched off and cools by only 12°C, when the electrolyser is switched back on, there is still a transient to the full working temperature.

The effect of the production rate on the overall time taken by the electrolyser to reach its full working temperature is then investigated by repeating the simulation. Instead of running the simulation directly from a renewable resource, the production rate of the electrolyser has been fixed at different values. The simulation is then run for each value with the electrolyser starting from an ambient of 30°C, this is shown in Figure 5-5. As can be seen, the thermal transient is much longer when the electrolyser is operating at lower production rates.
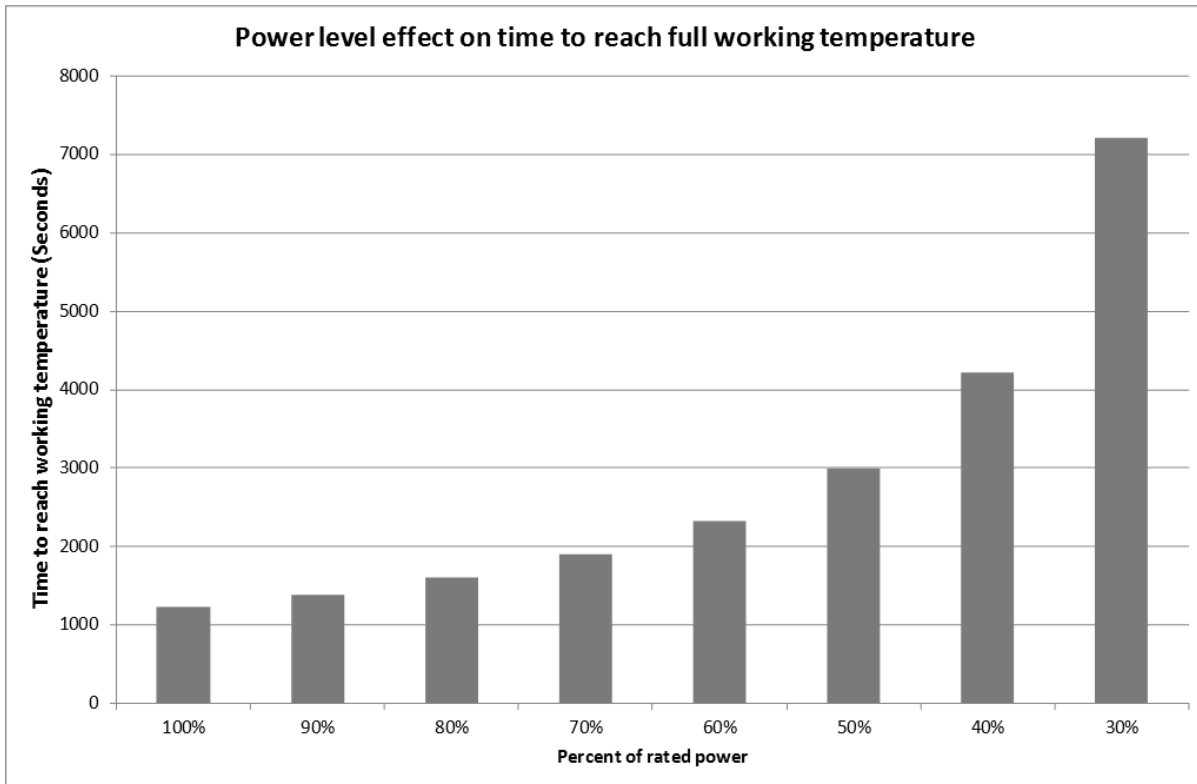
Figure 5-5: Effect of power level on thermal transient time

The implication of Figure 5-5 is that when operating an electrolyser in conjunction with renewable generation, there will be periods when the long thermal transients could have a significant impact on overall hydrogen production. Therefore, in the next section the impact of operating the electrolyser in combination with a renewable source on the overall hydrogen production will be explored.

5.4 Case Study - Effect of Electrolyser Thermal Transients When Connected to PV on Overall H₂ Production

As aforementioned, if an electrolyser is operated in conjunction with a RES in an intermittent and variable manner, the cumulative impact on hydrogen production of thermal transients should become more pronounced. In addition, in situations where renewable resources are lower, the electrolyser will operate at lower power rates more often. An example of this would be in the winter when there is much less light available to operate a PV array. This, in turn, will increase the time taken by the electrolyser to reach its full working temperature and therefore it's most efficient operating condition. The cumulative production of hydrogen will therefore be lower than what would be anticipated using a constant efficiency model.

5.4.1   Simulation Configuration

To investigate the level of impact thermal transients have on the production of hydrogen, an electrolyser has been modelled and simulated when coupled to a renewable source. The renewable generation source, in this case, is chosen to be a photovoltaic array. Figure 5-6 shows the system configuration for the simulated Hybrid energy system.
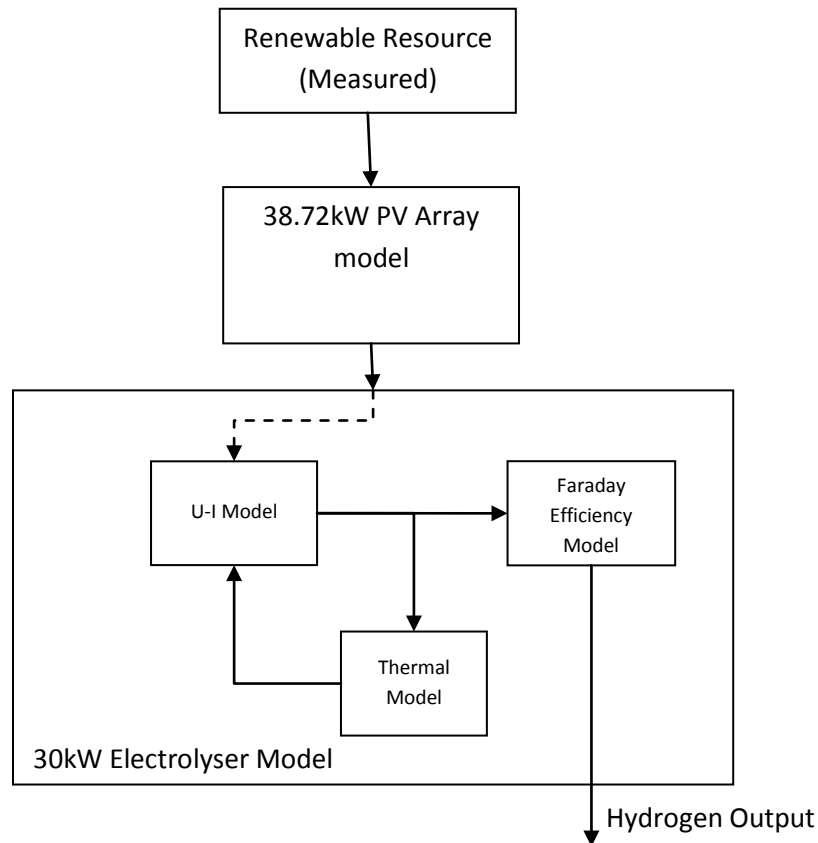
Figure 5-6: Overview of the simulated hybrid energy system

For the above system, the energy is produced from a Photo-Voltaic array (PV). No energy storage or grid connection is considered and it is assumed that all hydrogen production is vented (the rationale is that only the thermal effect on electrolyser's production is to be investigated here and not the storage). The system illustrated in Figure 5-6 will only operate the electrolyser when there is sufficient power available from the PV array. The minimum power required to start the electrolyser is 20% of the electrolyser maximum production.

The electrolyser simulated in this configuration is a 5.33Nm^{3}h^{-1} unit (30kW maximum power). Therefore, the electrolyser will only be switched on at a PV power output of 6kW, which is 20% of the

maximum power consumption of the electrolyser. This means that the electrolyser will start to operate at a level of 1.07Nm^{3}h^{-1} (at 6kW power). Simulation parameters for the electrolyser model are detailed in appendix B, Table 10-2.

The renewable energy is provided from a simulated array of BP380S 80Wp PV modules. PV modules are connected as four arrays each with 6 strings of 16 PV panels totalling 384 panels. This gives a maximum rated output of 30.72kW. As discussed, the electrolyser is configured to operate between 20% and 100% of its rated production levels. The mathematical models for the PV and electrolyser are shown in Appendix A, (sections 9.2 and 9.3 respectively).

The solar resource data used as input data for the simulation are those measured data taken from the meteorological station described in the previous chapter, and are recorded in watts per square meter. A summary of the simulation results is given in Table 5-1 and is discussed in the following section.

	Jan	Feb	Mar	Apr	May	Jun	Jul	Aug	Sep	Oct	Nov	Dec
Logged time (s)	44635	41755	44575	42780	31910	40445	44635	37280	41955	43780	43195	44635
PV output (kWh)	18	224	998	1958	2351	2940	2719	1752	1362	620	108	9
Electrolyser consumption (kWh)	0	54	650	1484	2000	2350	2130	1270	965	350	6	0
Unused (kWh)	18	170	348	474	351	590	589	482	397	270	102	9
H$_2$ mass (kg)	0	0.185	2.411	5.633	7.701	9.040	8.121	4.797	3.599	1.250	0.017	0
Effect of Thermal transient	0%	6%	2%	2%	1%	1%	1%	2%	2%	4%	14%	0%

Table 5-1: Simulation summary data

5.4.2   Cumulative Thermal Transient Effects

The electrolyser production has been simulated with an ambient temperature of 20°C. The electrolyser operates at a working temperature of 60°C. Figure 5-7 illustrates the output of the simulation model.

Hydrogen production
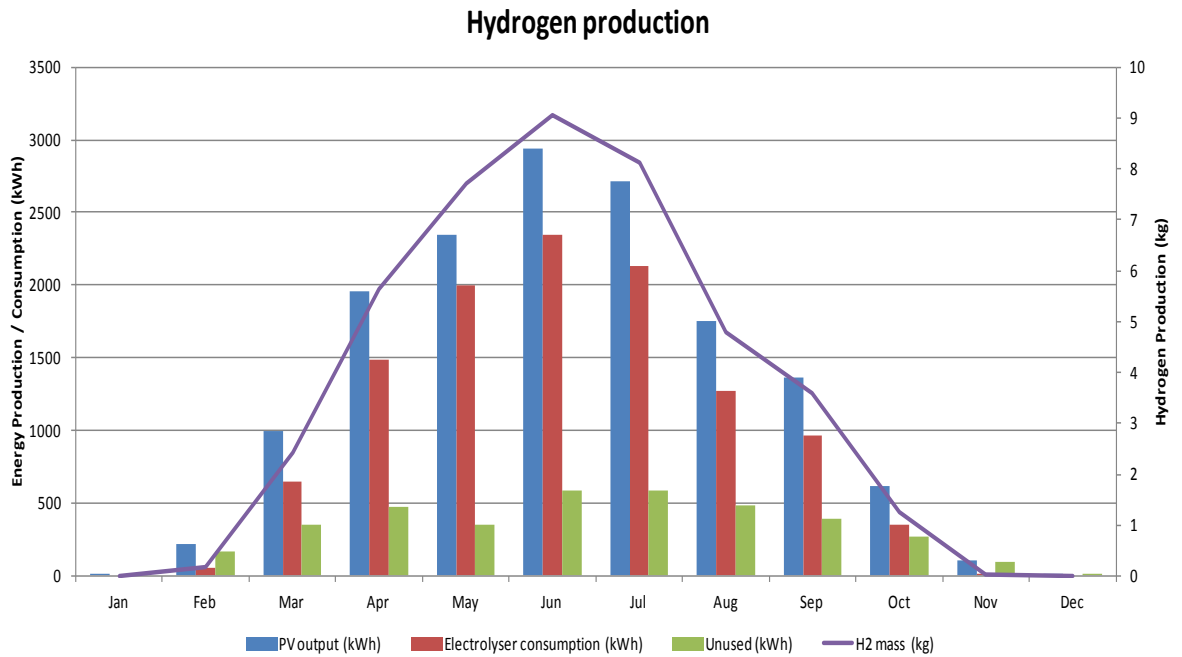
Figure 5-7: Simulation output of renewable H₂ production fed from PV

Figure 5-6 shows that there are much lower production rates during the winter months than in the summer months. During the winter months, the hydrogen production rate is very low, and much of the energy available for electrolysis is lost as the power available from the PV is not exceeding the 20% minimum threshold of the electrolyser to turn on. Conversely, during the summer months the production is much higher as the PV output improves.

The effect of the thermal transient is then considered by repeating the simulation for each month with the electrolyser temperature fixed to its working temperature (60°C), as was shown in Figure 5-3. The hydrogen production output from the thermally compensated model is then subtracted.

Subtracting the hydrogen output of the thermally compensated model from the hydrogen output of the fixed temperature model yields the cumulative effect of the thermal transients on overall hydrogen production during each month. The result of applying the proposed algorithm is shown in Figure 5-8. It can be seen that during the times of very low renewable production, the effect of thermal transients is much greater. This is due to low production levels and short durations of

operation, which accordingly limits the time available to bring the electrolyser up to full working temperature.
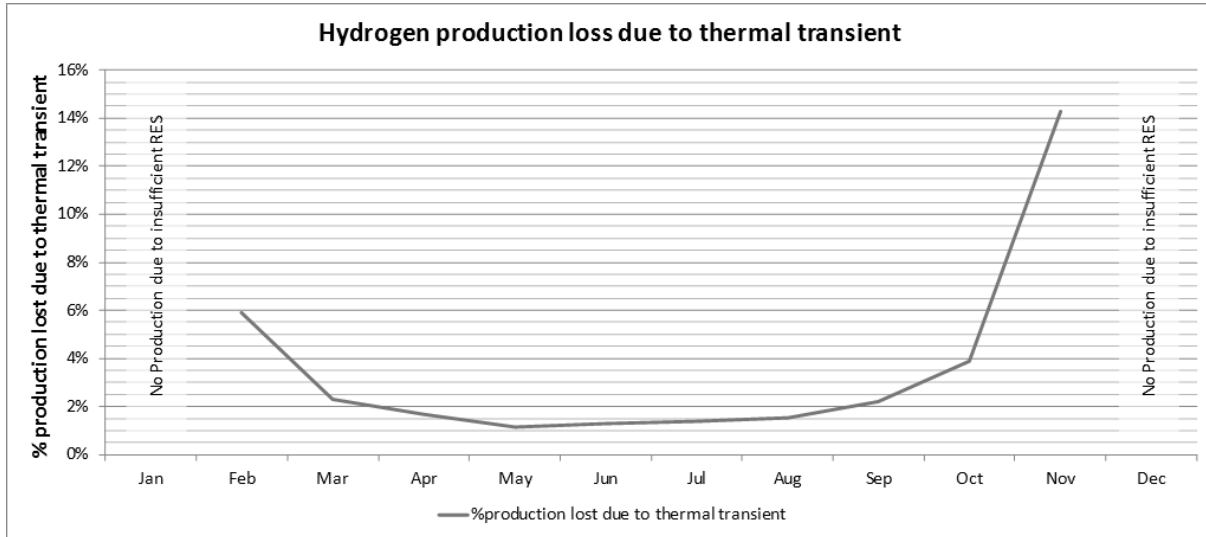
Figure 5-8: Effect of thermal Transient on hydrogen production (for a 30kW electrolyser)

5.4.2.1 Thermal Transfer Effects on Efficiency with Higher Temperature Electrolysis

As discussed previously, the higher the working temperature of an electrolyser, the better the hydrogen production efficiency becomes. Thus, the simulation summarised in Figure 5-8 was then repeated using a higher temperature alkaline electrolyser to identify whether or not a higher temperature electrolyser will incur a greater reduction on overall hydrogen production when operated in combination with renewable generation.

The electrolyser therefore considered for this simulation was a 26kW alkaline electrolyser with a working temperature of 80°C. The simulation process has been repeated using a smaller solar array model to match the slightly smaller power requirements of the higher temperature electrolyser. The PV array is also based around the BP380S 80Wp PV modules as used in the 30kW electrolyser simulation. To match the power output of the PV modules to the electrolyser, the PV modules are connected as four arrays each with 5 strings of 16 PV panels totalling 320 panels to give 25.6KW of electrical output.

As can be seen from the results of the comparison given in Figure 5-9, the impact of thermal transients on hydrogen production is very similar for both the 26kW and 30kW electrolysers. The very slight increase in thermal transient impact in the 26kW electrolyser can be attributed to the higher operational temperature. This originates from the longer time needed to reach this full working temperature as shown in Figure 5-10. Therefore it can be concluded that, the higher the temperature of operation, the longer the transient time period and the greater the impact on the overall production of hydrogen. This is particularly noticeable where the electrolyser works at the lowest limit of its production range (20%). This can be seen in the simulated PV output during the month of November when it was extremely low, resulting in extremely low hydrogen production and therefore an overall low hydrogen production efficiency in that month.
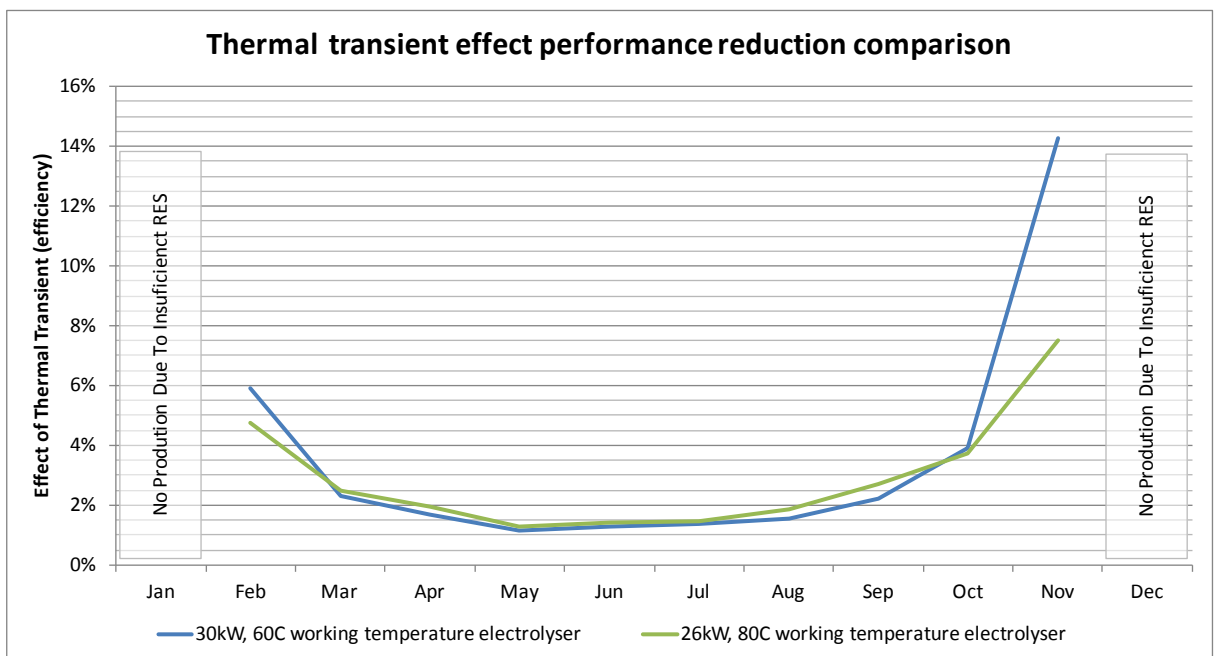
Figure 5-9: Comparison between 60°C and 80°C electrolysers
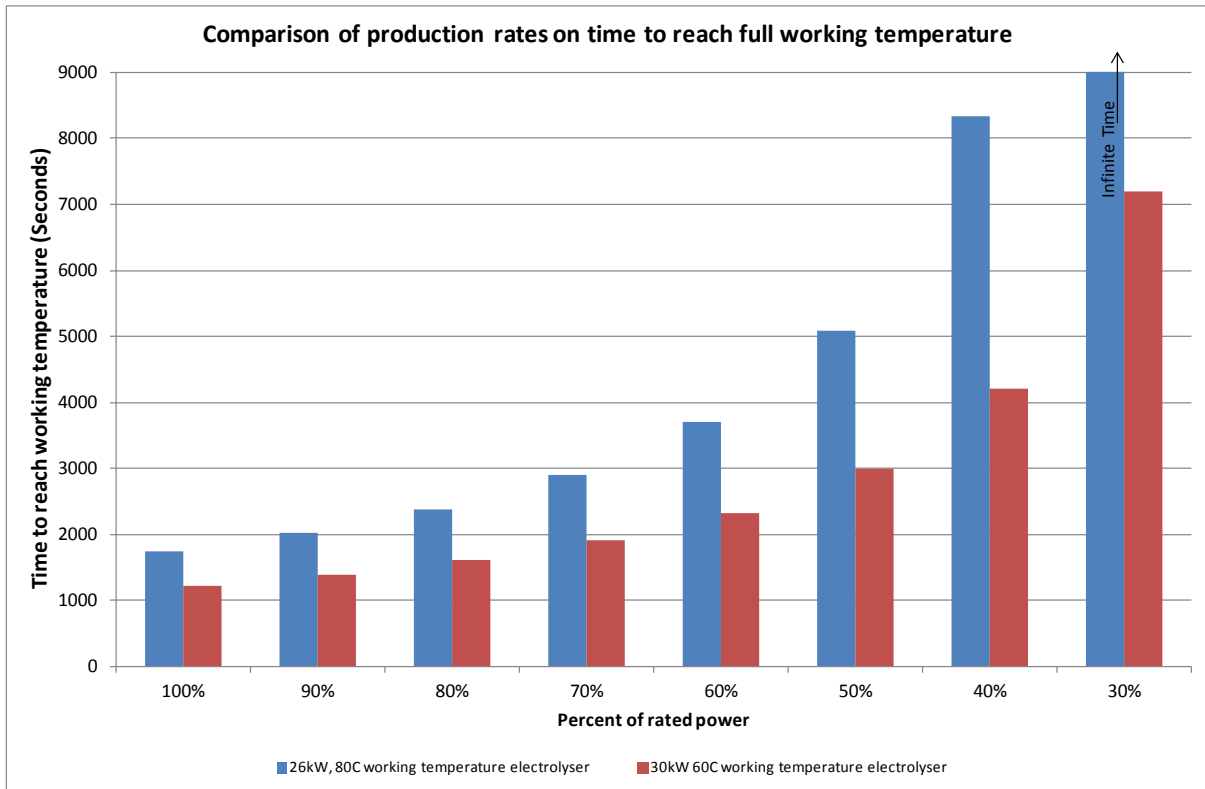
Figure 5-10: Comparison between 26kW and 30kW electrolysers' thermal transient time

5.5   Thermal Transients Summary

In this chapter, it has been shown that the effect of temperature on electrolyser performance has been well documented in literature. However, only one modelling tool, namely HydroGems, has the ability to simulate an electrolyser thermal characteristics effect on production efficiency. Furthermore, this tool has never been used to simulate the overall cumulative impact on hydrogen production from electrolysis when combined with renewable generation.

Therefore, a modelling algorithm has been developed here to simulate the impact of the electrolyser thermal transients (time taken for the electrolyser to reach its full working temperature) on the cumulative hydrogen production when operated in conjunction with renewable generation. The renewable generation can either be considered as grid constrained renewable generation, or as directly connected renewable generation.   In either case the electrolyser will be operated intermittently and at constantly changing variable power levels.

The proposed algorithm and the associated simulation in this chapter have shown that the variable and intermittent nature of a renewable energy source results in prolonged thermal transients. The prolonged thermal transients result in extended periods of time where the electrolyser is not producing hydrogen at its highest efficiency, therefore resulting in an overall reduction in hydrogen production. Using the proposed algorithm it was found that the typical effect of electrolyser thermal transients on production is to reduce cumulative hydrogen production in the region of between 1 to 3%. Where production is extremely low the effects can become much more pronounced, reducing overall hydrogen output to between a 6% and 14%. It could therefore be concluded that higher electrolyser utilisation minimises the effects of thermal transients on overall hydrogen production.

Furthermore, additional analysis has been conducted to investigate the potential impact of thermal transients on higher temperature electrolysers operating in combination with renewable generation. It has been found that hydrogen production for higher temperature electrolysers are only marginally more affected by the thermal production efficiency transient. It is then reasonable to conclude, that should extra high temperature electrolysis (in the region of 400°C) become commercially available, they will likely suffer from a much greater loss in the overall hydrogen production.

The simulations conducted demonstrate that thermal transients have a relatively low adverse effect on production, unless when prolonged production rates are extremely low. Therefore future HEST simulation could potentially use a thermally uncompensated model where high electrolyser utilisation is known to exist. However, the simulation has only been considered for two relatively small-scale electrolyser machines where the overall thermal mass is not too large. It is therefore reasonable to conclude that the thermal transient effect on large industrial scale electrolysers of 1MW and above will have the potential to be much larger. This is due to the much greater thermal mass associated with a very large electrolysis machine, hence having a much larger effect on hydrogen production. Therefore in such cases, the use of a constant temperature model is not suitable and it is sensible to investigate the thermal transient effect on overall hydrogen production.

6

---

6 Constrained Renewable for Hydrogen Refuelling

A recent pathways analysis study has found out that the use of hydrogen is essential for reducing the carbon emissions of the transport sector [125]. It has further been found (as discussed in chapter two) that the application of hydrogen production by electrolysis served the requirement for controllable demand side managed (DSM) loads to act as sinks for constrained renewable energy. Additionally (as investigated in chapter 3), hydrogen can realise a more competitive financial value if hydrogen produced from constrained renewable generation is delivered to market as a high value gas rather than used for conversion back to electrical energy for use 'on-grid'.

Whilst refuelling vehicles with hydrogen is a very quick process (in the order of 3 to 5 minutes), many hydrogen fuelling stations rely on a small, low power, low volume compressor to replenish the stationary fuel tanks between refuelling operations [126]. This process results in a dynamic miss-match between fuelling operations. It also affects the ability of a refuelling station to replenish its stationary storage tanks between refuelling operations. This mismatch increases when an intermittent renewable source is used as the source of energy to generate hydrogen for transport use. Therefore, it is important to check by simulation if a renewable resource is dynamically and

autonomously able to produce and store enough hydrogen for refuelling purposes. This is particularly important where constrained renewable energy is used, and it becomes vital to be able to simulate the dynamic ability of a refuelling station to replenish itself before the next vehicle refill.

A number of models have been developed in literature to simulate hydrogen pressure, volume and mass flows within a refuelling station to optimise hydrogen delivery into a vehicle [127]. However, a model that supports the analysis of refuelling station pressure volume and mass flows from a constrained renewable source of hydrogen production has not yet been investigated.

Therefore, a hydrogen mass transfer model for analysing the replenishment dynamics a hydrogen refuelling station between refuelling operations when supplied from a grid constrained renewable source is proposed in this chapter. Refuelling station configurations together with the best configuration for use with constrained renewable energy will be first investigated. The proposed mass transfer model for hydrogen refuelling station replenishment between refuelling operations is then developed. The developed model is then validated in a case-study. The aim is to analyse the ability of a small hydrogen refuelling station supplied by grid constrained renewable energy to meet the demands of a hydrogen vehicle.

6.1   Refuelling Station Operational Design

Hydrogen used for automotive applications can be stored on-board a vehicle in either a gaseous, liquid or solid form. The storage of hydrogen on board a vehicle in liquid form requires cryogenic cooling of hydrogen gas resulting in a very energy intensive storage process and is not commonly used [128]. In addition, metal hydride (solid) hydrogen storage is not commonly used outside of material handling applications (e.g., forklifts) as the storage medium incurs a significant weight disadvantage [129]. Therefore, gaseous hydrogen storage is the most commonly used form of hydrogen storage for transport applications and is the focus of this chapter.

Typically there are four configurations commonly used in the design of a gaseous hydrogen refuelling station [130]. These are:

- Direct compression

- High Pressure Buffer tank

- Hybrid High Pressure Buffer tank

- High pressure cascade

For each configuration, there is a source of hydrogen production and some form of compression to enable high pressure hydrogen to be rapidly delivered to a hydrogen fuelled vehicle. Usually the hydrogen is provided by an 'on-demand' source, such as reformed natural gas, bulk hydrogen storage, pipeline, or on-demand electrolysis. However for the case under investigation in this section, the hydrogen source is considered as supplied from a constrained renewable source. Therefore the replenishment phase for the refuelling station is shown in the four configurations that are described in more detail below.

6.1.1 Direct Compression

In a direct compression configuration, the output from the hydrogen source is held in a small volume, low pressure buffer tank. When a vehicle refuelling operation is conducted, the hydrogen gas is generated on-demand from the hydrogen source and compressed directly into the vehicles on-board storage tank. A simplified overview of a direct compression refuelling station is shown in Figure 6-1.

The advantage of direct compression refuelling operations is that there is very little hydrogen gas stored within the refuelling station. However, refuelling operations requires the power source to be available at the time of refuelling. Furthermore, a high-power, high-flow compressor must operate at the same time as the electrolyser produces hydrogen at refuelling time. The low volume of hydrogen storage coupled with a high-power, high-flow compressor significantly reduces the flexibility a refuelling station of this type has. Therefore, such a configuration would be unsuitable for operation in conjunction with an intermittent and variable renewable energy source.
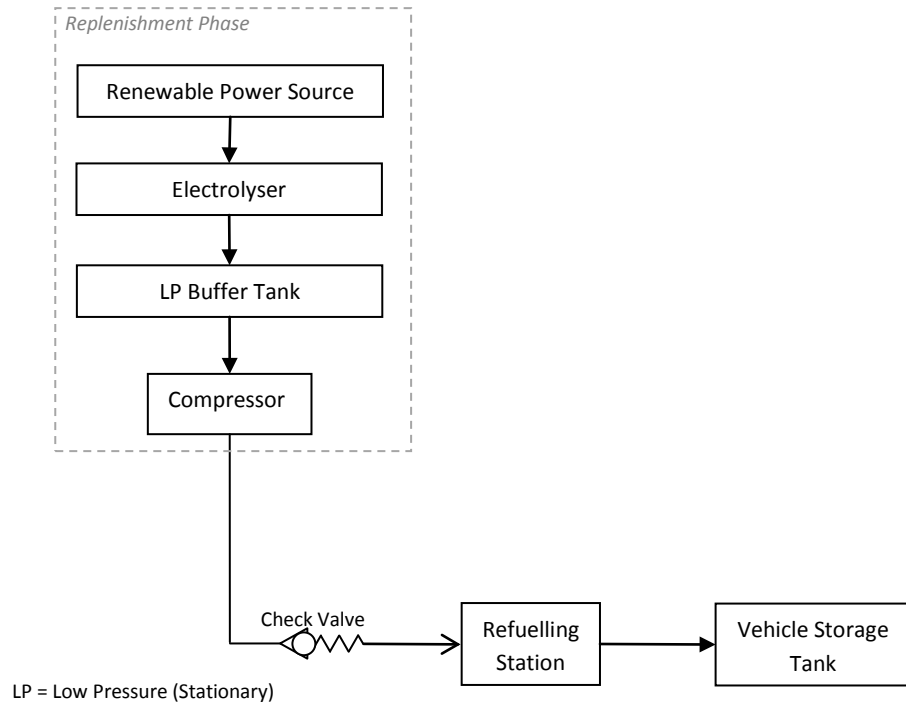
Figure 6-1: Example of a direct compression refuelling station

6.1.2   High Pressure Stationary Tank

To improve the flexibility of a hydrogen refuelling station for operation with a renewable energy source, a large stationary hydrogen storage tank can be added. An example of a simplified high pressure stationary tank refuelling station configuration is shown in Figure 6-2.

In a high pressure stationary tank design, hydrogen is produced and then compressed into a Large Stationary High Pressure Storage Tank (LSHPST) between refuelling operations. During a refuelling operation, high pressure hydrogen stored within the LSHPST is transferred to the vehicle through what is known as a mass transfer process. A mass of hydrogen within the LSHPST will flow into the lower pressure vehicle tank until the required 'full' pressure is reached. When the vehicle storage tank is connected to the refuelling station, a valve is opened allowing hydrogen to flow into the vehicle's on-board storage tank. Once the required mass of hydrogen has transferred to the vehicle and the required pressure is reached, the refuelling operation is stopped.

The main advantage of a high pressure buffer tank design over a direct compression design is that the refuelling phase can be completed very quickly. In addition, the high pressure buffer tank can be

replenished in a more flexible manner with a smaller compressor than direct compression refuelling station designed. However, in order to achieve a complete refuelling operation, the stationary high pressure storage tank must be very large. The stationary hydrogen storage must also be held at a much greater pressure than the vehicle storage tank so that refuelling operation can be successfully completed.

Replenishment Phase

Renewable Power Source

Electrolyser

LP Buffer Tank

Compressor

Check Valve

Large stationary HP Single Tank

Refuelling Station

Vehicle Storage Tank

LP = Low Pressure (Stationary)
HP = High Pressure (Stationary)
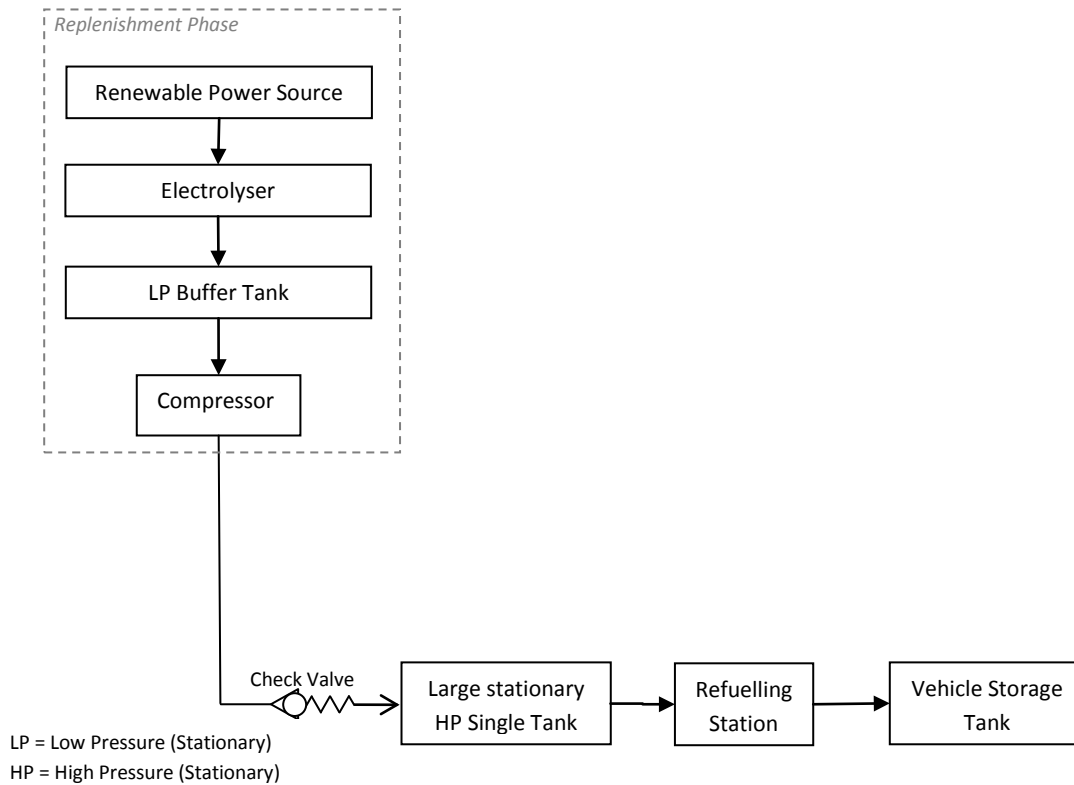
Figure 6-2: Example of a high pressure buffer tank refuelling station

6.1.3   Hybrid Intermediate Pressure Stationary Tank

To reduce the quantity of extremely high pressure hydrogen stored within a hydrogen refuelling station a hybrid configuration can be implemented. In the hybrid intermediate pressure stationary tank design, hydrogen is stored within the refuelling station at an intermediate pressure as shown in Figure 6-3.

During a refuelling operation, the stationary intermediate pressure tank is used to directly fill the on-board vehicle tank in a hydrogen mass transfer process similar to the high pressure stationary tank concept. However due to the intermediate pressure of the stationary storage, it is not possible to reach 100% of hydrogen transfer into the vehicle. This is because there is insufficient pressure to

push the required hydrogen mass into the vehicle storage tank. Therefore the remainder of the hydrogen transfer is completed by the refuelling station compressor. During a refuelling operation hydrogen cannot be replenished into the refuelling stations intermediate pressure storage.

The requirement to use the refuelling station compressor during the refuelling operation greatly increases the refuelling operation time. In addition to this, the use of the compressor during the refuelling operation reduces the flexibility of this type of design for use with an intermittent power source.

LP = Low Pressure (Stationary)
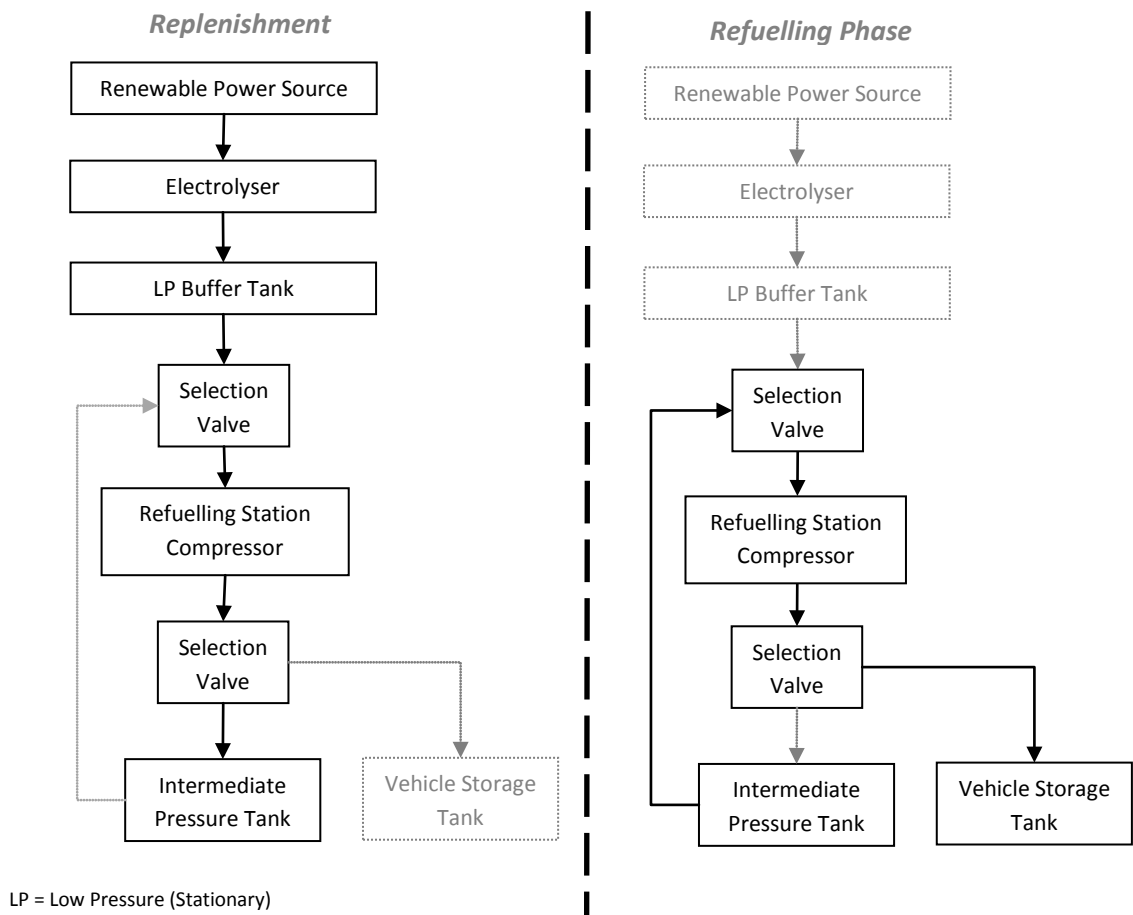
Note: Greyed out sections denote they are disconnected. During the replenishment phase, the vehicle cannot be refuelled. During refuelling operations, there is no hydrogen production.

Figure 6-3: Example of a hybrid pressure buffer tank refuelling station

6.1.4   High Pressure Cascade

A high pressure cascade refuelling station design offers a compromise to the aforementioned configurations. It uses a small compressor, in some instances known as a booster, to replenish the refuelling station's hydrogen store. In a cascade refuelling operation, hydrogen held in the stationary store is transferred into the vehicle fuel tank in three stages. This is illustrated in Figure 6-4.
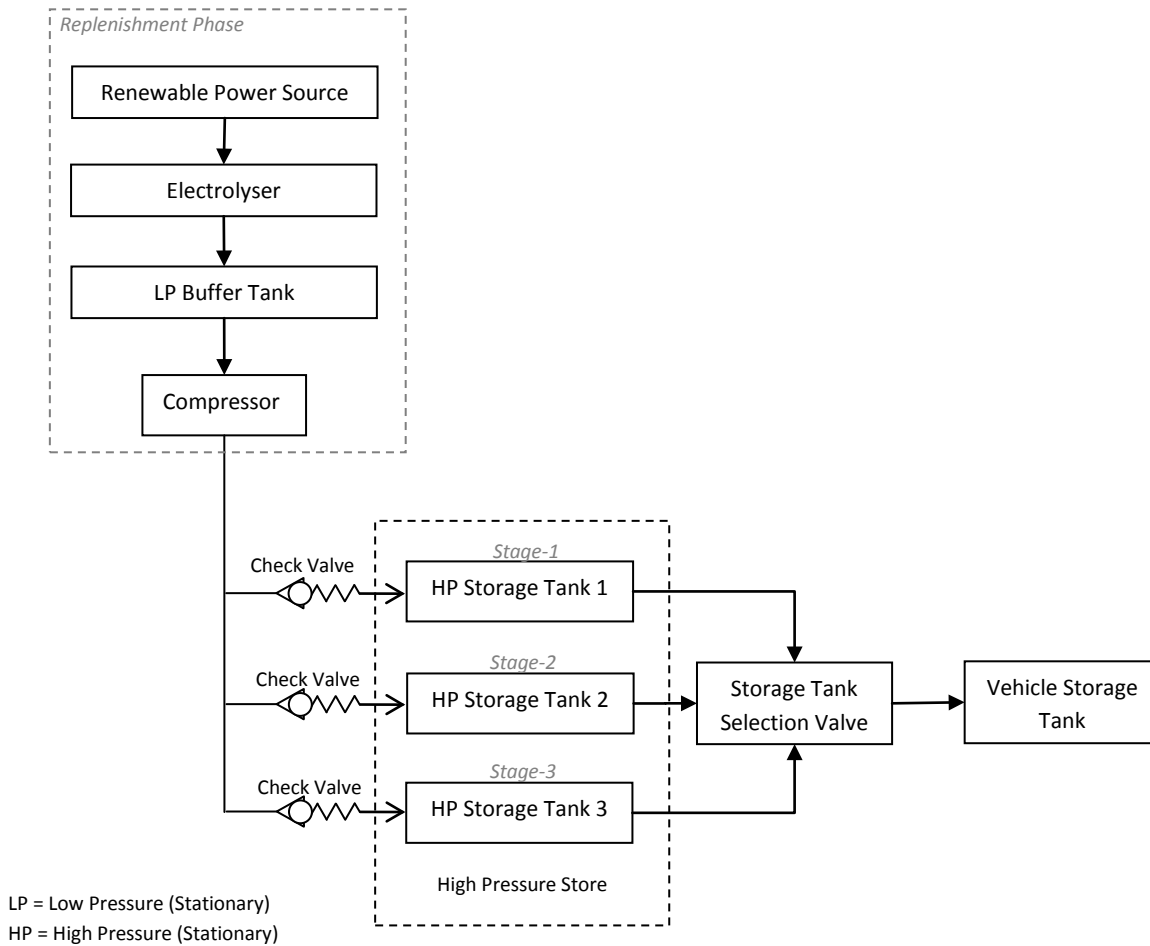
Figure 6-4: Example of a high pressure cascade refuelling station

The three stage cascade refuelling operation is conducted in three discrete steps as follows:

1.   The first stage involves connecting a stationary hydrogen storage tank, known as tank-1 (with pressure equal to P_1), to the automotive storage tank (V-tank). When these are connected, hydrogen from tank-1 is released into the automotive vehicle tank and the pressure between the two tanks equalises to give pressure (P_2).

2.   The first stage (tank-1) is then disconnected from the vehicle storage tank. The second stationary hydrogen storage tank, known as tank 2 (P_3), is then connected to the vehicle

tank (V-Tank). The pressure is again allowed to equalise between the two pressure vessels.

3. The second stage (tank 2) is now disconnected from the vehicle storage tank. The third stationary hydrogen storage tank, known as tank 3, is then connected to the vehicle refuelling tank. Once more the pressure (P4) equalises between the two pressure vessels for the final time to achieve the desired 'full' pressure.

Once a three-stage refuelling operation is completed, the hydrogen refuelling station is replenished with hydrogen from an electrolyser that is powered from an intermittent renewable resource. The use of a three stage cascade refuelling station design provides the most efficient refuelling station design due to the use of small compressor/booster. Additionally, the use of 3-stage cascade refuelling has the benefit of reducing the quantity of hydrogen stored within the refuelling station by up to 20% [131].

6.2   A Renewable Hydrogen Refuelling Station Mass Transfer Model

The use of a high pressure cascade refuelling station combines the advantages of a simple high pressure equalisation process with the flexibility of onsite hydrogen storage. The primary advantage of a cascade refuelling station design is that it can deliver hydrogen with a 20% reduction in on-site storage requirements. In addition, and in contrast to direct compression refuelling, the requirement for a very high power, high flow compressor is removed.

The thermo-dynamic modelling of hydrogen refuelling stations has been used to optimise the configuration of pressure vessels within a refuelling station for achieving the quickest possible refuelling time [132]. Thermodynamic modelling has also been applied to on-board vehicle hydrogen storage to identify the impact of thermal effects during hydrogen transfer [133]. Furthermore, previous studies using a combination of thermodynamics and Computational Fluid Dynamics (CFD) modelling techniques found that over and under filling of hydrogen storage tanks resulted from cascade refuelling operations. However, it was acknowledged that hydrogen fuelled vehicles are nowadays designed with communication equipment installed to communicate real values of hydrogen mass transferred from refuelling station to the vehicle. This removes the potential for over and under filling caused by the thermodynamic effects of expanding and contracting hydrogen gas in refuelling operations [134].

The application of spatial planning techniques has also been used to identify the most suitable location for hydrogen refuelling infrastructure when used in conjunction with renewable generation [135]. However, no reference to modelling the ability of constrained renewable sources to deliver hydrogen into a cascade refuelling application can be found in literature. In other words, no models have been developed to define if there will be sufficient hydrogen generated and transferred into a refuelling station from constrained renewable generation to refill a vehicle within these constrains.

Therefore, a refuelling station hydrogen mass transfer model specifically developed for systems with constrained energy availability is proposed. The proposed model considers the use of a high pressure cascade refuelling station concept due to the benefits that such a design offers. The proposed model enables the hydrogen mass flow simulation of a high pressure cascade refuelling station coupled with a constrained renewable hydrogen resource. The model is developed based on the renewable hydrogen fuelling station shown in Figure 6-4.

Note: The proposed model described enables the simulation of hydrogen mass transfer from each of the high pressure tanks to the vehicle. The replenishing of the high pressure hydrogen storage tanks from an electrolysis source and booster compressor is also shown.

Before the first refuelling operation occurs, it is assumed that the stationary high pressure (HP) tank is full. As such and as the HP tank is full, the refuelling station can begin the refuelling operation. The three stages for filling the vehicle tank are as described in section 6.1 and the developed model for each stage is given in the following section. Once a cascade refuelling operation has been completed, the refuelling station then replenishes its internal hydrogen stores as soon as renewable power is available. It is further considered that the refuelling process utilises the communication processes described above to remove the thermo-dynamic effects of hydrogen mass transfer, therefore enabling the correct amount of hydrogen to be delivered to the vehicle.

6.2.1 Cascade Refuelling Stage-1

Using ideal gas laws, gas constants and 'real gas' Z correction factors (described in Appendix A), the first stage of hydrogen refuelling can be modelled by equations 6-1 to 6-8 as follows:

Cascade refuelling Stage-1 Inputs

T = Ambient temperature

P_1 = Pressure of stationary cascade hydrogen storage tank-1

V_1 = Volume of stationary cascade hydrogen storage tank-1

T_1 = Temperature of stationary cascade hydrogen storage tank-1

n_1 = moles of hydrogen stored in stationary cascade hydrogen storage tank-1

R = Universal Gas Constant: R=8.314472 J/(mol K)

P_2 = Pressure at the end of stage-1 refuelling operation

V_2 = (V_1) + (volume of automotive application (V_{Tank}))

T_2 = temperature of storage tank-1 and vehicle tank after stage-1 refueling.

n_2 =molar quantity of hydrogen after stage 1 refuelling is complete

M = Molar Mass (2.01588g/mol)

V_{Tank} = Automotive hydrogen storage tank volume

n_{Tank} = Automotive tank stored hydrogen molar quantity

Z_1 = correction factor for stationary cascade hydrogen storage tank-1

Z_2 = correction factor after stage-1 refuelling operation

Where:

$$P_1V_1 = Z_1 n_1 \bar{R} T_1 \ \therefore \ n_1 = \frac{P_1V_1}{Z_1RT_1} \qquad\qquad (6\text{-}1)$$

$$P_2V_2 = Z_2 n_2 \bar{R} T_2 \ \therefore \ n_2 = \frac{P_2V_2}{Z_2RT_2} \qquad\qquad (6\text{-}2)$$

During the first stage of refuelling, the moles of gas present before (n_1) and after (n_2) the refuelling operation will be the same since the vehicle tank is empty. Therefore:

$$n_1 = n_2 \qquad\qquad (6\text{-}3)$$

Equations 6-1 and 6-2 can therefore be combined with equation 6-3 to give equation 6-4

$$\frac{P_1V_1}{Z_1RT_1} = \frac{P_2V_2}{Z_2RT_2} \qquad\qquad (6\text{-}4)$$

When the empty vehicle hydrogen storage tank (*V-tank*) is connected to the full tank-1 hydrogen storage tank (with volume V_1), the final cascade refuelling pressure (P_2) at the end of stage 1 must be calculated by solving the equation 6-4 for P_2 as follows:

$$P_2 = \frac{P_1 V_1 Z_2 R T_2}{Z_1 R T_1 V_2}$$

(6-5)

At the end of stage-1 we consider the end pressures, volumes, temperatures and densities of hydrogen gas to have reached equilibrium after hydrogen gas equalisation has completed. The flow rate of hydrogen between tanks is closely controlled in the refuelling station to minimise large temperature changes that occur when gas is expanded from one vessel to another. This means we can consider $T = T_1 = T_2$ and therefore equation 6-5 can be simplified to equation 6-6 for finding P_2:

$$P_2 = \frac{P_1 V_1 Z_2}{Z_1 V_2}$$

(6-6)

Using the values of P_2 and Z_2 and only the automotive tank volume (V-Tank) as V_2 in equation 6-7, it is then possible to calculate the number of hydrogen moles transferred.

$$n_{tank} = \frac{P_2 V_{tank}}{R T Z_2}$$

(6-7)

The mass (m) of the hydrogen contained within the automotive tank (V-Tank) is then found as the product of the number of moles of gas molecules present (n) and the molar mass (M) of Hydrogen as shown in equation 6-8.

$$m = n.M$$

(6-8)

At the end of cascade refuelling operation stage 1, the developed mathematical model provides:

- Final equalisation pressure and therefore pressure of automotive tank (P_2)
- Mass of hydrogen transferred to automotive storage tank (Kg)

- Number of moles of hydrogen (n_{tank}) transferred to automotive storage tank (which is required for calculating stage 2 refuelling operation)

6.2.2   Cascade Refuelling Stage-2

The stage-2 cascade refuelling model utilises the same equations-set as stage 1, however the calculation methodology is slightly different due to the fact that the automotive hydrogen tank now contains a quantity of hydrogen. Stage-2 of the cascade refuelling model starts with the number of moles of hydrogen contained within the automotive tank (n_{tank}) calculated from stage-1.

The first equation in the stage-2 model (equation 6-9) calculates the molar quantity of hydrogen (n_3) contained within tank-2, the stage-2 hydrogen storage. The automotive tank already contains hydrogen at the start of stage-2 refuelling therefore $n_{tank} \neq n_3$ in this case. Thus n_3 can be found as follows:

$$P_3 V_3 = Z_3 n_3 \bar{R} T_3 \quad \therefore \quad n_3 = \frac{P_3 V_3}{Z_3 R T_3} \tag{6-9}$$

Where: n_3 = molar quantity of hydrogen stored in stationary tank-2

V_3 = volume of stationary storage tank-2

T_3 = T = temperature of storage tank-2

P_3 = pressure of storage tank-2

Z_3 = correction factor for stationary cascade hydrogen storage tank-2

The total molar quantity of hydrogen now present when the automotive tank is attached to the hydrogen storage tank-2 can be expressed as n_4 as shown in equation 6-10.

$$n_4 = n_{tank} + n_3 = n_{tank} + \frac{P_3 V_3}{Z_3 R T_3} \tag{6-10}$$

The total moles n_4 is therefore contained within the combined volume of the automotive tank (V_{tank}) and hydrogen storage tank-2 (V_3). Consequently the equalisation pressure (P_4) of the total molar quantity of hydrogen n_4 can now be calculated using equation 6-11.

$$P_4 = \frac{Z_4 n_4 \bar{R} T_4}{(V_{tank} + V_3)} \qquad (6\text{-}11)$$

Where: P_4 = combined molar quantity of hydrogen stored in stationary tank-2 + V_{tank}

      T_4 = T = temperature of storage tank-2

      n_4 = combined molar quantity of hydrogen in stationary tank-2 + V_{tank}

      Z_4 = correction factor for combined hydrogen storage tank-2 + V_{tank}

      V_3 = volume of stationary storage tank-2

      V_{tank} = automotive hydrogen tank volume

With the equalisation pressure (P_4) now known, along with the volume of the automotive tank (V_{tank}), the corresponding molar quantity (n_5) and mass (m_{tank}) of hydrogen contained within the automotive tank can be found as shown in equation 6-12.

$$m_{tank} = M n_5 = M \frac{P_4 V_{tank}}{Z_4 R T_4} \qquad (6\text{-}12)$$

At the end of cascade refuelling operation stage 2, the model provides:

1. Final equalisation pressure and therefore pressure of automotive tank (P_4)

2. Mass of hydrogen (m_{tank}) transferred to automotive storage tank (Kg)

3. Number of moles of hydrogen (n_5) transferred to automotive storage tank (required for calculating stage 3 refuelling operation)

6.2.3 Cascade Refuelling Stage-3

The model for the final refuelling stage is similar to the stage 2 model with the molar quantity of stage 2 passed to stage 3, and the stationary value of hydrogen tank-3 used.

6.2.4 Replenishment Phase

When a cascade refuelling operation is completed, the mass and pressure of hydrogen within the three high pressure tanks (shown in Figure 6-4) are known after the vehicle storage tank is disconnected. This is calculated using the previously described 3-stage refuelling station model.

When the refuelling station is in a hydrogen depleted state after a refuelling operation, it requires to be replenished. This is known as the replenishment phase. During the replenishment phase, 'new' renewably produced hydrogen is generated using an electrolyser powered from constrained renewable energy. The produced hydrogen is momentarily stored in a low pressure (LP) buffer tank until sufficient pressure has been developed to allow the booster compressor to start. Hydrogen is then transferred from the low pressure (LP) buffer into the high pressure (HP) refuelling station cascade storage tanks.

It is possible to simulate the transfer of hydrogen from the electrolyser and associated low pressure (LP) hydrogen buffer using the transfer characteristics for the hydrogen booster/compressor. The proposed algorithm that simulates the replenishment of the refuelling station is shown in Figure 6-5.
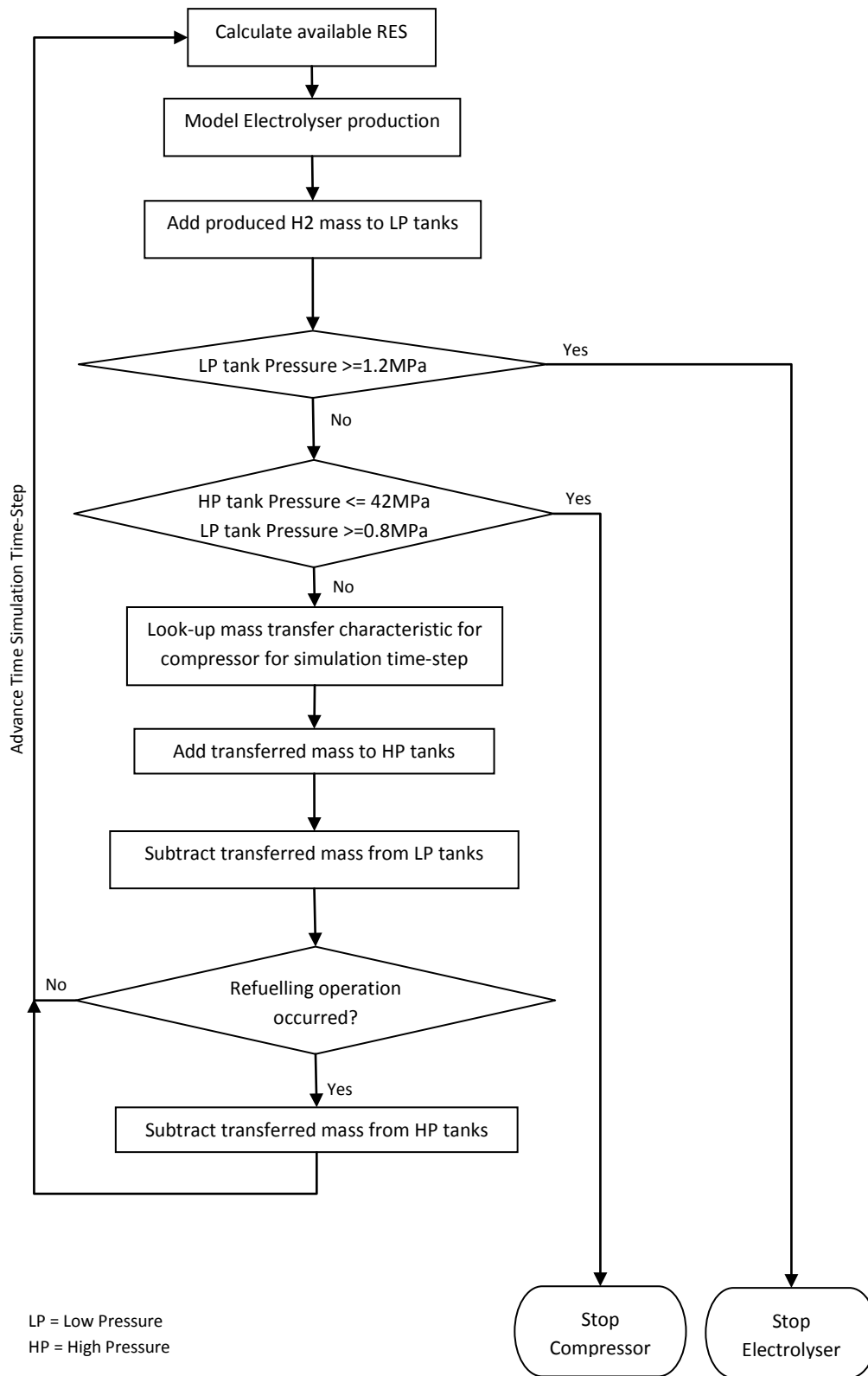
Figure 6-5: Proposed algorithm that simulates the replenishment of the refuelling station

Manufacturer's mass transfer characteristic of a hydrogen compressor is used to simulate the transfer of hydrogen from the LP buffer to the HP cascade storage. The transfer rate of the hydrogen

compressor is affected by the inlet pressure (LP Tank pressure) and outlet pressure (HP tank pressure). Therefore the hydrogen's mass transfer rate is a function of the compression ratio of the compressor.

Due to the low thermal mass of the compressor and internal hydrogen volume, the very tight management of gas temperatures in commercial compressors and the slow transfer speed, the thermal behaviour of hydrogen under compression is not considered. Furthermore, the transfer characteristic of the compressor is already thermally compensated meaning that the effects of temperature have already been factored into the compressors transfer flow rate. An example of a compressor characteristic 'curve' is shown in Figure 6-6, where the values of gas transfer are shown.
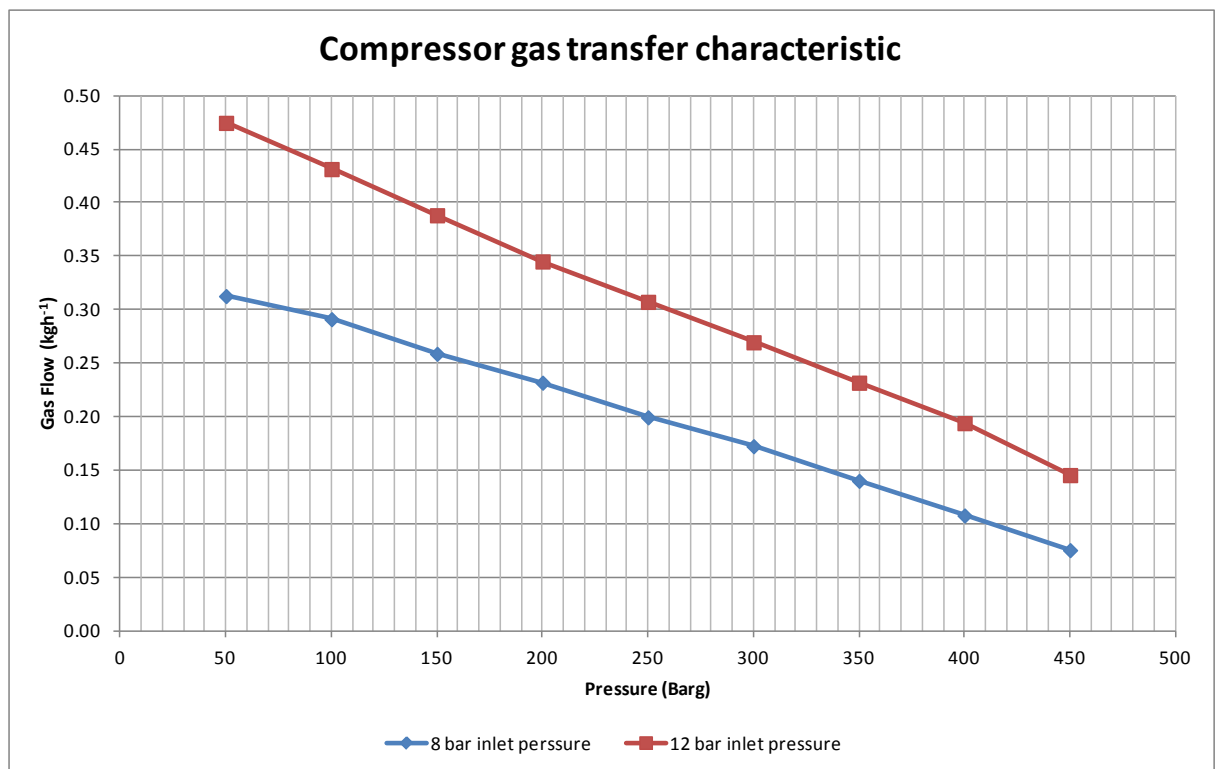
Figure 6-6: Gas compressor typical gas transfer characteristic

6.3 Case Study

The following case study is used to illustrate the application of the proposed hydrogen mass transfer model for analysing the replenishment dynamics of a hydrogen refuelling station between refuelling operations when supplied from a grid constrained renewable source.

The selected case study is based on Renewable Biogas that being produced at Comhairle nan Eilean Siar (CnES)'s Integrated Waste Management Facility (IWMF) from the anaerobic digestion of municipal organic waste [64]. The rate of biogas production varies depending on the composition and quantities of organic waste fed into the anaerobic digester.

The produced biogas is fed to a 240kWe gas engine generating electricity and heat which are partially re-used to supply the IWMF's energy demands. Excess electricity export is restricted by the electricity Distribution Network Operator (DNO) due to stability constraints. As there are constraints on exporting the electrical energy on to the power grid network, the excess is used to provide power for hydrogen production and storage. This hydrogen is then used for a transport application. Unfortunately, the biogas production rate is variable and results in the gas engine operating intermittently, but in a predictable fashion. In other words, it is possible to determine when electrical power will be available from the biogas plant.

Note: When the biogas engine is generating electricity, the Hebridean Hydrogen Seed (H$_2$SEED) facility uses the limited and constrained excess electricity to power a 5.33Nm^3.hr^{-1} or 0.46kg.hr^{-1} alkaline electrolyser at Standard Temperature and Pressure to generate hydrogen for typically 10 hours per day.

6.3.1   The Hydrogen Vehicle

The hydrogen demand in this case study is based on the characteristics of the converted petrol-hydrogen bi-fuelled Ford Transit supplied as a technology demonstrator [136]. The case study hydrogen vehicle utilises 350 bar on-board hydrogen storage tanks that are similar to many other demonstration vehicles [137,138]. The case study vehicle details are given in Table 6-1 :

Parameter	Value
Model year	2009
Fuel	Petrol / compressed hydrogen (350bar)
Fuel capacity	Petrol: 80litre. Hydrogen: three tanks (2x74litre, 1x39litre) totally 4.5kg at 350bar (Low pressure alarm/warning occurs at 20 bar)
Engine	2.3 litre displacement capacity with spark ignition
Engine Cylinders	Straight 4
Engine Power	104kW (petrol); 75kW (estimated, hydrogen)
Supercharger	Belt-driven with intercooler provides additional combustion air when running on hydrogen gas
Vehicle range (un-laden)	Urban - 82 miles; Motorway - 135 miles (estimated)

Table 6-1: **Manufacturer's vehicle details [136]**

The total on-board hydrogen capacity of the vehicle is 4.52kg H_2 at 350bar and 15°C. Due to the low pressure safety alarm the transient on-board capacity is considered as 4.2kg H_2. This is based on the "low pressure" alarm occurring at 20bar with the expectation that the vehicle will be switched to petrol operation at this point.

Note: 20bar equates to 6% (20/350) of the full capacity of 350bar, therefore 94% of 4.52kg of H_2 is found to be 4.2kg H_2.

The vehicles range has been reported to be between 80 – 85 miles (130 – 160km) on one re-fill. The vehicle starts its journey with a full tank at 350bar and stops at the "low pressure" alarm of 20 bars. Hydrogen consumption can therefore be considered as 19-20 miles/kg (given the range 80–85 miles/4.2kg), or 31-38km/kg (130–160km/4.2kg).

The vehicle is operated up to a maximum of 6 days a week (Monday to Saturday inclusive) covering close to the maximum range reported by the vehicle manufacturer every day. Therefore, it is reasonable to consider that the vehicle will require a full refill of hydrogen each day.

As the vehicle can only consume a maximum of 4.2kg due to the presence of the 'low pressure' alarm safety feature, the weekly demand for hydrogen can be calculated as 4.2 x 6 = 25.2kg. Whilst there is no demand for hydrogen on the 7th day (Sunday), it is possible for the refuelling infrastructure to be replenishing in this time.

6.3.2 HEST Configuration

The selected HEST configuration for the case study is the one shown in Figure 6-4. The hydrogen produced from the electrolyser passes directly to a low-pressure (LP) buffer storage at up to 1,200 KPa prior to compression to the high pressure (HP) storage at up to 42 MPa pressure. The Low Pressure (LP) buffer storage consists of two Manifold Cylinder Pack (MCP) modules providing a nominal storage volume (geometric capacity) of 9,600 litres. At 15°C and 1,200 kPa, the LP storage holds approximately 9.46kg of hydrogen.

The transient (or usable) capacity of the LP storage is dependent on the operating set points of the hydrogen compression system. With an upper set point of 12bar and lower set point of 9bar the transient capacity provided is 2.35kg. The transient capacity defines the quantity of hydrogen that can be transferred from the LP buffer storage to the HP storage prior to replenishing the buffer by operating the electrolyser.

The high pressure storage consists of a total of fifteen composite cylinders each with a nominal geometric capacity of 82 Litres, providing a total nominal volume of 1,230 litres. At 15°C and 42 MPa pressure, the HP storage holds approximately 34.1kg of hydrogen.

The refuelling station is capable of dispensing the stored hydrogen at up to 350bar to the vehicle storage vessels. A summary of the HEST case study system for transport application is shown in Figure 6-7
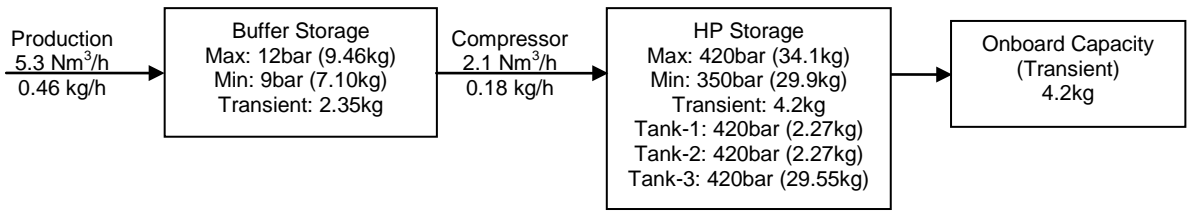
Figure 6-7: Overview of the hydrogen system for transport application

6.3.3 Case Study Simulation and Model Application

Starting from a full stationary tank, a simulation has been undertaken to identify if the vehicles daily hydrogen demand can be met by the onsite hydrogen infrastructure and constrained renewable energy.

A typical 7 day simulated profile of production, compression and demand are shown in Figure 6-8, Figure 6-9 and Figure 6-10. These have been simulated using the proposed model described in the previous section.
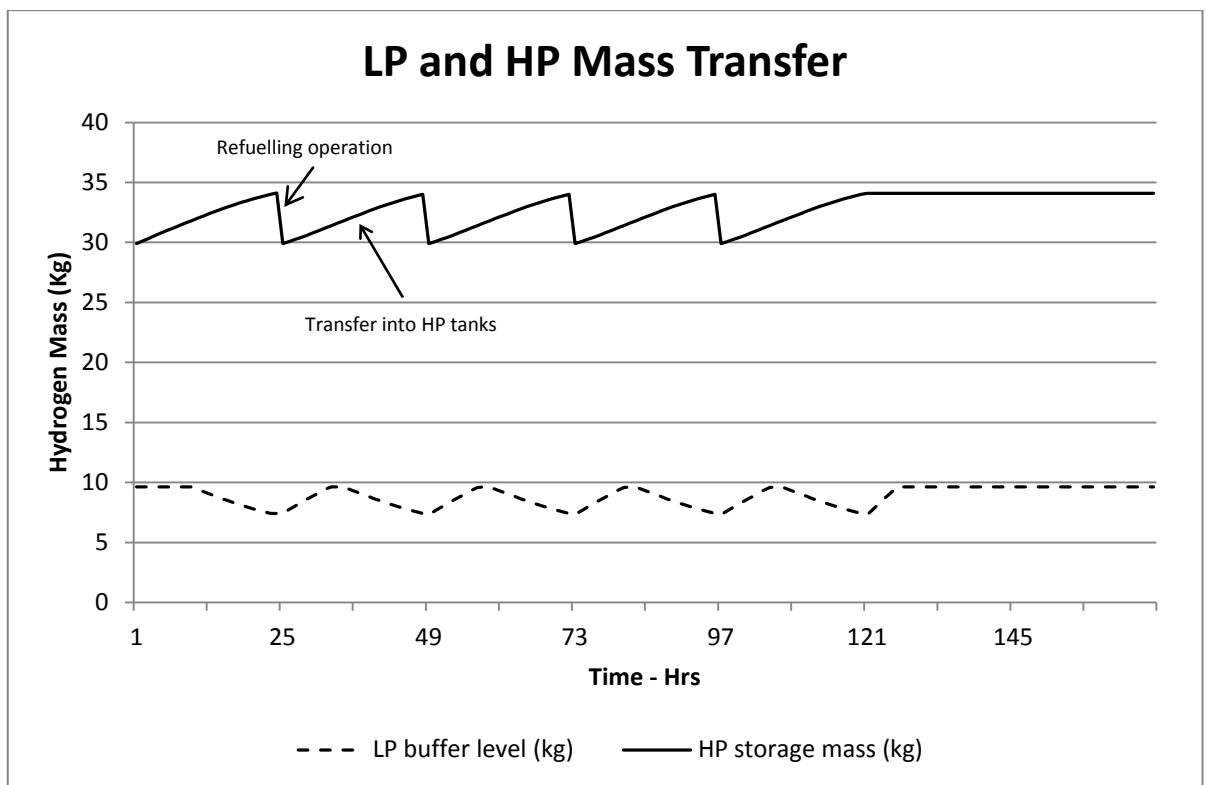
Figure 6-8: Hydrogen mass transfer between LP and HP storage systems

In Figure 6-8, the simulation shows the HP storage tanks hydrogen mass is oscillating between 34.1kg and 29.9kg. The sudden drop in HP storage mass is attributed to the refuelling operation occurring once per day (Monday to Saturday). As the HP storage tank level increases, the LP storage tank level falls. The slow rise from 29.9kg to 34.1kg results from hydrogen being transferred from the LP buffer to the HP storage by the hydrogen compressor. It has been found from the system simulation that the transfer process takes approximately 23 hours to be complete. The slow increase in the LP buffer vessel from 7.1Kg to 9.5kg results from the generation of new hydrogen from constrained renewable energy from the bio gas engine.

Figure 6-9: **Hydrogen production and transfer profile for 10hrs per day production**

In Figure 6-9 the simulation shows the Hydrogen mass transfer from the LP to the HP storage. The rate of transfer is given by the hydrogen compressors mass transfer characteristic (as shown in Figure 6-6). The hydrogen production rate (restricted by available renewable energy) is also shown.

Figure 6-10 shows the simulation results for the HP storage pressure profile during the refuelling and replenishing periods. The pressure cycling range of 35 to 42MPa (350 to 430 bar) shows that the

refuelling operation can always achieve 35MPa into the vehicle, and be replenished to 42MPa from the electrolyser and LP buffer tank. However, whilst the model has found that there is enough hydrogen produced from the constrained renewable energy via on-site electrolysis, there is a requirement to operate the compressor/booster for much longer periods of time to facilitate hydrogen transfer into to the high pressure cascade tanks.

Figure 6-8 and Figure 6-10 together show that the vehicle will always be able to refuel to its full pressure of 35MPa (350Bar), and full mass of 4.2kg as long as there is some auxiliary power available to maintain the compressor/booster operation. This is seen in the high pressure refuelling station storage tanks always obtaining 42kPA (420 Bar) of pressure. In other words the high pressure tanks always become full between refuelling operations. This therefore demonstrates that the modestly sized 5.3Nm^3/h, 30kW, 1,200KPa (12Bar) electrolyser powered from the grid constrained renewable energy is capable of meeting the hydrogen fuel demands of the vehicle. However, the hydrogen mass transfer requires a much longer time than that available from constrained renewable energy. Therefore an auxiliary 'always-on' supply would be required for the small compressor/booster.
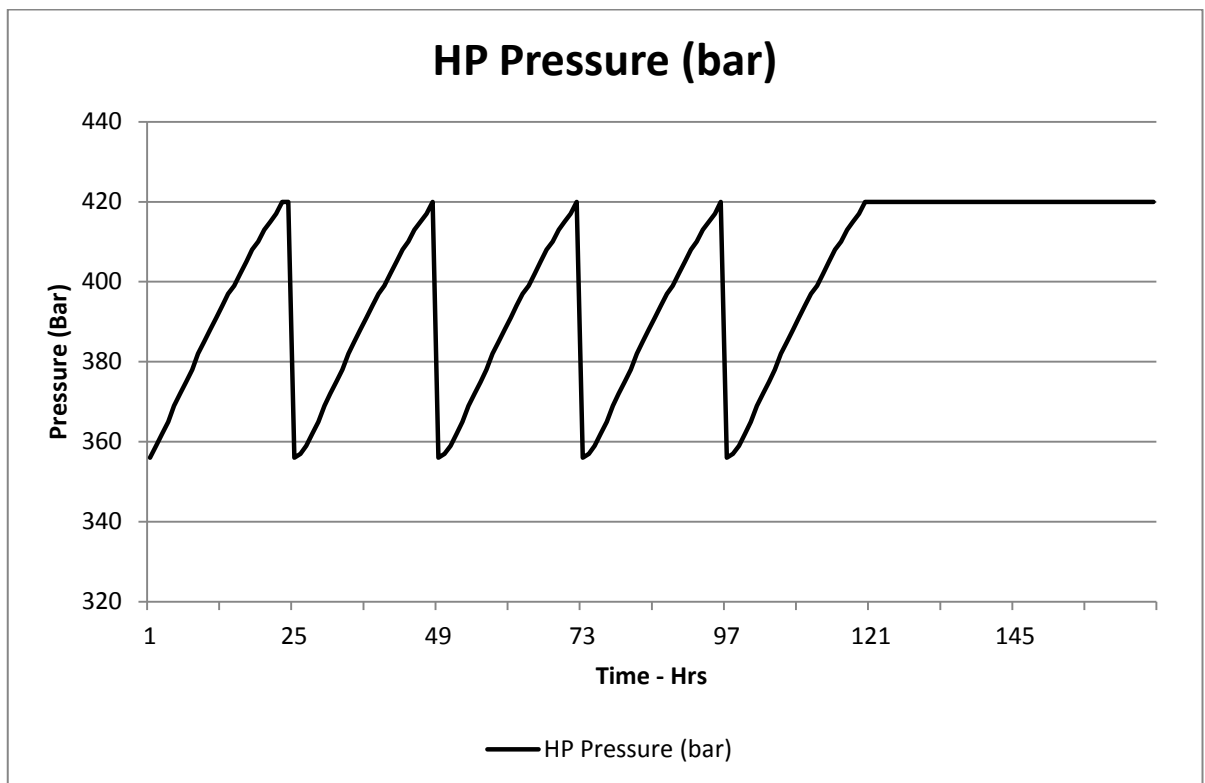

Figure 6-10: HP pressure cycle profile for 1 week of operation

6.4 Conclusion

In this chapter, it has been shown that high pressure cascading refuelling station configurations enable high speed refuelling operations with a 20% reduction in required hydrogen to be stored. Yet, modelling of hydrogen refuelling stations has been found to be limited. Existing models in literature focused on the complex thermo-dynamics of a refuelling stations ability to refuel a connected vehicle during refuelling operation. On the other hand, it has been found that the latest generation of hydrogen vehicles utilise a two-way communication with the refuelling station. This removes refuelling errors caused by the thermo dynamic effects of expanding and contracting gases, thereby reducing the need for complex thermo-dynamics refuelling station models for assessing the dynamics of replenishing the refuelling station.

Further to this, no dynamic analysis of the replenishment of a hydrogen refuelling station from a constrained renewable source has been found in literature. As such, a new analysis model has been proposed in this chapter. The aim was not only to assess the dynamic ability of a constrained source to produce enough hydrogen for fuelling, but also to quantify if the constrained RES is able to replenish the refuelling station before the next refuelling operations.

This chapter presented the development of the proposed hydrogen mass transfer model that can be applied to analyse replenishment of hydrogen into a refuelling station. The proposed model allows quantifying if a constrained renewable resource will generate sufficient hydrogen for a refuelling application. It also enables the analysis of the replenishment ability of the refuelling station to be completed. This therefore allows an assessment of the dynamic ability of constrained renewable generation to create and transfer hydrogen into the refuelling station.

The proposed model has then been tested and validated by using a case study of a small refuelling station supplied from a constrained renewable source. The application of the developed model onto this case study has shown that a relatively small electrolyser of $5.33Nm^3$/h (30kW) can meet the daily demands of commercial delivery vehicle from a constrained RES. However, in order to replenish the refuelling station with the hydrogen produced it has been found that an 'always-on' auxiliary power supply would be required to keep the compressor operating. In this case the constrained RES generation allowed for such 'always-on' power.

7

---

7   Conclusions & Further Work

This research project focused on investigating Hydrogen Energy Storage Technologies (HEST) to support their wider uptake and application in stabilising the power grid in the presence of increased renewable generation integration.   Summarised below are the findings from each of the chapters within this thesis.

Chapter 1 introduced the problems facing the existing electrical infrastructure with the increasing numbers of renewable sources getting connected.   The lack of available tools that can quickly evaluate HEST as a potential solution for such problems has also been addressed.

Chapter 2 revealed that despite improvements that have been implemented in electrical power networks through the application of Smart Grids, VPP and DSM, there is now an urgent need to increase the electrical power grid capacity and flexibility. It has been concluded that such capacity and flexibility increase can be achieved through the application of energy storage, with a market

estimated to be worth $117 billion USD by 2017. In relation to this point, it has been further concluded that constrained renewable generation energy storage can be realised using hydrogen technologies.

In essence, when HEST are used, absorption of constrained renewable energy via electrolysis can be achieved. The absorption of excess renewable generation using electrolysis can thereby reduce constraints on the power grid for further renewable generation deployment. When taken within the context of "Smart Grid", it has been illustrated that electrolysis can offer the additional benefit of becoming a deferrable controllable load (or 'sink') using DSM and VPP control techniques. Hydrogen created by electrolysis from constrained renewable energy can then be stored in the form of compressed gas to be later re-used in many different applications such as in electrical power generation, transport fuelling, gas grid injection, cooking, heating, cooling, ammonia fuel/fertiliser and many more. It has also been concluded that HEST can provide enhanced grid stability functionality over other forms of energy storage devices as it offers a multitude of end-use applications for the stored energy.

Chapter 3 illustrated that the adoption of HEST has been significantly restricted due to high costs and limited availability of modelling tools that can quickly and easily identify early opportunities for its financial competitiveness. A financial competitive assessment of HEST has therefore been conducted. A new LC model has been developed within the example of constrained RES from a power grid network. The model has been applied to five different scenarios, where it has been found the application of HEST to store constrained renewable generation for later re-use on the power grid has been the least financially competitive scenario. Conversely it has been found that the most financially competitive scenario is achieved if HEST was used to absorb constrained renewable energy, and the hydrogen and oxygen produced were directly sold as gas..

Furthermore, the proposed model showed that HEST does not perform competitively in an energy arbitrage scenario (within the existing balancing mechanism of constraint payments in the UK power network). This is largely due to the comparatively low turnaround efficiency for electrolysis of constrained RES, storage as hydrogen gas, and conversion back to electrical energy via a fuel cell. Typical turn around efficiency for this process is in the region of 35 % to 40% for HEST, whilst other

bulk energy storage technologies such as PHS, CAES, NAS and NiCd have much higher turn around efficiencies that range from 65% to 85%.

It has also been found that whilst detailed cost analysis were conducted for HEST in traditional cost arbitrage markets, they did not consider the energy stored in the form of hydrogen is an output product available for direct sale as gas. Moreover, no model has been found in literature to include oxygen as a potentially valuable by-product from the electrolytic hydrogen production process, which can support the uptake of HEST.

In summary, the proposed LCM with the newly introduced sale of by-product oxygen revealed that selling hydrogen and oxygen gas produced from grid constrained renewable energy is the most financially competitive scenario, while the arbitrage scenario is the least financially competitive.

Chapter 4 determined that many of the available software tools do not offer the capability to simulate hydrogen energy storage technology as part of a hybrid renewable energy system. It has been concluded that currently available software that can simulate HEST and determine the size of an electrolyser, wind turbine, storage system, etc require a significant quantity of input data (i.e., CAPEX, OPEX, renewable resource, anticipated size of hardware, load data, number of simulation iterations, etc). It has been illustrated that these input data are often not available in early stage project development, thereby requiring substantial guess work to be undertaken by the software users. Due to the large input data requirements for the existing software and the significant computing resources needed for more advanced techniques, a deterministic sizing methodology has been developed to offer a very rapid initial system sizing.

The proposed deterministic sizing method requires a very limited number of input data (only two, namely the load and renewable resource) and can offer an initial system size for a hybrid renewable hydrogen energy storage system very quickly. This method plays an important role in the very early initial design phase. This therefore, assists in the early decision making process for the implementation of such HEST systems.

The proposed deterministic sizing method has shown that application of electrolytic hydrogen production, storage and re-use can significantly increase the utilisation of renewable generation that would otherwise not be used. This has been demonstrated using the case study described in chapter 4. However, it has been shown that the "turn-around" efficiency of an HEST system was only 29%, which further illustrates that scenario E (Chapter 3) is highly inefficient and would need substantial increase in efficiency for it to become a viable solution. One of the main reasons for the low turn around efficiency is that typical commercially available fuel cells are not able to utilise the HHV of the hydrogen gas. Due to the low turn around efficiency, the application of hydrogen technologies for renewable energy storage to subsequently supply an electrical load results in potentially very large storage requirements.

Nevertheless, the application of HEST has been found to increase the utilisation of constrained renewable energy. Even with a very modest storage system, it has been shown that the level of constrained renewable energy has been greatly reduced.   Therefore, where grid constrained renewable energy exists the application of even a small HEST solution can enable a greater renewable penetration without causing additional constraints.

Chapter 5 investigated the effect of temperature on electrolyser performance has been well documented in literature. However, it was shown that only one modelling tool has the ability to simulate an electrolysers' thermal characteristics effect on production efficiency, namely HydroGems.   Yet it has never been used to simulate the cumulative impact that the electrolyser temperature has on hydrogen production when combined with renewable generation.

Therefore an algorithm has been proposed to investigate the impact of thermal transients (time taken for the electrolyser to reach its full working temperature) on cumulative hydrogen production when used in conjunction with renewable generation. From the proposed algorithm and associated simulations, it has been found that the variable and intermittent nature of a renewable energy source results in prolonged thermal transients.   The prolonged thermal transients resulted in extended periods of time where the electrolyser is not producing hydrogen at its highest efficiency, therefore resulting in an overall reduction in hydrogen production. It has been found that the typical effect of the thermal transient on production is a reduction in cumulative hydrogen production in the region of between 1 to 3%. Where production is extremely low the effects can become much more

pronounced, increasing to between 6% and 14%. Therefore, it has been concluded that higher utilisation minimises the effects of thermal transients on overall hydrogen production.

Chapter 6 investigated the Hydrogen storage modelling for refuelling applications. It has been found that existing models in literature focus on the thermo-dynamics of refuelling stations to refuel a connected vehicle during refuelling operations. It has also been found in literature that the thermodynamic affects of refuelling a hydrogen vehicle have been removed in the latest demonstration vehicles. Conversely, it has been found that the same dynamic analysis has not been conducted for the replenishment of a hydrogen refuelling station from constrained renewable source.

Therefore, a hydrogen mass transfer model has been developed to analyse replenishment dynamics of hydrogen into a refuelling station. Furthermore, the model has been tested by applying it to a small refuelling station supplied from a constrained renewable source to identify if it could meet a daily refuelling requirement. From the proposed mass-transfer model, it has been found that enough hydrogen could be generated from a constrained renewable source to meet the required refuelling schedule. However, the replenishment of the refuelling station took longer time than what the renewable power was available for. Therefore the proposed model has provided the analysis for the replenishment dynamics of a hydrogen refuelling station which are critical when supplied from a constrained renewable resource.

7.1   Knowledge Contribution

In conclusion, the contributions to knowledge that has been presented within this thesis can be summarised in the following:

- A novel LCM has been developed for investigating the HEST financial competitiveness, while incorporating the value of by-product oxygen. It has been identified that Hydrogen use as an energy storage mechanism achieves the most financial competitiveness when the by-product oxygen is utilised.
- A new deterministic sizing methodology that offers very rapid initial HEST system sizing has been proposed. The proposed method requires a very limited number of input data and can

offer an initial system size for a hybrid hydrogen energy storage system very quickly. This plays an important role in appropriately sizing a HRHES at the very early initial design phase. This, therefore, assists in the early decision making process for the implementation of such a system. For every component in the proposed HRHES (i.e. the RES, Electrolyser, H_2 storage and Fuel cell), a model has been developed to simulate its operation using Matlab/Simulink. These individually developed models have then been integrated together to develop the proposed sizing model.

- The impact of the prolonged thermal transients of the existing commercial alkaline electrolysers on the overall H_2 production has further been modelled. It has been concluded that prolonged thermal transients result in extended periods of time where the electrolyser is not producing hydrogen at its highest efficiency. This therefore results in an overall reduction in the hydrogen production when operation is in conjunction with renewable energy sources. Using the proposed algorithm, the typical effect of electrolyser thermal transients on H_2 production has been found as a reduction in the cumulative hydrogen production in the region between 1 to 3%. When available renewable energy is extremely low the effect on hydrogen production can become much more pronounced, reducing the overall hydrogen output to between 6% and 14%.

- A hydrogen mass transfer model has been further developed to analyse the replenishment dynamics of hydrogen into a refuelling station utilised from a constrained renewable source.

7.2 Further Work

The research work that has been presented in this thesis focused on the development of four key areas that has been identified as absent in existing literature on HRHES. These aspects were the analysis of HEST financial competitiveness, the quick deterministic sizing of a HRHES with the minimum input data, the analysis of the effect of the electrolyser thermal transience on H_2 production, and the dynamic analysis of replenishing hydrogen refuelling stations through mass flow modelling. Each of these has contributed to knowledge, however there is still more room for further development of the proposed work to allow a further improvement in the understanding of HEST and enables its wide deployment. For example:

- The developed models could be further expanded to allow the analysis of the hydrogen energy storage technologies in more applications. Of a particular interest is the application of hydrogen production, from grid constrained renewable generation, in 'sector-shifting'. As

discussed in chapter 3, the constrained renewable energy in the UK is rising almost exponentially. A potential storage mechanism, that could be further modelled, is the absorption of these significant quantities of constrained energy through injecting the H_2 gas produced into the existing natural gas infrastructure.

- The developed LCM model could be further expanded to incorporate more scenarios such as employing H_2 for ammonia production. This could be either used as a fertiliser or as fuel for the transport sector. This could further determine the most financially competitive application (e.g. marine, material handling, train, plane, automotive).The results obtained from a fertiliser model could then be compared to the LCM results of selling electricity as an export commodity. In other words, the LCM could be expanded upon to identify if it would be more financially competitive to invest in ammonia fertiliser production from constrained renewable sources, rather than storing and re-selling electricity.

- The deterministic model, detailed in chapter 4, could be further expanded to incorporate other types of renewable sources such as wave, tidal, etc. It would also be advantageous to integrate the LCM and introduce an optimisation method for the storage mechanism, which would allow the users to analyse a number of scenarios automatically.

- Further investigation of the effects of thermal transients in large utility scale electrolysers should be also developed. Within this case, a number of scenarios could be investigated such as low, medium and high utilisation patterns. Comparison of the operational scenarios with the performance characteristics of multi-mega-watt electrolysis could potentially identify the financial and hydrogen production losses that could result from thermal transients at this scale.

- A further application of the developed mass flow model to more complex refuelling station scenarios would also be advantageous to allow improving the model further. Expansion of this modelling approach to allow larger refuelling stations with more diverse refuelling patterns could potentially identify the maximum number of refuelling operations that may be performed by infrastructure based upon the increasingly popular design of high pressure cascade refuelling.

- A further application of stochastic or other advanced techniques (GA, PSO, AI) to refuelling station configurations would be of considerable interest, especially since there is a lack of such models. This could potentially offer a means to optimise the refuelling station configuration with hydrogen produced from constrained renewable generation.

8

8 References

[1]   Lord Nicholas Stern, "the Economics of Climate Change: The Stern Review", Cambridge University Press, Cambridge, October 2006

[2]   Ottmar Edenhofer, Ramon Pichs Madruga, Youba Sokona, Kristin Seyboth , Patrick Matschoss , Susanne Kadner, et al, "Renewable Energy Sources and Climate Change Mitigation: Special Report of the Intergovernmental Panel on Climate Change", Technical Support Unit Working Group III, Potsdam Institute for Climate Impact Research (PIK), Intergovernmental Panel on Climate Change 2012, ISBN 978-1-107-60710-1

[3]   International Energy Agency, "Energy Technology Perspectives 2008 – Scenarios and Perspectives to 2050", (Paris, 2008), 643 pp. (2010 edition now in print)

[4]   British Petrolium (BP) , "BP Energy Outlook 2030", BP, January 2011 Edition

[5]   British Petrolium (BP) , "BP Energy Outlook 2030", BP, January 2013 Edition

[6]   United States Department of Energy, Solar Technologies Programme, "The Importance of Flexible Electricity Supply", Solar Integration Series 1 of 3, DOE/GO-102011-3201, May 2011

[7]   Øystein Ulleberg, Hiroshi Ito, María Hildur Maack, Bengt Ridell, Shannon Miles, Nick Kelly, et al, "IEA Agreement on the Production and Utilization of Hydrogen", IEA-HIA Task 18 Sub-Task B Final Report, ISBN 978-0-9815041-0-0, November 2007

[8]   U.S. Energy Information Administration Office of Integrated Analysis and Forecasting, "International Energy Outlook 2010", DOE/EIA-0484(2010), July 2010

[9]   European Wind Energy Association (EWEA), "Large scale integration of wind energy in the European power supply: Analysis, Issues & Recommendations", Published by EWEA, December 2005

[10]   Tugrul U. Daima, Xin Li, Jisun Kim, Scott Simms, "Evaluation of energy storage technologies for integration with renewable electricity: Quantifying expert opinions", Environmental Innovation and Societal Transitions, Volume 3, Pages 29-49, 2012

[11]   Marc Beaudin, Hamidreza Zareipour, Anthony Schellenberglabe, William Rosehart, "Energy storage for mitigating the variability of renewable electricity sources: An updated review", Energy for Sustainable Development, Volume 14, Issue 4, Pages 302-314, 2010

[12]   Michael Giberson and Lynne Kiesling, "Analyzing the Blackout Report's Recommendations: Alternatives for a Flexible, Dynamic Grid", Volume 17, Issue 6, Pages 51-59, 2004

[13]   Barbara Tyran, "Advancements in Energy Storage: Utility-Scale Technologies and Demonstration Projects", ASERTTI Webinar August 20, 2012

[14]   A. Ahmadi-Khatir, R. Cherkaoui, "A probabilistic spinning reserve market model considering DisCo' different value of lost loads", Electrical Power System Research, Volume 81, Issue 4, Pages 862-872, 2011

[15]   Patrick J. Luickx, Erik D. Delarue, William D. D'haeseleer, "Considerations on the backup of wind power: Operational backup", Journal of Applied Energy, Volume 85, Issue 9, Pages 787-799, 2008

[16]   Debora Coll-Mayor, Mia Paget, Eric Lightner, "Future intelligent power grids: Analysis of the vision in the European Union and the United States", Energy Policy, Volume 35, Issue 4, Pages 2453-2465, 2007

[17]   Dr John Constable, Dr Lee Moroney, "High Rewards for Wind Farms Discarding Electricity 5-6th April 2011", Renewable Energy Foundation information note, May 2011

[18]   Frans Van Hulle, Nicolas Fichaux, Anne-Franziska Sinner, Poul Erik Morthorst, Jesper Munksgaard, Sudeshna Ray, et al, "Powering Europe: wind energy and the electricity grid", A report by the European Wind Energy Association, November 2010

[19]   Electricity Networks Strategy Group , "Our Electricity Transmission Network: A Vision For 2020", A Summary of an Updated Report to the Electricity Networks Strategy Group, URN 11D/955, February 2012

[20]   Department of Energy and Climate Change, "Electricity Market Reform: Consultation on proposals for implementation", Presented to Parliament by the Secretary of State for Energy and Climate Change, 2013

[21]   Sebastian Knab, Professor Kai Strunz, Dr. Heiko Lehmann , "Smart Grid: The Central Nervous System for Power Supply - New Paradigms, New Challenges, New Services", Universität sverlag der TU Berlin, 2010

[22]   Massimiliano Manfren, Paola Caputo, Gaia Costa, "Paradigm shift in urban energy systems through distributed generation: Methods and models", Journal of applied energy, Volume 88, Issue 4, Pages 1032-1048, 2011

[23]   Massimiliano Manfren, Paola Caputo, Gaia Costa, "Distributed energy generation and sustainable development", Renewable and Sustainable Energy Reviews, Volume 10, Issue 6, Pages 539-558, 2006

[24]   Council of European Energy Regulators (CEER), "The drive towards Smart Grids", European Regulators' Group for Electricity and Gas (ERGEG), FS-10-01, October 2010

[25]   Matthias Wissner, "The Smart Grid – A saucerful of secrets?", Elsevier Journal of applied energy, Volume 88, Issue 7, Pages 2509-2518, 2011

[26]   Dr. Joachim Luther, "Smart grids, smart loads, and energy storage", Chapter 24, Global Sustainability: A Nobel Cause, Cambridge University Press, March 2010,

[27]   Christopher Findlay, "Strength in Numbers: Merging Small Generators as Virtual Power Plants", Living Energy, Issue 4, January 2011

[28]   Waqar A.Qureshi, Nirmal-Kumar C.Nair, Mohammad M. Farid, "Impact of energy storage in buildings on electricity demand side management" Energy Conversion & Management, Volume 52, Issue 5, Pages 2110-2120, 2011

[29]   Pedro S. Moura, Aníbal T. de Almeida, "The role of demand-side management in the grid integration of wind power", Applied Energy, Volume 87, Issue 8, Pages 2581-2588, 2010

[30]   Eric D. Knapp, Raj Samani, "Chapter 4 - Privacy Concerns with the Smart Grid, Applied Cyber Security and the Smart Grid", Syngress, Boston, 2013, Pages 87-99, Applied Cyber Security and the Smart Grid, ISBN9781597499989, Pages 87–99, 2013

[31]   Samuel Gyamfi, Susan Krumdieck, Tania Urmee, "Residential peak electricity demand response—Highlights of some behavioural issues", Renewable and Sustainable Energy Reviews, Volume 25, Pages 71-77, 2013

[32]   European Commission Directorate-General For Energy, "DG ENER Working Paper: The future role and challenges of Energy Storage", 14 January 2013

[33]   Sam Koohi-Kamali, V.V.Tyagi, N.A.Rahim, N.L.Panwar, H.Mokhlis, "Emergence of energy storage technologies as the solution for reliable operation of smart power systems: A review", Renewable and Sustainable Energy Reviews, Volume 25, Pages 135-165, 2013

[34]   Paul Denholm, Erik Ela, Brendan Kirby, and Michael Milligan, "The Role of Energy Storage with Renewable Electricity Generation", National Renewable Energy Laboritory, Technical Report NREL/TP-6A2-47187, January 2010

[35] Fabio Orecchini, Adriano Santiangeli, "Beyond smart grids - The need of intelligent energy networks for a higher global efficiency through energy vectors integration", International Journal of hydrogen energy, Volume 36, Issue 13, Pages 8126-8133, 2011

[36] N.S. Wade, P.C.Taylor, P.D.Lang, P.R.Jones, "Evaluating the benefits of an electrical energy storage system in a future smart grid", Energy Policy, Volume 38, Issue 11, Pages 7180-7188, 2010

[37] D.B. Nelson, M.H. Nehrir, C. Wang, "Unit sizing and cost analysis of stand-alone hybrid wind/PV/fuel cell power generation systems", Renewable Energy, Volume 31, Issue 10, Pages 1641-1656, 2006

[38] Rodica Loisel, "Power system flexibility with electricity storage technologies: A technical–economic assessment of a large-scale storage facility" Electrical Power and Energy Systems, Volume 42, Issue 1, Pages 542-552, 2012

[39] Cornelius Pieper & Holger Rubel, "Electricity Storage - Making Large-Scale Adoption of Wind & Solar Energies A Reality", Balanced Growth: Finding Strategies for Sustainable Development, Pages 163-181, ISBN 978-3-642-24652-4, 2012

[40] I.A. Grant Wilson, Peter G. McGregor, David G. Infield, Peter J. Hall, "Grid-connected renewables, storage and the UK electricity market", Renewable Energy , Volume 36, Issue 8, Pages 2166-2170, 2011

[41] J.McDowall, "Integrating Energy Storage with Wind Power in weak Electricity Grids", Power Sources, Volume 162, Issue 2, Pages 959-964, 2006

[42] Oliver Edberg, Chris Naish, Colin McNaught, "Energy Storage and Management Study", AEA Technology for the Scottish Government, ELL/000/077, revision 4, October 2010

[43] J. Buekers, E. Steen Redeker, E. Smolders, "Lead toxity to wildlife: Derivation of a critical blood concentration for wildlife monitoring based on literature data", Science of the Total Environment, Volume 407, Issue 11, Pages 3431-3438, 2009

[44] NGK Insulators, Ltd. "NAS Battery Fire Incident and Response", Press Release, October 28, 2011

[45] John Robertson, "Danger of Lerwick battery fire forces SSE to halt connection", Shetland Times, November 25th, 2011

[46] Piergiorgio Alotto, Massimo Guarnieri, Federico Moro "Redox flow batteries for the storage of renewable energy: A review", Renewable and Sustainable Energy Reviews, Volume 29, Pages 325-335, 2014

[47] Adam Z. Weber, Matthew M. Mench, Jeremy P. Meyers, Philip N. Ross, Jeffrey T. Gostick, Qinghua Liu, "Redox flow batteries: a review", Applied Electrochemistry, Volume 41, Issue 10 , pages 1137-1164, 2011

[48] A.J. Appleby, "From Sir William Grove to today: fuel cells and the future", Power sources, Volume 29, Issues 1–2, Pages 3-11, 1990

[49] Dan Rastler, "Electricity Energy Storage Technology Options: System Cost Benchmarking", IPHE Workshop 'Hydrogen- A competitive Energy Storage Medium for large scale integration of renewable electricity', November 2012

[50] Bjarne Steffen, "Prospects for Pumped-Hydro Storage In Germany", Energy Policy, Volume 45, Pages 420-429, 2012

[51] Dimitris Al. Katsaprakakis, Dimitris G. Christakis, Ioannis Stefanakis, Petros Spanos, Nikos Stefanakis, "Technical details regarding the design, the construction and the operation of seawater pumped storage systems", Energy, Volume 55, Pages 619-630, 2013

[52] Preetesh U.Mushi, Jesse Pichel, Elaine S. Kwei, "Energy storage: game - changing component of the future grid", Piper Jaffrey, Investment Research, February 2009

[53] European Commission – Community Research, "Hydrogen and Fuel Cells - A Handbook for Communities", Roads To HyCom, Volume A: Introduction, October 2007

[54] Gerda Gahleitner, "Hydrogen from renewable electricity: An international review of power-to-gas pilot plants for stationary applications", International Journal of Hydrogen Energy, Volume 38, Issue 5, Pages 2039-2061, 2013

[55] Professor D. Gray, "Smart Grids and Virtual Power Plants: Point of departure", Robert Gordon University, February 2011

[56] Tessenderlo Group, "Annual Report, Tessenderlo Group, 2003

[57] Guy Maisonnier, Jérôme Perrin, Dr. Robert Steinberger-Wilckens, "Industrial surplus hydrogen and markets and production", deliverable 2.1 and 2.1a, Roads2HyCom, Document Number: R2H2006PU.1, March 2007

[58] R.G.M. Crockett, M.Newborough, D.J. Highgate, "Electrolyser Based Energy Management: A Means for optimising the exploitation of variable renewable energy resources in standalone applications" Solar Energy, Volume 61, Issue 5, Pages 293-302, 1997

[59] Dr. Christoph Stiller, Dr. Alexander Stubinitzky, "Hydrogen for grid scale storage of renewable energy", World Hydrogen Energy Conference, June 2012

[60] Fuel Cell Today, "Water Electrolysis and Renewable Energy Systems", May 2013

[61] Peter Forsberga, Magnus Karlström, "On optimal investment strategies for a hydrogen refuelling station", International Journal of Hydrogen Energy, Volume 32, Issue 5, Pages 647-660, 2007

[62] Daniel Aklil-D'Halluin, Elizabeth Johnson, Ross Gazey, Et al, "Remote Communities & Islands - An Economical Case For Hydrogen Technologies," UNIDO, May 2008

[63] Ross Neville Gazey, "Design and development of an integrated prototype renewable hydrogen energy system", MPhil Thesis, Robert Gordon University, 2006

[64] Tulloch, D. Aklil, R. Goodhand, M. González eguizábal, "The h2seed project", M., San Antonio Fuel Cell Seminar & Exposition, October 2007

[65] Dr Jason Stoyel, "Hydrogen Mini Grid System: An iconic development for Yorkshire Forward", June 2008

[66] Mark Kraemer, "Renewable Energy Storage and Hydrogen Energy", presentation to Grove Fuel Cell Symposium, London September 2009

[67] Øystein Ulleberg, Torgeir Nakken, Arnaud Ete´, "The wind/hydrogen demonstration system at Utsira in Norway: Evaluation of system performance using operational data and updated hydrogen energy system modelling tools", International Journal of Hydrogen Energy, Volume 35, Issue 5, Pages 1841-1852, 2010

[68] Fuel Cells Bulletin , "Hydrogen Office opens in Scotland", Fuel Cells Bulletin, Volume 2011, Issue 2, Pages 9-10, 2011

[69] John Petersen, "Grid-scale Energy Storage: Lux Predicts $113.5 Billion in Global Demand by 2017", Renewable Energy World.com April 2012, (http://www.renewableenergyworld.com /rea/news/article/2012/04/grid-scale-energy-storage-lux-predicts-113-5-billion-in-global-demand-by-2017) accessed 14-10-13

[70] A. Yilanci, I. Dincer and H.K. Ozturk, "A review on solar-hydrogen/fuel cell hybrid energy systems for stationary applications", Progress in Energy and Combustion Science, Volume 35, Issue 3, Pages 231-244, 2009

[71] Francisco Díaz-González, Andreas Sumper, Oriol Gomis-Bellmunt, Roberto Villafáfila-Robles, "A review of energy storage technologies for wind power applications", Renewable and Sustainable Energy Reviews, Volume 16, Issue 4, Pages 2154-2171, 2012

[72] Jinyang Zheng, Xianxin Liu, Ping Xu b, Pengfei Liu, Yongzhi Zhao, Jian Yang, "Development of high pressure gaseous hydrogen storage technologies", International Journal of Hydrogen Energy, Volume 37, Issue 1, Pages 1048-1057, 2012

[73] Daniel D. Aklil-D'Halluin, Elizabeth Johnson, Vincenzo Ortisi, "New Policies For Successful Hydrogen Deployment", 4th World Hydrogen Technologies Convention, 2011, Glasgow, U.K. Paper ID: 0107

[74] Haisheng Chen, Thang Ngoc Cong, Wei Yang, Chunqing Tan, Yongliang Li, Yulong Ding, "Progress in electrical energy storage system: A critical review", Progress in Natural Science, Volume 19, Issue 3, Pages 291-312, 2009

[75] Helder Lopes Ferreira, Raquel Garde, Gianluca Fulli, Wil Kling, Joao Pecas Lopes, "Characterisation of electrical energy storage technologies", Energy, Volume 53, Pages 288-298, 2013

[76] H. Ibrahima, A. Ilincaa, J. Perron, "Energy storage systems characteristics and comparisons", Renewable and Sustainable Energy Reviews, Volume 12, Issue 5, Pages 1221-1250, 2008

[77] Bruce Dunn, Haresh Kamath, Jean-Marie Tarascon, "Electrical Energy Storage for the Grid: A Battery of Choices", Science, Volume 334 no. 6058, pages 928-935, November 2011

[78] Eric Hittingera, J.F. Whitacrea, Jay Apta, "What properties of grid energy storage are most valuable?", Power Sources, Volume 206, Pages 436-449, 2012

[79] Rong-Ceng Leou, "An economic analysis model for the energy storage system applied to a distribution substation", Electrical Power and Energy Systems, Volume 34, Issue 1, Pages 132-137, 2012

[80] Amirsaman Arabali, Mahmoud Ghofrani, Mehdi Etezadi-Amoli, "Cost analysis of a power system using probabilistic optimal power flow with energy storage integration and wind generation", International Journal of Electrical Power & Energy Systems, Volume 53, Pages 832-841, 2013

[81] Philipp Grünewald, Tim Cockerill, Marcello Contestabile, Peter Pearson, "The role of large scale storage in a GB low carbon energy future: Issues and policy challenges", Energy Policy, Volume 39, Issue 9, Pages 4807-4815, 2011

[82] D. Rastler, "Electric Energy Storage Technology Options: A White Paper Primer on Applications, Costs and Benefits", Electric Power Research Institute (EPRI), Palo Alto, CA, 1020676 , December 2010

[83] Mott Macdonald, "UK Electricity Generation Costs Update", Report commissioned by the UK Department of Energy and Climate Change, June 2010

[84] Abbas A. Akhil, Georgianne Huff, Aileen B. Currier, Benjamin C. Kaun, Dan M. Rastler, Stella Bingqing Chen, et al, "DOE/EPRI 2013 Electricity Storage Handbook in Collaboration with NRECA", Sandia National Laboratories, SAND2013-5131, July 2013

[85] Kevin Harrison, "Analysis of Hydrogen and Competing Technologies for Utility-Scale Energy Storage", IPHE Workshop, Spain, November 2012

[86] J.Constable, L. Moroney, "Information Note: Scottish Wind Power Constraint Payments update" Renewable Energy Foundation, June 2011

[87] Baringa Partners, "Flexible Plug and Play Principles of Access Report", UK Power Networks, December 2012

[88] Renewable Energy Foundation Constrained Renewable Generation data, http://www.ref.org.uk/constraints, last accessed 19-10-2013

[89] ERP Analysis Team, led by Jonathan Radcliffe, "The future role for energy storage in the UK", Energy Research Partnership Technology Main Report, June 2011

[90] Department of energy and climate change, "UK Renewable Energy Roadmap Update 2012", UK Government, December 2012

[91] Sandhya Sundararagavan, Erin Baker, "Evaluating energy storage technologies for wind power integration", Solar Energy, Volume 86, Issue 9, Pages 2707-2717, 2012

[92] Benedikt Battke, Tobias S. Schmidt, David Grosspietsch, Volker H. Hoffmann, "A Review and probabilistic model of lifecycle costs of stationary batteries in multiple applications", Renewable and Sustainable Energy Reviews, Volume 25, Pages 240-250, 2013

[93] Department of Energy and Climate Change (DECC), "Electricity Generation Costs 2013", 13D/185, July 2013

[94] Data provided courtesy of the collaborating research partner the Pure Energy Centre.

[95] D. Steward, G. Saur, M. Penev, and T. Ramsden, "Cost Analysis Highlights Hydrogen's Potential for Electrical Energy Storage", Technical Report, NREL/TP-560-46719, November 2009.

[96] O. Erdinc, M Uzunoglu, "Optimum design of hybrid renewable energy systems: Overview of different approaches", Renewable and Sustainable Energy Reviews, Volume 16, Issue 3, Pages 1412-1425, 2012

[97] Lehmann H, Kruska M, Ichiro D, Ohbayashi M, Takase K, Tetsunari I, et al. , "Energy rich Japan: full report" Institute for Sustainable Solutions and Innovations, October 2003

[98] Koutroulis E, Kolokotsa D, "Design optimization of desalination systems power-supplied by PV and W/G energy sources", Desalination, Volume 258, Issues 1–3, Pages 171-181, 2010

[99] Yang H, Zhou W, Lu L, Fang Z, "Optimal sizing method for stand-alone hybrid solar–wind system with LPSP technology by using genetic algorithm", Solar Energy, Volume 82, Issue 4, Pages 354-367, 2008

[100] Yang H, Zhou W, Lou C, "Optimal design and techno-economic analysis of a hybrid solar–wind power generation system", Applied Energy, Volume 86, Issue 2, Pages 163-169, 2009

[101] Bilal BO, Sambou V, Ndiaye PA, Kébé CMF, Ndongo M, "Optimal design of a hybrid solar–wind–battery system using the minimization of the annualized cost system and the minimization of the loss of power supply probability (LPSP)", Renewable Energy, Volume 35, Issue 10, Pages 2388-2390, 2010

[102] Lagorse J, Paire D, Miraoui A, "Sizing optimization of a stand-alone street lighting system powered by a hybrid system using fuel cell, PV and battery", Renewable Energy, Volume 34, Issue 3, Pages 683-691, 2009

[103] Thiaux Y, Seigneurbieux J, Multon B, Ahmed HB, "Load profile impact on the gross energy requirement of stand-alone photovoltaic systems", Renewable Energy, Volume 35, Issue 3, Pages 602-613, 2010

[104] Kornelakis A, Koutroulis E, "Methodology for the design optimisation and the economic analysis of grid-connected photovoltaic systems", IET Renewable Power Generation, Volume 3, issue 4, Pages 476–492, 2009

[105] Katsigiannis YA, Georgilakis PS, Karapidakis ES, "Multiobjective genetic algorithm solution to the optimum economic and environmental performance problem of small autonomous hybrid power systems with renewables", IET Renewable Power Generation, Volume 4, Issue 5, pages 404–419, 2010

[106] Logenthiran T, Srinivasan D, Khambadkone AM, Raj TS, "Optimal sizing of an islanded microgrid using evolutionary strategy", 11th international conference on probabilistic methods applied to power systems (PMAPS), Pages 12-17, 2010

[107] Sánchez V, Ramirez JM, Arriaga G, "Optimal sizing of a hybrid renewable system", IEEE international conference on industrial technology (ICIT), Pages 949-954, 2010

[108] Avril S, Arnaud G, Florentin A, Vinard M, "Multi-objective optimization of batteries and hydrogen storage technologies for remote photovoltaic systems", Energy, Volume 35, Issue 12, Pages 5300-5308, 2010

[109] Kaviani AK, Riahy GH, Kouhsari SHM, "Optimal design of a reliable hydrogen based stand-alone wind/PV generating system, considering component outages", Renewable Energy, Volume 34, Issue 11, Pages 2380-2390, 2009

[110] Hakimi SM, Tafreshi SMM, "Optimal sizing of a stand-alone hybrid power system via particle swarm optimization for Kahnouj area in south-east of Iran", Renewable Energy, Volume 34, Issue 7, Pages 1855-1862, 2009.

[111] Haghi HV, Hakimi SM, Tafreshi SMM, "Optimal sizing of a hybrid power system considering wind power uncertainty using PSO-embedded stochastic simulation", 11th international conference on probabilistic methods applied to power systems (PMAPS), Pages 722–727 , 2010

[112] Garyfallos Giannakoudis, Athanasios I. Papadopoulos, Panos Seferlis, Spyros Voutetakis, "Optimum design and operation under uncertainty of power systems using renewable energy sources and hydrogen storage", International Journal of Hydrogen Energy, Volume 35, Issue 3, Pages 872-891, 2010

[113] M. Castaneda, L. M. Fernandez, H.Sanchez, A Cano, F. Jurado, "Sizing methods for stand-alone hybrid systems based on renewable energies and hydrogen", 16th IEEE Mediterranean Electrotechnical Conference (MELECON), Pages 832-835, 2012

[114] S. J. Watson, A. G. Ter-gazarian, "The Optimisation of Renewable Energy Sources in an Electrical Power System by Use of Simulation and Deterministic Planning Models", International Transactions in Operational Research, Volume 3, Issues 3–4, Pages 255-269, 1996

[115] Caisheng Wang, M. Hashem Nehrir, "Power Management of a Stand-Alone Wind/ Photovoltaic/ Fuel Cell Energy System", IEEE transactions on energy conversion, volume 23, no. 3, 2008

[116] Ø. Ulleberg, "Stand-alone power systems for the future: Optimal design, operation & control of solar-hydrogen energy systems," Ph.D. dissertation, Norwegian Univ. Sci. Technol., Trondheim, Norway, 1998.

[117]   Caisheng Wang, Hashem Nehrir, "Power Management of a Stand-Alone Wind/Photovoltaic/Fuel Cell Energy System", IEEE Transactions On Energy Conversion, volume 23, no. 3, 2008

[118] Shijun Liao, Jianwei Xia, Xinfa Dong, Baitao Li, "Guangdong 300KW PEM Fuel Cell Power Station and Fuel Cell R&D in SCUT", School of Chemistry and Chemical Engineering South China University of Technology, 2009

[119] Alfredo Ursu´a, Pablo Sanchis "Static-dynamic modelling of the electrical behaviour of a commercial advanced alkaline water electrolyser", International journal of hydrogen energy, Volume 37, Issue 24, Pages 18598-18614, 2012

[120] A. Bergen, L. Pitt, A. Rowe, P. Wild, N. Djilali, "Transient electrolyser response in a renewable-regenerative energy system", International Journal of Hydrogen Energy, Volume 34, Issue 1Pages 64-70, 2009

[121] Software developer statistics published on their home page: http://homerenergy.com/ Accessed 1st October 2013

[122] Tom Lambert, Paul Gilman, Peter Lilienthal "Micropower System Modeling With Homer", National Renewable Energy Laboratory, January 2005

[123] Øystein Ulleberg, Torgeir Nakken, Arnaud Ete, "The wind/hydrogen demonstration system at Utsira in Norway: Evaluation of system performance using operational data and updated hydrogen energy system modelling tools", International Journal of Hydrogen Energy, Volume 35, Issue 5, Pages 1841-1852, 2010

[124] D. Connolly, H. Lund, B.V. Mathiesen, M. Leahy, "A review of computer tools for analysing the integration of renewable energy into various energy systems", Applied Energy, Volume 87, Issue 4, Pages 1059-1082, 2010

[125] John Barton, Rupert Gammon, "The production of hydrogen fuel from renewable sources and its role in grid operations", Power Sources, Volume 195, Issue 24, Pages 8222-8235, 2010

[126] Daniel Symes, Bushra Al-Duri, Aman Dhir, Waldemar Bujalski, Ben Green, Alex Shields, et al, "Design for on-site Hydrogen Production for Hydrogen Fuel Cell Vehicle Refueling Station at University of Birmingham, U.K.", World Hydrogen Energy Conference 2012, Energy Procedia, Volume 29, Pages 606-615, ISSN 1876-6102, 2012

[127] Fernando Olmos, Vasilios I. Manousiouthakis, "Hydrogen car fill-up process modeling and Simulation", International Journal of Hydrogen Energy, Volume 38, Issue 8, Pages 3401-3418, 2013

[128] Salvador M. Aceves, Francisco Espinosa-Loza, Elias Ledesma-Orozco,Timothy O. Ross, Andrew H. Weisberg, Tobias C. Brunner, et al, "High-density automotive hydrogen storage with cryogenic capable pressure vessels", International Journal of Hydrogen Energy, Volume 35, Issue 3, Pages 1219-1226, 2010

[129] Jose´ Miguel Pasini, Claudio Corgnale, Bart A. van Hassel, Theodore Motyka, Sudarshan Kumar c, Kevin L. Simmons, "Metal hydride material requirements for automotive hydrogen storage systems", International Journal of Hydrogen Energy, Volume 38, Issue 23, Pages 9755-9765, 2013

[130] K. Stolzenburga, V. Tsatsami, H. Grubelc, "Lessons learned from infrastructure operation in the CUTE project", International Journal of Hydrogen Energy, Volume 34, Issue 16, Pages 7114-7124, 2009

[131] E. Rothuizen, W. Me´rida, M. Rokni, M. Wistoft-Ibsen, "Optimization of hydrogen vehicle refueling via dynamic simulation", International Journal of Hydrogen Energy, Volume 38, Issue 11, Pages 4221-4231, 2013

[132] M. Hosseini, I. Dincer, G.F. Naterer, M.A. Rosen, "Thermodynamic analysis of filling compressed gaseous hydrogen storage tanks" International Journal of Hydrogen Energy, Volume 37, Issue 6, Pages 5063-5071, 2012

[133] Jiann C. Yang, "A thermodynamic analysis of refueling of a hydrogen tank", International Journal of Hydrogen Energy, Volume 34, Issue 16, Pages 6712-6721, 2009

[134] Steffen Mausa, Jobst Hapke, Chakkrit Na Ranong, Erwin Wu¨chner, Gerardo Friedlmeier, David Wenger, "Filling procedure for vehicles with compressed hydrogen tanks", International Journal of Hydrogen Energy, Volume 33, Issue 17, Pages 4612-4621, September 2008

[135] Hanane Dagdougui, Ahmed Ouammi, Roberto Sacile, "Modelling and control of hydrogen and energy flows in a network of green hydrogen refuelling stations powered by mixed renewable energy systems", International Journal of Hydrogen Energy, Volume 37, Issue 6, Pages 5360-5371, 2012

[136] Steve Carroll, Peter Speers and Chris Walsh, "Cenex Stornoway Hydrogen Vehicle Trial", Centre of excellence for low carbon and fuel cell technologies, October 2011

[137] Thanh Hua, Rajesh Ahluwalia, J-K Peng, Matt Kromer, Stephen Lasher, Kurtis McKenney, Et Al, "Technical assessment of compressed hydrogen storage tank systems for automotive applications", International Journal of Hydrogen Energy, Volume 36, Issue 4, Pages 3037-3049, 2011

[138] Sjoerd Bakker, Harro van Lente, Marius T.H. Meeus, "Dominance in the prototyping phase—The case of hydrogen passenger cars", Research Policy, Volume 41, Issue 5, Pages 871-883, 2012

[139] Janardan Gupta, Ashwani Kumar, "Fixed pitch wind turbine-based permanent magnet synchronous machine model for wind energy conversion systems", Engineering and Technology, volume 2, issue 1, Jan-Jun 2012

[140] S.M. Muyeenj, Junji Tamura, Toshiaki Murata, "Stability Augmentation of a Grid-connected Wind Farm", Green Energy and Technology, 2009, DOI 10.1007/978-1-84800-316-3

[141] RWE npower renewables, "Wind Turbine Power Calculations", Mechanical and Electrical Engineering Power Industry, August 2009

[142] ENERCON GmbH, "ENERCON Wind energy converters: Product overview", July 2010

[143] Stathis Tselepis, Nikos Hatziargyriou, Aris Dimeas, Spyros Hatzivasiliadis, Michel Vandenbergh, Randolf Geipel, Et al, "Experimental validation of islanding mode of operation", Advanced Architectures and Control Concepts for MORE MICROGRIDS, Work Package F, PL019864, December 2009

[144] Kame Khouzam, Keith Hoffman, "Real-Time Simulation of Photovoltaic Modules", Solar Energy, Volume 56, Issue 6, Pages 521-526, 1996

[145] Øystein Ulleberg, "Modeling of advanced alkaline electrolyzers: a system simulation approach", International Journal of Hydrogen Energy, Volume 28, Issue 1, Pages 21-33, 2003

[146] R. García-Valverde, C. Miguel, R. Martínez-Béjar, A. Urbina, "Optimized photovoltaic generator–water electrolyser coupling through a controlled DC–DC converter", International Journal of Hydrogen Energy, Volume 33, Issue 20, October 2008, Pages 5352–5362

[147] Eric W. Lemmon and Marcia L. Huber, "Revised Standardized Equation for Hydrogen Gas Densities for Fuel Consumption Applications", Journal of Research of the National Institute of Standards and Technology, Volume 113, Number 6, November-December 2008

[148] M. E. Wieser, "Atomic Weights of The Elements 2005", Pure Applied Chemistry, Volume78, No. 11, pages 2051-2066, 2006

[149] P. J. Mohr, B. N. Taylor, and D. B. Newell, "Revised Modern Physics" 80, 633 (2008).

[150] P.J. Mohr, B.N. Taylor, and D.B. Newell, "CODATA Recommended Values of the Fundamental Physical Constants: 2006", Revised Modern Physics, Volume 80, Page 685, June 2008.

[151] Dr D.Ali, Dr D.Aklil, "Modeling a Proton Exchange Membrane (PEM) Fuel Cell System as a hybrid power supply for standalone applications", Power and Energy Engineering Conference (APPEEC), 2011 Asia-Pacific, Pages 1-5, 2011

[152] Jinfeng Wu, Xiao Zi Yuan, Jonathan J. Martin, Haijiang Wang, Jiujun Zhang, Jun Shen, et al, "A review of PEM fuel cell durability: Degradation mechanisms and mitigation strategies", Power Sources, Volume 184, Issue 1, Pages 104-119, 2008

9 Appendix

9 Appendix A - Model Summary

Within this appendix, the individual models developed for each component of the proposed HRHES are presented. These models have been developed in a Mathlab-Simulink environment to allow the development of the system sizing algorithm proposed in chapter 4. The developed electrolyser model has been further used to investigate the effect of the electrolyser thermal transients in chapter 5 and to model the refuelling station replenishment dynamics in chapter 6. The proposed HRHES overall simulation model is depicted in Figure 9-1.
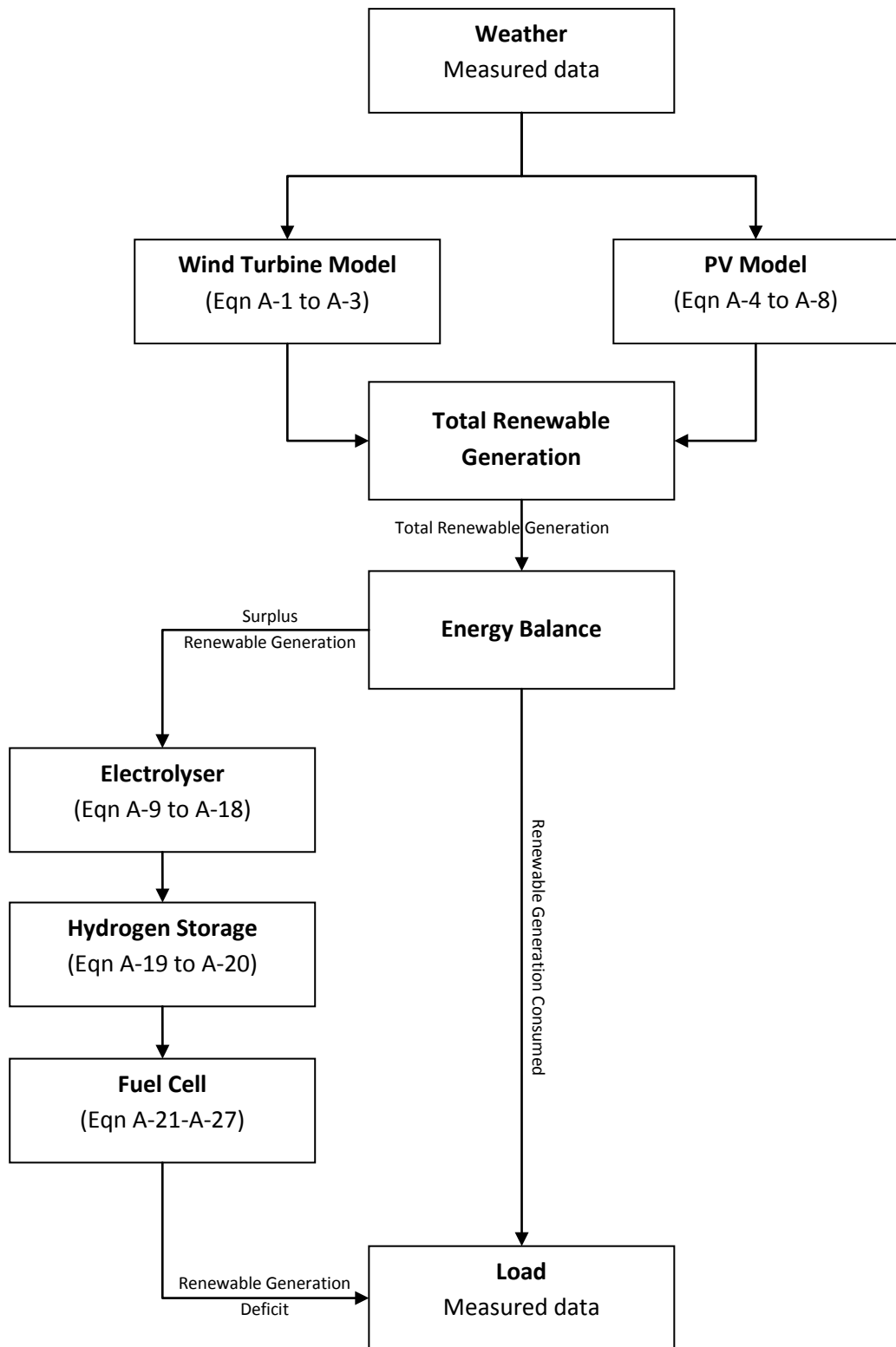
Figure 9-1: Chapter 4 simulation overview

9.1 Wind Turbine Model

The wind turbines commonly used in modern installations are typically designed to operate at a variable speed with either a fixed or variable pitch blade angle. The blade angle is the angle of the blades attack relative to the oncoming wind. In addition modern variable speed wind turbines have no transmission (gearbox) which improves efficiency and reduce operational noise, fatigue and wear and tear. The developed model, as summarised below, has been derived from the manufacturer's data sheet together with literature [139-142] to allow a reasonable approximation of the turbines expected performance.

The main factor affecting a wind turbines power output is its rotors coefficient of performance (Cp) value. The coefficient of performance is a measure of wind turbines blade rotor effectiveness at converting the power in the wind to mechanical power. The wind turbines coefficient of performance is calculated using equation A-1:

$$C_p(\lambda) = 0.5(\lambda - 0.02\beta^2 - 2.9)e^\lambda - 0.0303\lambda \qquad \text{(A-1)}$$

Where λ (or tip speed ratio as it is commonly known) is found from equation A-2 and β is the blades pitch angle. The tip speed ratio (λ) is the relationship between the ratio of the wind speed and the speed at which the wind turbines rotor tips are travelling.

$$\lambda = \frac{\dfrac{\pi n D}{60}}{v} \qquad \text{(A-2)}$$

Where: n = Turbine RPM

D = Turbine rotor diameter

v = Wind speed.

The overall power output from a wind turbine can therefore be modelled by applying the Cp value to the swept area of the wind turbines rotor, wind speed and air density as shown in equation A-3:

$$P_{wind} = \frac{1}{2}\rho A v^3\left(0.5(\lambda - 0.02\beta^2 - 2.9)e^{(\lambda)} - 0.0303\lambda\right) \qquad \text{(A-3)}$$

Where: P_{wind} = Wind turbine output

ρ = Air density

A = Swept rotor area

v = Wind speed

λ = Tip speed ratio

β = Blade pitch angle

9.2 PV Model

An interpolation model has been used here to simulate the performance of the photovoltaic panel arrays [143-144] This PV Panel model uses commonly the available data presented by the manufacturers on their data sheets as an industry norm. The proposed interpolation model is shown by equation A-4, which utilises values directly from the manufacturer standard data.

$$I = I_{SC}\left[1 - C_1\left(exp\left(\frac{V_R}{C_2 V_{oc}}\right) - 1\right)\right] + D_I \tag{A-4}$$

Using the PV panel manufacturer data for short circuit current (I_{sc}), open circuit voltage (V_{oc}), and the Maximum Power Point (MPP) voltage and current (V_{MP}) and (I_{MP}) respectively, enables the performance characteristics to be interpolated for difference light conditions. The two constants C_1 and C_2 are first calculated by using the short circuit, MPP and Open circuit reference points in equations A-5 and A-6,

$$C_1 = \left(1 - \frac{I_{mp}}{I_{sc}}\right) exp\left(-\frac{V_{mp}}{C_2 V_{oc}}\right) \tag{A-5}$$

$$C_2 = \frac{\left(\frac{V_{mp}}{V_{oc}} - 1\right)}{\ln\left(1 - \frac{I_{mp}}{I_{sc}}\right)} \tag{A-6}$$

The effects of temperature and irradiance are then accounted for in equations A-7 and A-8:

$$V_R = V + \beta\left(T - T_{ref}\right) + R_s D_I \tag{A-7}$$

$$D_I = \alpha\Phi\left(T - T_{ref}\right) + I_{sc}(\Phi - 1) \tag{A-8}$$

Where: I_{sc} = Short Circuit Current

V_{mp} = Maximum Power Point Voltage

I_{mp} = Maximum Power Point Current

V_{oc} = Open Circuit Voltage

Φ = Solar Irradiance

T = Cell Temperature

T_{ref} = Reference Temperature (25 ^{o}C)

α, β = Coefficients of I_{sc} and V_{oc} variation depending on temperature.

R_s = Series Resistance.

9.3 Electrolyser Model

The proposed electrolyser model has three distinct model elements. These are the U-I curve, faraday efficiency, and thermal models. These model elements have been combined to simulate the operation of an electrolyser. An electrolyser model that accurately predicts the electrochemical and thermal dynamic behaviour of an advanced alkaline electrolyser has been developed in literature by Øystein Ulleberg [145] and is summarised in the next section.

9.3.1 U-I curve

An electrolyser operating characteristic is determined by its voltage and current profile. In essence, the quantity of hydrogen produced by an electrolyser varies with the amount of current passing through the electrolytic cell stack.

An electrolyser U-I curve depicts how electrolytic cell voltage develops as more current is absorbed by the electrolyser to increase the gas output flow. For an ideal electrolyser this relationship would be a straight line. However, due to the losses that occur in the electrochemistry and cell structure, there is a non-linear relationship. This relationship is affected by the ohmic resistance of the electrolyte and electrodes as well as the parasitic loss of 'stray' electrolysis. The parasitic loss of stray electrolysis is a phenomenon where the electrons flow down the electrolyte fluid channels instead of directly between the electrodes themselves.

The voltage (U) required to breakdown water can be expressed in terms of the over voltage beyond the reversible electrochemical cell voltage (U_{rev}). The voltage required to facilitate electrolytic

dissociation of water molecules is temperature dependant and can be expressed as shown in equation A-9.

$$U = U_{rev} + \frac{(r_1 + r_2 T)}{A} I + s \log\left(\left(\frac{t_1 + \frac{t_2}{T} + \frac{t_3}{T^2}}{A} I\right) + 1\right)$$

(A-9)

Where: U = Voltage (V)

U_{rev} = reversible voltage (V)

$r_{1,2}$ = empirical ohmic resistance parameter of electrolyte (Ωm^2)

T = temperature ($^O K$)

$t_{1,2,3}$ = empirical over voltage parameter of electrode ($mA^{-1}m^2$)

s = over voltage parameter of electrode (V)

A = electrode area (m^2)

I = current (I)

The reversible cell voltage (U_{rev}) is calculated using an empirical Nernst equation for electrolysis [146]. This is found using equation A-10.

$$U_{rev,T(K)} = 1.5184 - 1.5421 \times 10^{-3}T + 9.523 \times 10^{-5}T \ln T + 9.84 \times 10^{-8}T^2$$

(A-10)

9.3.2   Faraday Efficiency

The Faraday efficiency is the ratio between actual and maximum theoretical hydrogen mass that can be produced in an electrolyser. Faraday efficiency losses are caused by parasitic current losses within the electrolysis cell stack. The parasitic current loss will increase as a percentage of the overall current with decreasing current densities and increasing temperatures. Therefore the percentage of parasitic current loss to the total current flow increases with decreasing current densities.

An empirical equation for the Faraday efficiency is shown in equation A-11:

$$\eta_F = \frac{\left(\frac{I}{A}\right)^2}{f_1 + \left(\frac{I}{A}\right)^2} f_2$$

(A-11)

Where: η_F = Faraday Efficiency

           A = Electrode area (m^2)

           I = Current (I)

           f_1 = Faraday efficiency parameter mA^2cm^{-4}

           f_2 = Faraday efficiency parameter (number between 0 and 1)

f_1 and f_2 are the two constants used in the definition of the Faraday efficiency of hydrogen production. The first constant (f_1) is defined in units of mA^2cm^{-4} while the second constant used (f_2) is defined as an arbitrary number between the values of 0 and 1. These values are selected empirically

Faraday's law also models the production rate of hydrogen in an electrolytic cell. The production rate of hydrogen is directly proportional to the transfer rate of electrons at the electrodes. This is equivalent to the electrical current provided by the power supply. Therefore the total hydrogen production rate in an electrolysis stack consisting of several cells connected in series can be expressed as shown in equation A-12:

$$\dot{n}_{H_2} = \eta_F \frac{n_c I}{zF} \qquad \text{(A-12)}$$

Where: $\dot{n}_{H_2}$ = Molar flow rate ($mol\ s^{-1}$)

           η_F = Faraday Efficiency

           z = 2 (number of electrons transferred per reaction)

           I = Current (I)

           F = Faraday constant 96485 $Cmol^{-1}$

           n_c = Number of cells in electrolyser cell stack

9.3.3   Thermal Model

The production of heat in an electrolyser is primarily caused by electrical inefficiencies. The energy efficiency can be calculated from the thermo-neutral voltage (U_{tn}) and the cell voltage (U) using equation A-13:

$$\eta_e = \frac{U_{tn}}{U} \qquad \text{(A-13)}$$

Where: η_e =Energy Efficiency

U_{tn} =Thermo Neutral Voltage $\cong$ 1.477V

U =Cell Voltage

As found in literature [145] the value for U_{tn} remains almost constant in the pressure and temperature range considered within this thesis (0-1200kPa pressure, 0-80°C temperature), therefore the value used for U_{tn} is 1.477V

The operating temperature of an electrolyser can be found from the overall thermal energy balance of the electrolysis system. The thermal energy balance of the electrolyser can be expressed as shown in equation A-14. Equation A-15 calculates the thermal energy created by the electrolysis process, and equation A-16 is used to calculate the thermal losses of the electrolyser system. To maintain the electrolyser temperature at or below the maximum specified by the manufacturer equation A-17 is applied. In this case it is always assumed that the electrolyser cooling system is sufficient to remove the excess heat generated by the electrolysis process.

$$C_t \frac{dT}{dt} = \dot{Q}_{gen} - \dot{Q}_{loss} - \dot{Q}_{cool} \tag{A-14}$$

$$\dot{Q}_{gen} = n_c(U - U_{tn})I = n_c UI(1 - \eta_e) \tag{A-15}$$

$$\dot{Q}_{loss} = \frac{1}{R_t}(T - T_a) \tag{A-16}$$

$$\dot{Q}_{cool} > \dot{Q}_{gen} - \dot{Q}_{loss} \tag{A-17}$$

Where: $\dot{Q}_{gen}$ = Thermal Energy Created by electrolysis process

$\dot{Q}_{loss}$ = Thermal Energy lost to the environment

$\dot{Q}_{cool}$ = Thermal energy dissipated by cooling system

C_t = Thermal capacity (or inertia) of electrolyser (JK^{-1})

R_t = Thermal resistance of electrolyser (W^{-1}K)

n_c = number of cells in the electrolysis stack (n)

η_e = Energy Efficiency (%)

U_{tn} = Thermo Neutral Voltage (V)

U = Cell Voltage (V)

T = Electrolyser Temperature (K)

T_a = Ambient temperature (K)

t = Time

To calculate the electrolyser temperature as time passes, it is assumed that the electrolyser exhibits a constant heat generation and heat transfer profile for a small time interval of not more than a few seconds. Therefore an intra-time-step steady-state thermal model can be expressed as shown in equation A-18, where T_{ini} is the initial temperature and Δ_t is the change in time

$$T = T_{ini} + \frac{\Delta t}{C_t}\left(\dot{Q}_{gen} - \dot{Q}_{loss} - \dot{Q}_{cool}\right)$$
(A-18)

9.4 Pressurised Hydrogen Storage Model

The ideal gas relationship can only be used to describe the behaviour of real hydrogen gas accurately at relatively low pressures up to approximately 1MPa. At higher pressures, the results become increasingly inaccurate. One of the easiest ways to account for this additional compression is through the addition of a compressibility factor, designated in the literature by the symbol Z [147].

Compressibility factors (or "Z factors") are derived from data obtained through experimentation and depend on temperature, pressure and the nature of the gas. The Z factor is then used as a multiplier to adjust the ideal gas law to fit actual gas behaviour as shown in equation A-19.

$$P = Z\rho RT$$
(A-19)

Where: P = Absolute pressure in Pascal

ρ = Molar density

T = Absolute temperature in Kelvin

R = Universal gas constant = 8.31434 Nm/mol K

9.4.1 Pressure Correction Factor

Research conducted by the National Institute for Standards and Technology developed a mathematical method for calculating compressibility factors using a virial equation based on Pressure (MPa) and Temperature (^{o}K). An equation for the density of hydrogen gas that agrees with measurement standards to within 0.01% from 220°K to 1000°K with pressures up to 70MPa, and to within 0.01 % from 255°K to 1000°K with pressures to 120MPa, and to within 0.1 % from 200°K to 1000°K up to 200MPa has been developed [147].

Using equation A-20 and the variable values listed in Table 9-1, the compressibility factor for hydrogen at different pressures and temperatures can be calculated to a high degree of accuracy.

$$Z(P,T) = \frac{P}{\rho RT} = 1 + \sum_{i=1}^{9} a_i \left(\frac{100}{T}\right)^{b_i} \left(\frac{P}{1}\right)^{c_i} \tag{A-20}$$

The equation and its constants are defined for pressures in Mega-Pascal (MPa) and temperatures in Kelvin (^{o}K). The mass of diatomic hydrogen (H_2) and the molar gas constant given in Table 9-1 are obtained from recent publications [148-150].

I	a_i	b_i	c_i
1	0.05888460	1.325	1.0
2	−0.06136111	1.87	1.0
3	−0.002650473	2.5	2.0
4	0.002731125	2.8	2.0
5	0.001802374	2.938	2.42
6	−0.001150707	3.14	2.63
7	0.9588528×10^{-4}	3.37	3.0
8	$−0.1109040 \times 10^{-6}$	3.75	4.0
9	0.1264403×10^{-9}	4.0	5.0
Molar Mass: M = 2.01588g/mol			
Universal Gas Constant: R=8.314472 J/(mol K)			

Table 9-1: Table of constants required to calculate Z for Hydrogen gas

9.5   Fuel Cell Model

A fuel cell in common with an electrolyser is an electro-chemical device. However its mode of operation is to release the energy stored within a fuel (hydrogen in the case of this research project) and produce electricity. Many examples of fuel cell models can be found in literature, however the model used in this thesis has been developed by Dr. Dallia Ali, and is summarised below [151]

The basic chemical reaction of a bipolar FC cell is shown in equation A-21 where H_2, O_2, and H_2O are Hydrogen Gas, Oxygen Gas, and water respectively.

$$H_2(g) + \frac{1}{2}O_2(g) \rightarrow H_2O + heat \tag{A-21}$$
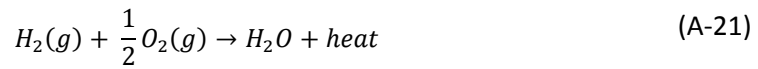
Each cell in a fuel cell will suffer from a number of losses. These losses are typically characterised in terms of the overall cell voltage (U) in relation to the reversible cell voltage (U_{rev}) and associated activation (U_a), ohmic (U_o) and concentration (U_c) losses as shown in equation A-22.

$$U = Urev - Ua - Uo - Uc \tag{A-22}$$

The reversible or ideal voltage of a fuel cell can be found using the Nernst equation for the open circuit voltage of a fuel cell. This takes into consideration changes in temperature as shown in equation A-23 [151].

$$Urev = 1.229 - 0.85 \times 10^{-3} \times (T - 298.15) + 4.3085 \times 10^{-5}T \left[\ln(P_{h2}) + (\frac{1}{2})\ln(P_{O2}) \right] \tag{A-23}$$

Where T is the temperature in degrees Kelvin, P_{h2} and P_{O2} are the partial pressures of the hydrogen and oxygen in Pascals.

Activation losses (U_a) are due to the time it takes for the electrochemical reactions to take place on the surface of the fuel cell electrodes. A small fraction of the voltage is lost promoting the chemical reaction to take place that transfers electrons to and from the anode and cathode electrodes. Equation A-24 represents the activation losses [151].

$$U_a = -\left[\xi_1 + \xi_2 T + \xi_3 T \ln(C_{O2}) + \xi_4 T \ln(i_{fc}) \right] \tag{A-24}$$

Where: i_{fc} = Cell operating current

           C_{O2} = Concentration of oxygen at the catalytic interface of the cathode

           T   = Cell temperature in degrees Kelvin

           ξ = Parametric coefficients of each FC Cell

Ohmic losses (U_o) occur due to the parasitic current flows within the electrode and cell assembly. This is caused by stray electrons passing directly through the Membrane Electrode Assembly (MEA) instead of around the external electric circuit. The ohmic losses for NAFION® based membrane electrode assemblies are expressed in equation A-25. (Perfluorosulfonic acid (PFSA) membranes such as Nafion® represent the majority of PEM fuel cells membranes [152])

$$U_o = I_{FC}\left(\rho_M\left(\frac{L}{A}\right) + R_C\right) \tag{A-25}$$

Where: I_{FC} = The cell operating current

           R_C = Resistive constant

           L   = Membrane Thickness

           A   = Membrane Active Area

The value of ρ_M is corrected for temperature using equation A-26:

$$\rho_M = \frac{181.6\left[1 + 0.03\left(\frac{I_{fc}}{A}\right) + 0.062\left(\frac{T}{303}\right)^2 \cdot \left(\frac{I_{fc}}{A}\right)^{2.5}\right]}{\left[\psi - 0.634 - 3\left(\frac{I_{fc}}{A}\right)\right] \cdot \exp\left[4.18\left(\frac{T - 303}{T}\right)\right]} \tag{A-26}$$

Where: I_{fc} = Cell operating current

           A   = Membrane Active Area

           T   = Cell temperature in degrees Kelvin

           Ψ = Humidification level of the membrane (14=ideal, 23=over saturated)

The concentration losses within a fuel cell are caused by the change in the concentration of the reactants at the surface of the electrodes within each cell. At high current densities the reactant concentration drops causing greater losses. Therefore the concentration losses are most prevalent when the fuel cell is operating at high power levels. The effect of concentration losses is expressed as shown in equation A-27

$$U_C = -B \ln\big(1 - (j/j_{max})\big) \qquad\qquad (\text{A-27})$$

Where: j = Current density (I_{FC}/A)

       j_{max} = maximum current density

       A   = Membrane Active Area

       B   = parametric coefficient, measured in Volts

10 Appendix B

Appendix B –Model value tables

Variable	Description	Unit	Value
r_1	electrolyte ohmic resistive parameter	Ωm^2	0.0001127
r_2	electrolyte ohmic resistive parameter	Ωm^2	-0.000001269
A	electrode area	m^2	0.06
S	over voltage parameter of electrode	V	0.2982
t_1	empirical over voltage parameter of electrode	$A^{-1}m^2$	0.173
t_2	empirical over voltage parameter of electrode	$A^{-1}m^2$	0.00424
t_3	empirical over voltage parameter of electrode	$A^{-1}m^2$	-0.000036
f_1	Faraday efficiency parameter	mA^2cm^{-4}	20000
f_2	Faraday efficiency parameter	$0.....1$	0.93
R_t	Thermal resistance of electrolyser	$W^{-1}K$	0.018
C_t	Thermal capacity of electrolyser	JK^{-1}	320000
n_c	Number of cells in electrolysis stack	N	48
T_{max}	Maximum operating temperature of electrolyser	^{O}C	80

Table 10-1: 26kW Electrolyser model parameter values

Variable	Description	Unit	Value
r_1	electrolyte ohmic resistive parameter	Ωm^2	0.0000453
r_2	electrolyte ohmic resistive parameter	Ωm^2	-0.0000012
A	electrode area	m^2	0.02
S	over voltage parameter of electrode	V	0.31
t_1	empirical over voltage parameter of electrode	$A^{-1}m^2$	0.8
t_2	empirical over voltage parameter of electrode	$A^{-1}m^2$	8.537
t_3	empirical over voltage parameter of electrode	$A^{-1}m^2$	900
f_1	Faraday efficiency parameter	mA^2cm^{-4}	200000
f_2	Faraday efficiency parameter	$0.....1$	0.985
R_t	Thermal resistance of electrolyser	$W^{-1}K$	0.018
C_t	Thermal capacity of electrolyser	JK^{-1}	300000
n_c	Number of cells in electrolysis stack	N	180
T_{max}	Maximum operating temperature of electrolyser	^{O}C	60

Table 10-2: 30kW Electrolyser model parameter values

Variable	Description	Unit	Value
r_1	electrolyte ohmic resistive parameter	Ωm^2	0.0000253
r_2	electrolyte ohmic resistive parameter	Ωm^2	-0.00000155
A	electrode area	m^2	0.08
S	over voltage parameter of electrode	V	0.31
t_1	empirical over voltage parameter of electrode	$A^{-1}m^2$	0.8
t_2	empirical over voltage parameter of electrode	$A^{-1}m^2$	8.537
t_3	empirical over voltage parameter of electrode	$A^{-1}m^2$	900
f_1	Faraday efficiency parameter	mA^2cm^{-4}	280000
f_2	Faraday efficiency parameter	$0.....1$	0.98
R_t	Thermal resistance of electrolyser	$W^{-1}K$	0.015
C_t	Thermal capacity of electrolyser	JK^{-1}	400000
n_c	Number of cells in electrolysis stack	N	140
T_{max}	Maximum operating temperature of electrolyser	^{O}C	60

Table 10-3: 200kW Electrolyser model parameters

Variable	Description	Unit	Value
D	Rotor Diameter	m	33.4
n	Rotational Speed	RPM	45
$β$	Blade Pitch Angle	^{o}	0
P_{wind}	Rated Power Output (at rated wind speed 13m/s)	kW	335
A	*Rotor* Sweep Area	m^2	876

Table 10-4: E33 Wind turbine model values

Variable	Description	Unit	Value
P_{mpp}	STC Power Rating	*Watts*	80
V_{oc}	Open Circuit Voltage	V	22.1
I_{sc}	Short Circuit Current	I	4.8
V_{mpp}	Maximum power point voltage	V	17.6
I_{mpp}	Maximum power point Current	I	4.5
$α$	I_{sc} Coefficient	$\%/^oC$	0.065
B	V_{oc} Coefficient	$\%/^oC$	-0.34
$Tref$	*Reference temperature*	^oC	25

Table 10-5: BP380S Photovoltaic Model Values

Variable	Description	Unit	Value
A	*Active Cell Area (per stack module, 8 modules used)*	cm^2	*350*
N	number of cells (per stack module)	n	100
B	parametric coefficient	V	0.016
Ψ	Humidification level of membrane	n	20
Rc	*Ressistive coefficient*	$Ω$	*0.0003*
L	Membrane thickness	cm	0.0178
T	Working temperature	^oK	343
$ξ1$	*Parametric coefficient*	n	*-0.948*
$ξ2$	*Parametric coefficient (@ working temp)*	n	*$-1.35x10^{-16}$*
$ξ3$	*Parametric coefficient*	n	*0.000076*
$ξ4$	*Parametric coefficient*	n	*-0.000193*
Jmax	Maximum current density	A/cm^2	1
P_{02}	partial pressure of oxygen	Atm	1
P_{H2}	partial pressure of oxygen	Atm	1

Table 10-6: Fuel Cell Model Values

11 Appendix - C

11 Appendix C – Publication List

R. Gazey, Dallia Ali, Daniel Aklil "Real World Renewable Hydrogen Transport", Journal of Technology Innovations in Renewable Energy, 2012, 1, 14-22. DOI: http://dx.doi.org/10.6000/1929-6002.2012.01.01.2

R.Gazey, Dr D. Ali, Dr D. Aklil, "Evaluation of hydrogen office wind/hydrogen demonstration system using simulation tools" 4th World Hydrogen Technologies Convention, 2011, Paper ID: 0109

R. Gazey, Dr. D. Ali, Dr. D. Aklil, "Techno-Economic Assessment of Energy Storage Systems For Enabling Projected Increase Of Renewables Onto Electrical Power Grids" IET Renewable Power Generation Conference Proceedings 2011. DOI: 10.1049/cp.2011.0135

R. Gazey, D. Ali, D. Aklil, "The Hydrogen office: open and storing wind", Poster presentation in the Power Storage Session, All Energy 2011 Conference and Exhibition, 18-20 May, Aberdeen, UK

Ross Gazey, Dr. Dallia Ali, Dr. Daniel Aklil, "Smart Grid Operation while integrating Photo-voltaic through Green Hydrogen Technology", Poster Presentation, 2nd TAMUQ Annual Research and Industry Forum

Ross Gazey, Dr. Dallia Ali, Dr. Daniel Aklil, "Modelling Hydrogen Energy Technology to facilitate increased renewable penetration", Poster Presentation in the ETP Annual Conference 2013 / All Energy 2013